Luo, Rui (2010) *Neutrino masses and Baryogenesis via Leptogenesis in the Exceptional Supersymmetric Standard Model.* PhD thesis.

http://theses.gla.ac.uk/1557/

Copyright and moral rights for this thesis are retained by the author

A copy can be downloaded for personal non-commercial research or study, without prior permission or charge

This thesis cannot be reproduced or quoted extensively from without first obtaining permission in writing from the Author

The content must not be changed in any way or sold commercially in any format or medium without the formal permission of the Author

When referring to this work, full bibliographic details including the author, title, awarding institution and date of the thesis must be given

Glasgow Theses Service
http://theses.gla.ac.uk/
theses@gla.ac.uk

Neutrino masses and Baryogenesis via Leptogenesis in the Exceptional Supersymmetric Standard Model

Rui Luo

Submitted in fulfilment of the requirements for the Degree of Ph.D.

Department of Physics and Astronomy

University of Glasgow

February 2010

Abstract

Netrino oscillation experiments discover that (left-handed) neutrinos have masses much less than charged leptons and quarks in the Standard Model. One solution to the light neutrino mass puzzle is the seesaw model where right-handed neutrinos are introduced with large Majorana masses. The heavy Majorana right-handed neutrinos lead to lepton number violation in the early universe. They decay into either leptons or anti-leptons via Yukawa couplings. The CP asymmetries of these decays result in lepton number asymmetry in the universe. The lepton number asymmetry can be converted into baryon number asymmetry via the electroweak sphaleron process. This mechanism explains the baryon asymmetry of universe problem and is called leptogenesis.

However, one finds that in order to generated enough baryon number in the universe, the reheating temperature, which is required to be of order of the lightest right-handed neutrino mass, has to be higher than $\sim 10^9$ GeV. The high reheating temperature would lead to the over-produced gravitinos in the universe, contrasting with the present observation. We investigate leptogenesis in the Exceptional Supersymmetric Standard Model. We find that the extra Yukawa couplings would enhance the CP asymmetries of the RH neutrino decay drastically. And the evolution of lepton/baryon asymmetries is described by Boltzmann Equations. Numerical calculation of the Boltzmann Equations shows that a correct amount of baryon number in the universe can be achieved when the lightest right-handed neutrino mass is $\sim 10^7$ GeV, and then the gravitino-over-production problem is avoided.

Contents

Acknowledgement

I would like to thank all the staff and students in the particle physics theory group at Glasgow University for their help and encouragement. Especially, I owe my deepest gratitude to my supervisor David J. Miller for support in my research and letting me do this project, which I really like. I feel very easy to discuss physics with him, although I am not good at expressing myself and I mostly speak Chinglish during the discussion. I am also very grateful to my collaborator Roman Nevzorov. He has made his support by helping me understanding the model and the solving problems in the calculation.

I would also like to thank Andrew Davies for helping me solving the problems in the book of Peskin and Schroeder in the first year. Furthermore, I am grateful to Peter Athron, John Campbell, Christine Davies, Colin Froggatt, Ian Kendall, Erik Gregory, Craig McNeile, David Sutherland, Dave Thompson and my previous flatmate Kit Wong for discussing physics and other sorts of things in the past four years. This thesis would not have been possible without them.

In particular, I am indebted to my collaborators Steve F. King in Southampton and Stefan Antusch in Munich. We have had so much valuable discussion in these projects.

Finally, thanks to all my families and friends. I can feel you all the time.

Declaration

I declare that none of the material presented in this thesis has previously been presented for a degree at this or any other university.

Chapter 1 is an overview of the background and related topics of my research. Chapter 2 is devoted to a review of the E_6SSM model I am using in this thesis. Chapter 3 is based on work in collaboration with Prof. Steve F. King, my supervisor Dr David J. Miller and Dr Roman Nevzorov. Chapter 4 is based on an ongoing work in collaboration with Dr Stefan Antusch, Prof Steve F. King, Dr David J. Miller and Dr Roman Nevzorov. My work described here has appeared in the following publications,

- S. F. King, R. Luo, D. J. . Miller and R. Nevzorov,
  "Leptogenesis in the Exceptional Supersymmetric Standard Model: flavour dependent lepton asymmetries,"
  JHEP **0812** (2008) 042 [arXiv:0806.0330 [hep-ph]].

- S. F. King, R. Luo, D. J. . Miller and R. Nevzorov,
  "Leptogenesis in the E_6SSM: Flavour Dependent Lepton Asymmetries,"
  AIP Conf. Proc. **1078** (2009) 509 [arXiv:0808.3739 [hep-ph]].

- S. F. King, R. Luo, D. J. . Miller and R. Nevzorov,
  "Leptogenesis in the E(6)SSM,"
  J. Phys. Conf. Ser. **110** (2008) 082009.

- S. F. King, R. Luo, D. J. . Miller and R. Nevzorov,
  "Generation of Flavour Dependent Lepton Asymmetries in the E_6SSM,"
  arXiv:0810.0516 [hep-ph].

- P. Athron, S. F. King, R. Luo, D. J. Miller, S. Moretti and R. Nevzorov,
  "Unification of Gauge Couplings in the E(6)SSM,"
  arXiv:0909.4530 [hep-ph].

Chapter 1

Introduction

1.1 Overview

Neutrinos are particles which are generated in various sources. They can be generated in the nuclear reaction in the core of the Sun and propagate together with the light to the Earth. Also they can be generated in the upper layer of the Earth atmosphere, in the nuclear power station and accelerators (human-made experiment), etc. They interact with other particles with a fairly low rate, so even when billions of neutrinos pass through a huge detector, we can only see a few signals produced by these neutrinos in one month. In our daily life, although billions of neutrinos pass through our body, we can not be hurt or even feel them.

Neutrinos are mysterious and we do not know too much about them. Initially, people assume they are massless, like photons, which means they can propagate at the speed of light. However, people found that there are three types of neutrinos. During the propagation, from the source to the detector, neutrinos can change from one type to another one. Precise measurement of the transition rate tells that this phenomenon can be explained by neutrino masses, and it is called neutrino oscillation. Neutrino oscillations and other experiments tell that neutrinos have masses much smaller than other elementary

particles, *e.g.* electron. The smallness of neutrino masses indicates the physics beyond our current knowledge, and one needs to explain how the neutrino masses are generated in theory. One elegant mechanism is called the seesaw model with hypothetical heavy particles. The neutrino mass term is an effective term generated via the heavy particles. Whether the neutrinos are Majorana particles can be tested by experiments including neutrinoless double beta decay where lepton number violation is induced by Majorana mass terms of light neutrinos.

Another intriguing puzzle of the particle cosmology is the Baryon Asymmetry of Universe (BAU) problem, based on the fact that the universe contains baryons (matter) rather than anti-baryons (anti-matter). In the canonical theory, there is no substantial asymmetry of baryon and anti-baryon during the evolution of the Universe, therefore one need a mechanism to explain how the matter asymmetry is generated. One elegant mechanism is leptogenesis. In leptogenesis, one proposes heavy right-handed neutrinos, which have not been discovered in experiments. The right-handed neutrinos can both decay into leptons (electrons and two other types, which have the same properties but different masses) and anti-particles of leptons, however rates of these two decay channels can be different, which leads to an asymmetry of leptons. The asymmetry of leptons can be converted into baryons, and therefore form the present matter in the Universe.

In the rest part of Chapter 1, we discuss the background of neutrino, the mass type of neutrinos, the model of neutrino oscillation, the experiments of exact scale of neutrinos, the seesaw model, the measurement of Baryon Asymmetry of the Universe, how the electroweak sphaleron process happens, how to calculate the lepton to baryon transition ratio, the framework of Leptogenesis and a brief discussion of Affleck-Dine mechanism and Electroweak Baryogenesis.

In Chapter 2, we discuss the Exceptional Supersymmetric Standard Model and its phenomenology. We present the Yukawa interactions of RH neutrino in this model. In Chapter 3, we calculate the CP asymmetry of RH neutrino decay in Exceptional Supersymmetric Standard Model, illustrating that the CP asymmetry can be enhanced

drastically with respect to the the CP asymmetry in the canonical scenario, by Yukawa couplings of right-handed neutrino and exotic particles (exotic leptons, inert Higgses or leptoquarks) in this model. In Chapter 4, we calculate the Boltzmann Equations for Leptogenesis. We show that baryon number density can be generated in the Exceptional Supersymmetric Standard Model with the first RH neutrino mass $M_1 \sim 10^6\, GEV$. And in Chapter 5, we conclude and point out related research areas. We list some important notation of the Standard Model in Appendix A. The ingredients of Minimal Supersymmetric Model are present in Appendix B. The hypercharges of MSSM particles are list in Appendix C. And Appendix D is devoted to the theory of Big Bang Nucleosynthesis. We will mention cosmological thermal dynamics in Appendix E. In Appendix F, an alternative method to the flavoured Boltzmann Equations for leptogenesis is presented. Finally, in appendix G we present an analogy of the Boltzmann Equations to illustrate how spectator processes play the role in leptogenesis.

1.2 Neutrinos

Electron neutrino ν_e was first postulated by Pauli in 1930 to explain the missing energy and momentum in nucleon decays [1]. The electron neutrino was firstly detected by Cowan and Reines in 1956 [2][3]. The second family neutrino ν_μ, associated with muon, and the third family neutrino ν_τ, associated with tau were detected in 1962 and 1975 respectively [4][5]. The number of neutrinos that interact with W and Z boson are lighter than Z boson is proved to be 3 via the invisible decay width of Z[1] [6]. Neutrinos were initially assumed to be massless. The neutrinos interact electroweakly are assumed to be left-handed, and no right-handed component is imposed to form mass terms. There was no experiment evidence of neutrino mass until people find the phenomena of solar neutrino oscillation and atmospheric neutrino oscillation.

Neutrino masses lead to neutrino oscillation and therefore answered the problem of

[1]We do not consider sterile neutrino(s), which do not participate in the weak interaction.

missing electron neutrinos in the solar neutrino beam: electron neutrinos oscillate into other flavours of neutrinos during the propagation from the Sun to the Earth. Atmospheric and terrestrial neutrino experiments [7]-[18] tested other neutrino oscillation channels oscillation, where three generations of neutrino have different masses and mix.

Today, there are still several unsolved/open problems of neutrino: what is the exact scale of neutrino masses? Is the neutrino mass pattern a normal hierarchy or inverted hierarchy? Is the neutrino mass Dirac or Majorana? What is the origin of the neutrino mass? Is there an explanation of why neutrino mixing is different from the quark mixing?

1.2.1 Neutrino Masses and Mixings

Neutrinos are the only neutral fermions under gauge transformations of the SM, which allows them to be identical to their antiparticles $\nu_i(h)^C = \nu_i(h)$, where h is a given helicity. In this case, we call neutrinos Majorana particles and we can write down the Majorana mass term for neutrinos [19][20],

$$\mathcal{L}_{\text{Majorana}} = m_\nu \bar{\nu}_L \nu_L^C + \text{h.c.}\,, \tag{1.1}$$

where $\nu_L^C = C\bar{\nu}_L^T$ is the charge conjugate of ν_L[2]. Notice that ν_L is not the mass eigenstate of the neutrino. We define $\nu_i \equiv \nu_L + \nu_L^C$, and it is easy to see that $\nu_i^C = \nu_i$ is the Majorana masss eigenstate.

An important feature of the neutrino Majorana mass term is it leads to lepton number violation. Due to this reason, Majorana neutrinos are preferred and widely assumed, although Dirac neutrinos are not excluded. In this case, the mass term for neutrinos is similar to that of quarks and charged leptons:

$$\mathcal{L}_{\text{Dirac}} = m_\nu \bar{\nu}_L \nu_R + \text{h.c.}\,, \tag{1.2}$$

with ν_R the RH neutrino, which is not allowed to participate the SM interaction. If neutrinos carry energy much higher than its mass, (solar and reactor neutrinos carry the

[2]The definition of charge conjugate can be found in Appendix (A)

lowest energy ∼1 MeV) the left-hand to right-hand transition in a neutrino beam cannot be observed.

A Majorana mass term for neutrinos is not allowed in the SM, because the term $\frac{1}{M}(HL)(HL)$ is non-renormalizable whereas the Dirac mass term for neutrinos is permitted if the RH neutrino is introduced. However, in either case, why neutrino masses are so small needs to be explained.

1.2.2 Neutrino Oscillation

Neutrino oscillations are the first indication that neutrinos have non-zero masses. Also neutrino oscillations are the most precise measurement of neutrino masses and mixings so far. In this section, we review the model of neutrino oscillations, showing that this model explains neutrino disappearance and appearance experiments[3].

1.2.2.a Solar Neutrino Oscillation Experiments

In the 1960s, Ray Davis and John Bahcall began the Homestake [24] experiment to measure the electron neutrino flux from the sun. The electron neutrino ν_e is produced in nuclear reaction around the core of the Sun. The energy the electron neutrinos carries is $\sim 1 - 10$ MeV. The flux of ν_e can be calculated via the Standard Solar Model. In the Homestake experiment, the electron neutrino induce the reaction $\nu_e + {}^{37}\mathrm{Cl} \rightarrow {}^{37}\mathrm{Ar} + \mathrm{e}$. One can separate ^{37}Ar in the water tank and count their number by observing their later decay. Therefore the electron neutrino flux can be measured indirectly. In the next 30 years, they found a defecit in electron neutrino number with respect to the description in the Standard Solar Model: The detected electron neutrino number in the flux is only $\sim 1/3$ of that predicted by the Standard Solar Model. This puzzle of missing electron neutrinos is called the Solar Neutrino Problem (SNP). Several types of explanation have

[3]For more details of neutrino oscillation and other neutrino experiments, we refer readers to [21] [22] and [23].

been proposed, including neutrino decay, neutrino oscillations and modification of the Standard Solar Model.

The result of Homestake was confirmed by the SNO [25], GALLEX [26], GNO [27] and Super-Kamkiokande [28], which can measure separately ν_e and $\nu_{\mu,\tau}$. It is the first solar neutrino appearance experiment, which used heavy water instead of water in the detector. The electron neutrino can break deuterons in the heavy water via charged current (CC) process $\nu_e + d \rightarrow p + p + e$. And all three flavours of neutrinos can scatter with deuterons via neutral current (NC) process $\nu_{e,\mu,\tau} + d \rightarrow \nu_{e,\mu,\tau} + p + n$. SNO finds the ν_e flux Φ_e and the total neutrino flux $\Phi_{e,\mu,\tau}$ has the relation $\Phi_e/\Phi_{e,\mu,\tau} < 1/2$. This indicates during the propagation, electron neutrino changes to muon neutrino and tau neutrino. And This can be explained by neutrino oscillation enhanced by matter effects (electron neutrinos scattering with electrons in the Sun).

In the neutrino oscillation model, the total neutrino flux is conserved. However, the active neutrino might change into sterile neutrinos, which do not participate in the electroweak interaction. The solar neutrino experiments measure the total neutrino flux and have results in agreement with the one predicted by the Standard Solar Model. So the change of active neutrinos to sterile neutrinos is negligible, and this provide the evidence of neutrino flavour changing during the propagation.

1.2.2.b Atmospheric Neutrino Oscillation Experiments

Another neutrino experiment, Super-Kamiokande [7] measured the atmospheric neutrino flux, which is produced by the collision of cosmic rays in the upper level of the Earth's atmosphere. A high energy cosmic ray (proton) hits a nuclei in the atmosphere, creating pions[4] via a QCD process (the "colour" interaction described by $SU(3)_c$, with guons as

[4]Pions are mesons with composition $u\bar{d}$ (π^+), $d\bar{d} - u\bar{u}$ (π^0) and $d\bar{u}$ (π^-).

the exchange particles), which majorly decay into muons and muon neutrinos[5]

$$\pi^- \to \mu^- + \bar{\nu}_\mu \,, \quad \pi^+ \to \mu^+ + \nu_\mu \,. \tag{1.3}$$

The subsequent decay of muons results in equal numbers of electron neutrinos and muon neutrinos (with energy $> 100\,\mathrm{MeV}$) in the flux:

$$\mu^- \to e^- \,\bar{\nu}_e \,\nu_\mu \,, \quad \mu^+ \to e^+ \,\nu_e \,\bar{\nu}_\mu \,. \tag{1.4}$$

Therefore one would derive that the total flux of ν_μ and ν_e are produced in proportion 2 : 1. Muons with energy above GeV collide with the atmosphere before decaying, resulting that at higher energy, the $\nu_\mu : \nu_e$ ratio is larger than 2.

Super-Kamiokande measured the $\nu_\mu + \bar{\nu}_\mu$ and $\nu_e + \bar{\nu}_e$ flux as a function of energy and the zenith angle. The atmospheric neutrinos scatter with nucleons in the water in the cylindrical tank of Super-Kamiokande via CC interaction $\nu_\ell + N \to \ell + N'$, where $\ell = e, \mu, \tau$ and N, N' are nucleons. The produced charged leptons ℓ yield Cerenkov rings, which can be detected by the photomultipliers surrounding the water tank of Super-Kamiokande. In the water tank, high energy leptons ($E_\ell \gg m_N$) produced by scatterings roughly keep the direction of the incoming neutrino, so that we can know the direction of neutrinos by measuring the direction of scattered leptons. The zenith angle is relevant to the neutrino propagating distance. For the down-going neutrino beam, the propagating length is about 15 km (the height of the atmosphere) whereas the up-going neutrinos fly 13,000 km (the diameter of the Earth) from the other side of the Earth. The Super-Kamiokande experiment found an asymmetry between the up-going and down-going ν_μ flux and no significant asymmetry for ν_e. The asymmetry shows the disappearance of ν_μ neutrino and indicates that there is a transition of muon neutrino flavour and the transition rate depends on the flight length of neutrinos.

[5]Here, in contrast with charged leptons and quarks, the expressions of electron neutrino, muon neutrino and tau neutrino all represent flavour eigenstates rather than mass eigenstates.

1.2.2.c Terrestrial Neutrino Oscillation Experiments

Neutrinos accelerator experiments are important in the neutrino studies (*e.g.* K2K [8], T2K [9], NOνA [10] MINOS [11]-[13] OPERA [14]), with a relatively high energy ($E \sim 1-10\,\mathrm{GeV}$) and relatively short travelling distance between the source and detector ($L \sim \mathcal{O}(100\,\mathrm{m}) - \mathcal{O}(10^3\,\mathrm{km})$). As we will discuss in the next section, the transition amplitude is measurable when $\Delta m^2 L/E \sim 1$, where Δm^2 is the square mass difference. For accelerator neutrino oscillation experiments, the mass square difference corresponds to the $\nu_\mu \leftrightarrow \nu_e$ flavour transition. Conventionally, high energy protons are used to hit the target to produce mesons. The charged mesons are focused in the magnetic horns. The decay of mesons (majorly pions and Kaons) produce the ν_μ neutrino beams. Hence most accelerator neutrino experiments are dedicated to studies of $\nu_\mu \leftrightarrow \nu_e$ and $\nu_\mu \leftrightarrow \nu_\mu$ transition. However, alternatively, in an improved method, neutrino beams are also produced by decays of μ^- or μ^+. In this case the neutrino beam in the source consists of $\nu_\mu + \bar{\nu}_e$ or $\bar{\nu}_\mu + \nu_e$, allowing the research of $\bar{\nu}_\mu \leftrightarrow \bar{\nu}_e$ transition. If the accelerator neutrino beam energy is high (*e.g.* MINOS, OPERA), we can detect the $\nu_\mu \leftrightarrow \nu_\tau$ transition.

Another important type of neutrino source of is nuclear reactors (*e.g.* CHOOZ [15]-[17] and KamLAND [18]). In fission reactions (usually in commercial power reactors), neutrons are yielded via, for example ${}^{235}_{92}\mathrm{U} + \mathrm{n} \rightarrow {}^{94}_{40}\mathrm{Zr} + {}^{140}_{58}\mathrm{Ce} + 2\mathrm{n}$. Neutrons decay to reach stable matter and generate anti-electron neutrinos $\bar{\nu}_e$. Reactor neutrinos carry low energy from beta decays ($\sim 1 - 10\,\mathrm{MeV}$). Both CHOOZ and KamLAND search for the disappearance of anti-electron neutrinos ($\bar{\nu}_e \rightarrow \bar{\nu}_e$). The neutrino travelling baselines (distance from reactor to detector) are: ~ 1 km for CHOOZ and 250 km for KamLAND. The neutrino oscillation amplitudes are sensitive to $\Delta m^2 L/E$, where Δm^2 is the mass square difference, L is the oscillation baseline and E is the energy of the neutrino beam. When $\Delta m^2 L/E \sim 1$, one can obtain the maximal corresponding transition rate.

1.2.2.d Cosmic Neutrino

Another interesting neutrino source is the Ultra High Energy Cosmic Ray (UHECR) [29] with energy $\sim 10^{20}\,\mathrm{eV}$. However, it is not clear how the UHECR neutrinos are produced and how long the oscillation length is. One possibility is that the proton is accelerated in some galactic or extra-galatic object, and the proton hits background photons via $p + \gamma_{3\mathrm{K}} \rightarrow \Delta^* \rightarrow N + \pi$. And the decay of ultra energy π produce neutrinos. The neutrinos propagate $10^{-1} - 10^4\,\mathrm{Mpc}$ from the source to the Earth, and we can detect them in AMANDA [30]-[33], AUGER [34] and the coming ICECUBE [35]-[38] experiment. Unfortunately, we are still far away from detecting the UHECR neutrino oscillation. But we hope to see some interesting phenomena at ICECUBE.

We summarize the neutrino oscillation experiments briefly in Table 1.1. Different neutrino appearance/disappearance detection indicate neutrinos change their flavours during their propagating, and the transition rates depend on the energy of the neutrino and the length of the baseline (the distance from the neutrino source to the detector). A coherent model is needed to explain all these phenomena.

Experiment	Source neutrino	Neutrino detected	Energy	Oscillation length
Solar	ν_e	$\nu_{e,\mu,\tau}$	$< 50\,\mathrm{MeV}$	$< 7 \times 10^8\,\mathrm{m}$
Atmospheric	$\nu_e\,,\bar{\nu}_e\,,\nu_\mu\,,\bar{\nu}_\mu$	$\nu_{e,\mu,\tau}\,,\bar{\nu}_{e,\mu,\tau}$	$\sim 1\,\mathrm{GeV}$	$15 - 13,000\,\mathrm{km}$
Accelerator	$\nu_e\,,\bar{\nu}_e\,,\nu_\mu\,,\bar{\nu}_\mu$	$\nu_{e,\mu,\tau}\,,\bar{\nu}_{e,\mu,\tau}$	$\sim 1 - 10\,\mathrm{GeV}$	$\sim 100\,\mathrm{m} - 1000\,\mathrm{km}$
Reactor	$\bar{\nu}_e$	$\bar{\nu}_{e,\mu,\tau}$	$\sim 1\,\mathrm{MeV}$	$\sim 100\,\mathrm{m} - 100\,\mathrm{km}$
UHECR	$\nu_e\,,\bar{\nu}_e\,,\nu_\mu\,,\bar{\nu}_\mu$	$\nu_{e,\mu,\tau}\,,\bar{\nu}_{e,\mu,\tau}$	$\sim 10^{12-22}\,\mathrm{eV}$	$> 1\,\mathrm{Mpc}$

Table 1.1: A brief summary of neutrino oscillation experiments. Notice for solar neutrino, the oscillation happens in the outer layer of the Sun.

1.2.2.e The Oscillation Model

The neutrino oscillation is an analogy of the $K^0 - \bar{K}^0$ oscillation [39]. K^0 and $\bar{K}^0$ are mesons with quark composition $d\bar{s}$ and $s\bar{d}$. They have an identical mass due to the conservation of CPT (the combination of parity, charge conjugation and time reversal). Leading order diagrams (box diagrams) of the weak interaction generate off-diagonal elements in their mass matrix, resulting in a mixing of K^0 and $\bar{K}^0$. Therefore the mass eigenstates of the Kaon is a combination of K^0 and $\bar{K}^0$ ($K_1 = \frac{1}{\sqrt{2}}(K^0 + \bar{K}^0)$ and $K_2 = \frac{1}{\sqrt{2}}(K^0 - \bar{K}^0)$), which can be seen by diagonalising the $K^0, \bar{K}^0$ mass matrix. As the K^0 or $\bar{K}^0$ propagates, K^0 can convert to $\bar{K}^0$ and vice versa.

In the SM, left-handed neutrinos only feel the weak force. Therefore neutrinos are always generated (and detected) via weak interactions. The Lagrangian of the charged current and W gauge boson is written as

$$\mathcal{L}_W = -\frac{g}{\sqrt{2}} \sum_{\alpha} \left(\overline{\ell}_{L\alpha} \gamma^{\lambda} \nu_{L\alpha} W^{-}_{\lambda} + \text{h.c.} \right) , \tag{1.5}$$

where $\alpha = e, \mu, \tau$ are the index for the charged lepton mass eigenstates, and neutrinos are written in their flavour eigenstates ν_α, associated with each corresponding charged lepton. Therefore, neutrinos generated via weak interaction *e.g.* charged lepton decay or leptonic nuclear process, are in their flavour eigenstates. If neutrinos are massless (or have identical masses), one can not distinguish different mass eigenstates. Provided different masses for three generation neutrinos are introduced, the flavour eigenstates of neutrinos are in principle certain superpositions of mass eigenstates,

$$\nu_\alpha = \sum_i U^*_{\alpha i} \, \nu_i \, . \tag{1.6}$$

Or we can invert Eq.(1.6), writing neutrino mass eigenstates as a combination of flavour eigenstates

$$\nu_i = \sum_\alpha U_{i\alpha} \, \nu_\alpha \, . \tag{1.7}$$

The neutrino mixing matrix $U_{i\alpha}$ is called the PMNS (Pontecorvo Maki Nakagawa Sakata)

[141] matrix and it is required to be unitary[6].

Conventionally the PMNS matrix is parametrised in three rotation angles, similar to CKM (Cabibbo-Kobayashi-Maskawa) matrix [41], and potential Majorana phases

$$V^{\nu\,\dagger} = P\, R_{23} U_{13} R_{12} P_{12}\,, \tag{1.8}$$

where

$$\begin{aligned}
P &= \begin{pmatrix} e^{i\omega_1} & 0 & 0 \\ 0 & e^{i\omega_2} & 0 \\ 0 & 0 & e^{i\omega_3} \end{pmatrix}, \qquad & R_{23} &= \begin{pmatrix} 1 & 0 & 0 \\ 0 & c^\nu_{23} & s^\nu_{23} \\ 0 & -s^\nu_{23} & c^\nu_{23} \end{pmatrix}, \\
U_{13} &= \begin{pmatrix} c^\nu_{13} & 0 & s^\nu_{13}\, e^{-i\delta^\nu} \\ 0 & 1 & 0 \\ -s^\nu_{13}\, e^{i\delta^\nu} & 0 & c^\nu_{13} \end{pmatrix}, \qquad & R_{12} &= \begin{pmatrix} c^\nu_{12} & s^\nu_{12} & 0 \\ -s^\nu_{12} & c^\nu_{12} & 0 \\ 0 & 0 & 1 \end{pmatrix}, \\
P_{12} &= \begin{pmatrix} e^{i\beta_1} & 0 & 0 \\ 0 & e^{i\beta_2} & 0 \\ 0 & 0 & 1 \end{pmatrix},
\end{aligned} \tag{1.9}$$

and $s^\nu_{ij} = \sin\theta^\nu_{ij}$, $c^\nu_{ij} = \cos\theta^\nu_{ij}$. The phase matrix P in the right hand side of Eq. (1.8) may always be removed by an additional charged lepton phase rotation. The PMNS neutrino mixing matrix $U_{\rm PMNS}$ [141] is a product of unitary matrices V^E and $V^{\nu\,\dagger}$, where V^E is associated with the diagonalisation of the charged lepton mass matrix. Since the charged lepton mixing angles are expected to be small $U_{\rm PMNS} \approx V^{\nu\,\dagger}$ in the first approximation.

One comment about the quark mixing: the quark generated in the electroweak interaction is also a superposition of three mass eigenstates. However, quark oscillations are not observed, since the superposition state loses its coherence in a extremely short time/distance after the quark is produced, due to the heavy masses of quarks.[42]. In contrast, the neutrino decoherence distance is a much larger scale because the masses of neutrinos are 10 orders of magnitude smaller than quarks.

[6]Taking into account of the seesaw model, which will be discussed in Section (1.2.5), this matrix is quasi-unitary, as a result of left-handed right-handed neutrino mixing. However, the violation of unitarity is strongly suppressed by the RH neutrino mass.

The propagation of each neutrino mass eigenstate in vacuum can be described by the equation for energy eigenstates:

$$i\,\frac{\partial}{\partial t}\,|\nu_i\rangle = E_i\,|\nu_i\rangle\,, \tag{1.10}$$

a free particle solution of which is

$$|\nu_i(t)\rangle = e^{-iE_it}\,|\nu_i(0)\rangle\,, \tag{1.11}$$

where $|\nu_i(0)\rangle$ is the initial state of the neutrino. Due to the smallness of neutrino mass, we have an approximation in the ultra-relativistic limit of $E \simeq p \gg m$,

$$E_i = \sqrt{p_i^2 + m_i^2} \simeq p_i + \frac{m_i^2}{2\,p_i}\,. \tag{1.12}$$

We can assume that $p_i = p \simeq E = E_i$, due to the fact that different mass eigenstates are produced coherently[7]. Since the generation and detection of neutrinos are always associated with a charged lepton signal, (*e.g.* a scintillation detector observes neutrino by the process $\nu_e + p \to n + e^-$) we are interested in the transition probabilities of flavour eigenstates associated with charged lepton mass eigenstates. Inserting Eq. (1.12) into Eq. (1.11), the neutrino mass eigenstate after propagating over distance L (also called length of baseline) becomes

$$|\nu_i(t)\rangle = e^{-iEt}e^{-im_i^2L/2E}|\nu_i(0)\rangle\,. \tag{1.13}$$

We notice that the factor $e^{-iE(t-L)}$ is a common factor for all mass eigenstates. Using the mixing relation Eq.(1.6), the amplitude of finding neutrino flavour β in a coherent flavour α neutrino beam is

$$\mathrm{Amp}(\nu_\alpha \to \nu_\beta) = \langle\nu_\beta|\nu_\alpha(t)\rangle = e^{-iEt}\sum_i U^*_{\alpha i}e^{-im_i^2L/2E}U_{\beta i}\,. \tag{1.14}$$

The transition probability of α to β is the modulus squared of amplitude

$$\begin{aligned}
\mathrm{P}(\nu_\alpha \to \nu_\beta) &= |\mathrm{Amp}\,(\nu_\alpha \to \nu_\beta)|^2 \\
&= \delta_{\alpha\beta} - 4\sum_{i>j}\mathrm{Re}(U^*_{\alpha i}U_{\beta i}U_{\alpha j}U^*_{\beta j})\sin^2(\Delta m^2_{ij}L/4E) \\
&\quad + 2\sum_{i>j}\mathrm{Im}(U^*_{\alpha i}U_{\beta i}U_{\alpha j}U^*_{\beta j})\sin^2(\Delta m^2_{ij}L/4E)\,,
\end{aligned} \tag{1.15}$$

[7]At the time of writting, the 'same energy, same momentum' assumption is re-investigated in [43].

where $\Delta m^2_{ij} \equiv m^2_i - m^2_j$ is the mass square difference of two neutrinos. We can notice that violation of unitarity would lead to non-conservation of total neutrino particle number in the neutrino flux.

We also notice that one can not detect the mass hierarchies (the sign of Δm^2_{ij}) of neutrino by measuring the oscillation possibilities in vacuum. However the transition probability in Eq.(1.15) describe the neutrino oscillation in vacuum. Taking into account matter effects [44], when neutrinos propagate in matter, only the electron flavour neutrino scatters with the electrons in matter (in the Sun or the Earth) via the charged current process, and all the three flavours interact with electrons and neutron/protons via neutral current. The charged current process gives an extra potential term for the electon neutrino. Then the oscillation can be enhanced or suppressed by this extra term. Especially when solar neutrinos propagate in the outer side of the sun, the matter effect of electrons in the sun changes the transition rate of neutrinos drastically. This effect is called the MSW [45] effect, which shows that $\delta m^2_{12} < 0$. The terrestrial neutrino experiments hope to clarify the hierarchy of the neutrino via matter effect.

The parameters of neutrino oscillations are now well measured. Global fitting results in [46] However, the separate masses for three neutrinos are still unknown. At least one

Parameter	Best fit	2σ	3σ
Δm^2_{21} $[10^{-5}\mathrm{eV}^2]$	7.6	7.3–8.1	7.1–8.3
$\lvert\Delta m^2_{23}\rvert$ $[10^{-3}\mathrm{eV}^2]$	2.4	2.1–2.7	2.0–2.8
$\sin^2\theta_{12}$	0.32	0.28–0.37	0.26–0.40
$\sin^2\theta_{23}$	0.50	0.38–0.63	0.34–0.67
$\sin^2\theta_{13}$	0.007	≤ 0.033	≤ 0.050

Table 1.2: Best-fit, 2σ and 3σ data for the three flavour neutrino oscillation parameters from global data.

extra independent mass measurement is required to determine the masses of neutrinos.

In the scenario of strong hierarchical neutrino masses, the second and third neutrino mass can be expresses approximately by

$$m_2 = \sqrt{m_1^2 + \Delta m_{21}^2}\,, \quad m_3 = \sqrt{m_1^2 + \Delta m_{31}^2}\,, \tag{1.16}$$

for normal hierarchy, and

$$m_1 \approx m_2 = \sqrt{\Delta m_{23}^2}\,, \tag{1.17}$$

for inverted hierarchy. However, in order to know the exact neutrino mass pattern, we need measure the absolute scale of neutrino mass.

1.2.3 Absolute Scale on Neutrino Masses

Neutrino oscillations only measure two mass squared differences. The absolute scales of neutrino masses are not given by measuring the transition probabilities. We do not know the hierarchy of neutrinos, whether the third generation is lighter (inverted hierarchy) or heavier (normal hierarchy) than the first and second generation of neutrino. These two possible patterns are illustrated in Fig. 1.1. To know the absolute scale of neutrino mass, one looks into the non-oscillation experiments.

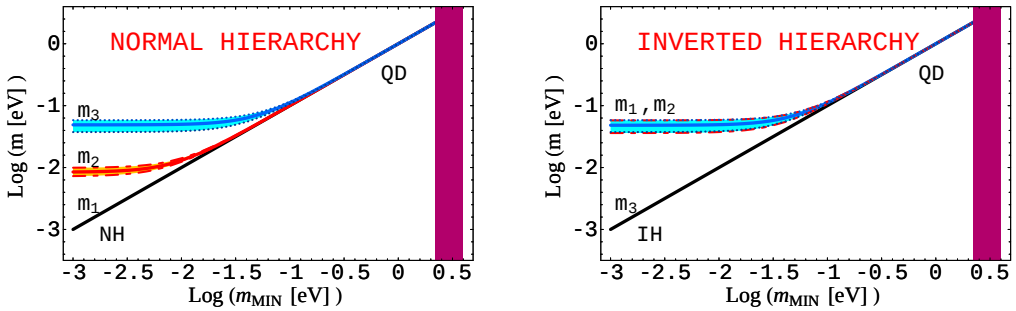

Figure 1.1: Neutrino masses versus the lightest neutrino mass for normal hierarchy and inverted hierarchy. Figure is taken from [56].

Neutrino masses can be measured via cosmological methods. The small perturbations in the early universe, which possibly come from the quantum fluctuation evolve to the large scale structure (LSS) of the present universe. After thermal decoupling, the

neutrino becomes a free-streaming particle with a certain wavelength and wave-number, which are functions of the neutrino mass. The masses of neutrinos change the temperature anisotropy spectrum and matter power spectrum of the Cosmology Microwave Background (CMB) Radiation. With Wilkinson Microwave Anisotropy Probe (WMAP) CMB data together with Galaxy redshift surveys and Lyman-α forest data [47] [48], one can arrive at the upper bounds of the neutrino abundance and the summation of neutrino mass [49]

$$\sum_i m_i < 0.61 \text{ eV} \quad (95\%\text{CL}) \,. \tag{1.18}$$

From this upper limit, one still can not tell the hierarchy of neutrino masses. However, future experiments including PLANCK lensing and CMBpol lensing will provide a sensitivity of 0.05 eV, sufficient to distinguish the pattern of neutrino masses.

Terrestrial neutrino mass experiments include the Tritium β decay experiment, *e.g.* Mainz neutrino experiment [50] and KATRIN [51], which measure the energy spectrum of $^3\text{H} \rightarrow {}^3\text{He}+\text{e}^- + \overline{\nu}_e$. The maximal energy of the electron is $Q - m_\nu$, where $Q = m_{^3\text{H}} - m_{^3\text{He}}$. Around the end-point the electron energy spectrum depends on the neutrino phase space $E_\nu \, p_\nu$. Assuming there is one generation of neutrino with mass m_{ν_e}, the electron energy spectrum can be expressed as

$$\frac{\mathrm{d}N_e}{\mathrm{d}E_e} = F(E_e)(Q - E_e)\sqrt{(Q - E_e)^2 - m_{\nu_e}^2} \,, \tag{1.19}$$

where $F(E_e)$ can be considered as a constant. When three generations of light neutrinos are taken into account, the electron neutrino is combination of three neutrino mass eigentates, with masses m_i, $i = 1, 2, 3$. And therefore the spectrum has the form

$$\frac{\mathrm{d}N_e}{\mathrm{d}E_e} = \sum_i |U_{ei}|^2 F(E_e)(Q - E_e)\sqrt{(Q - E_e)^2 - m_{\nu_i}^2} \,. \tag{1.20}$$

Comparing Eq.(1.19) and Eq.(1.20), we can see that the tritium β decay experiment is sensitive to the single effective parameter [52]

$$m_{\nu_e} = \sqrt{\sum_{i=1}^{3} |U_{ei}|^2 m_i^2} \,. \tag{1.21}$$

The recent tritium β decay experiments have sensitivity of ~ 2 eV, which is not small enough to distinguish the hierarchical and inverted hierarchical pattern.

Another important experiment is the neutrinoless double beta decay experiment. Most promisingly, if there are left-handed (light) neutrino Majorana mass terms, neutrinoless double beta decay ($0\nu\beta\beta$) [53] of a nucleus is allowed[8]. The neutrinoless double beta decay ($(Z, A) \rightarrow (Z + 2, A) + 2e^-$) is a rare nuclear process (Fig. 1.2). The rate of neutrinoless double beta decay depends on the nuclear matrix element [54] [55], which can be calculated separately and the effective Majorana neutrino mass

$$|\langle m_{ee}\rangle| = \left|\sum_{i=1}^{3} U_{ei}^2 m_i\right| . \tag{1.22}$$

One should notice that if the light neutrino mass is Dirac, the neutrinoless double beta decay would not happen. Hence this experiment is critical to test if the neutrino masses are Majorana.

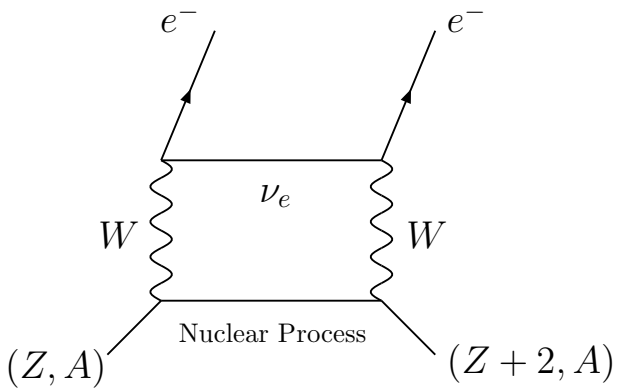

Figure 1.2: Feynman Diagram for neutrinoless double beta decay.

Since we know the element U_{e3} of neutrino mixing matrix $U_{\alpha i}$ is small, but U_{e2} and U_{e1} are relatively large, the hierarchy of neutrino masses is crucial for the width of neutrinoless double beta decay. According to Eq. (1.22), in order to have a relatively large value of m_{ee}, neutrino masses must have an inverted hierarchy, where the third family of neutrino

[8]In supersymmetric models, neutralinos being Majorana particles also contribute to $0\nu\beta\beta$ in the case of R parity violation.

is the lightest one. On the other hand, if $\langle m_{ee} \rangle < 0.01$ eV is measured, the inverted mass hierarchy would be ruled out, as inverted hierarchy leads to $|\langle m_{ee} \rangle| \sim \Delta m_{13} \sim \Delta m_{\rm atm}$.

1.2.4 The Neutrino Mass and Mixing Pattern

The quark mixing (CKM matrix) and neutrino mixing (PMNS matrix) are quite different. The mixing angles in the CKM matrix are relatively small, whereas two of the three mixing angles in the PMNS matrix are measured to be large, leaving the third one θ_{13} small. Notice that the possibility of a zero mixing θ_{13} is not ruled out experimentally. The values of mixing angles can be found in Table 1.2.

One finds an interesting approximation $\sin\theta_{12} \simeq \sqrt{1/3}$, $\sin\theta_{23} \simeq \sqrt{1/2}$ and $\sin\theta_{13} \simeq 0$, and therefore we can write the PMNS matrix in an approximate scheme [57]

$$U_{tri-bi} = \begin{pmatrix} \sqrt{\frac{2}{3}} & \sqrt{\frac{1}{3}} & 0 \\ -\sqrt{\frac{1}{6}} & \sqrt{\frac{1}{3}} & \sqrt{\frac{1}{2}} \\ \sqrt{\frac{1}{6}} & -\sqrt{\frac{1}{3}} & \sqrt{\frac{1}{2}} \end{pmatrix} . \tag{1.23}$$

The reason for large mixing of neutrinos is unknown. One interesting approach is to introduce certain flavour symmetries with the seesaw model, which gives natural small Majorana masses to neutrinos.

1.2.5 The Seesaw Model

The fact that the heaviest neutrino is six orders of magnitude lighter than the lightest charged fermion, the electron, requires an explanation. However the answer might be the physics at a scale higher than the scale of the SM. From the point of view of an effective theory, light neutrino masses can be obtained via a dimension 5 operator, after integrating out heavy particles or extra dimensions.

The canonical seesaw model includes RH neutrinos (at least 2 generations in order to

obtain correct masses and mixing patterns for light neutrinos[9], but naturally assumed to be of 3 generations), which are not observed yet. The RH neutrino can be introduced in Grand Unification Models, and they have to be neutral in the SM gauge, otherwise it would lead to unwanted signal in colliders. They couple to left-handed lepton doublets via Yukawa couplings and have Majorana mass M_R much larger than the electroweak scale. The Lagrangian for a RH neutrino Yukawa interaction reads

$$\mathcal{L}_{mass} = h\bar{N}\ell_L H - \frac{1}{2}M_R N_R N_R^C + \text{h.c.}\,, \tag{1.24}$$

where h is the Yukawa coupling and H is the Higgs field doublet in the SM. After the electroweak symmetry breaking, the neutral component of Higgs field develops a vacuum expectation value (vev) v, and therefore yields Dirac mass terms $hv\nu N$, to neutrinos. Here we ignore the flavour index and write the mass term of ν and N in a form of matrix, where $N \simeq N_R + N_R^C$,

$$\mathcal{L}_{mass} = \frac{1}{2}\begin{pmatrix}\nu & N\end{pmatrix}\begin{pmatrix}0 & hv\\ hv & M_R\end{pmatrix}\begin{pmatrix}\nu\\ N\end{pmatrix}, \tag{1.25}$$

The light neutrino mass appears in the 1-1 entry of the mass matrix after diagonalising

$$m_\nu = \frac{1}{2}\left(M_R - \sqrt{M_R^2 + 4(hv)^2}\right). \tag{1.26}$$

In the limit of $M_R \gg v$, the light neutrino mass is written as

$$m_\nu = -\frac{(hv)^2}{M_R}\,. \tag{1.27}$$

We see that the light neutrino mass is inversely proportional to the RH neutrino Majorana mass. If one sets Yukawa couplings to be of order 1, a RH neutrino mass $\mathcal{O}(10^{15})\,\text{GeV}$ leads to a light neutrino mass $m_\nu \sim \sqrt{\delta m^2_{atm}} \sim 0.05\,\text{eV}$, the lower bound on the heaviest left-handed neutrino mass.

Another limit is where the RH neutrino Majorana masses vanish $M_R = 0$, which means the masses we detect in neutrino oscillation are Dirac-type. In this scenario, light

[9]For the case of only one generation of RH neutrino, 3 light neutrino masses and 3 mixing angles can be expressed by the 4 parameters – the RH neutrino mass and 3 Yukawa couplings. One finds that it cannot match the oscillation data.

neutrino masses still can be explained by several mechanisms, *e.g.* higher dimensional theories [58].

In the Dirac neutrino seesaw model [59], the bare Yukawa couplings are forbidden between LH neutrinos and RH neutrinos, and the LH neutrinos and RH neutrinos both couple to a vector-like lepton, which is assumed to be heavy. Integrating out the heavy field gives a strong suppression on the effective Yukawa coupling.

In extra dimensional models [60], the RH neutrinos live in the 5-dimensional bulk, and SM particles live in a (3+1)-dimensional hyperplane. Integrating out the extra dimensions, the effective 4-dimension Yukawa couplings are suppressed by a factor M^*/M_{pl}. And therefore a small Dirac neutrino mass is obtained.

Nevertheless, a Majorana neutrino is more interesting, as it leads to several lepton number violating processes *e.g.* neutrinoless double beta decay .

1.3 Baryogenesis and Leptogenesis

Light neutrino Majorana masses would lead to low energy lepton number violating phenomenology, including neutrinoless double beta decay [53], whereas heavy RH neutrino masses would have consequences at high energy, including lepton number violating processes in LHC [61] and lepton number violating decays of RH neutrinos, which plays a crucial role for Leptogenesis. For a review of Leptogenesis, we refer readers to [62] and three Ph.D. theses [63][64][65].

In this section, we introduce three major mechanisms to generating net baryon number in the present universe: Leptogenesis, Affleck-Dine Leptogenesis and electroweak Baryogenesis. We discuss major obstacles of each mechanism and possible ways to solve them.

1.3.1 Measuring the Baryon Asymmetry of Universe

How can we know that the universe is made of matter rather than anti-matter or a mixture of matter and anti-matter? Firstly, we can verify the earth is clearly matter. Secondly, the sun radiates electrons rather than positrons from nuclear reactions, and therefore we know the sun is made of matter too. Based on the fact that no electron-positron annihilation is observed when the solar electron flux reaches other planets, we can make sure the solar system is majorly made of matter. In fact, cosmic observation has verified that the universe is made of matter at least at scale of 50-60 Mpc [66]. Hence, there is no need to doubt the matter universe.

There are two independent methods to measure the net baryon abundance $\eta_B \equiv n_B/n_\gamma$ of the universe, where n_B and n_γ are the number density of baryon and photon respectively. One is to measure the ratios of light elements produced by Big Bang Nucleosynthesis. Another is to measure the spectrum of the Cosmic Microwave Background radiation.

1.3.1.a Big Bang Nucleosynthesis

According to the big bang theory of the universe, light elements (D, ^{3}He, ^{4}He, ^{7}Li ...) are produced when the universe cools to the binding energy of the nuclei $T \sim 1$ MeV. Their density evolution can be described by Boltzmann Equations

$$\frac{\mathrm{d}\, n_i}{\mathrm{d}\, t} \;=\; -3H\, n_i \;+\; \Gamma_i\,, \tag{1.28}$$

where n_i are the densities of light elements $i = \mathrm{n}, \mathrm{p}, \mathrm{D} \cdots$, H is the Hubble expansion rate and Γ_i is the reaction rate relevant to each element. The nucleosynthesis interaction network[10] includes the processes generating primordial elements and intermediate elements. Reaction rates are proportional to the number densities of initial state particles, which could be light elements and photons. Therefore the ratios of light elements are sensitive to the baryon number density and the photon density. In [67] [68], the ratio of ^{4}He to

[10] A full set of interactions can be found in Appendix (D)

baryon Y_p, the ratio of D to H Y_D, the mass fraction of ^{3}He y_3 and mass fraction $y_{\rm Li}$ are given by a fit around $\eta_B \simeq 6 \times 10^{-10}$

$$
\begin{aligned}
Y_p &\simeq 0.2485 \pm 0.0006 + 0.0016(\eta_{10} - 6)\,, && (1.29)\\
y_D &= 2.64(1 \pm 0.03) \left(\frac{6}{\eta_{10}}\right)^{1.6}\,, && (1.30)\\
y_3 &\simeq 3.1(1 \pm 0.01)\, \eta_{10}^{-0.6}\,, && (1.31)\\
y_{\rm Li} &\simeq \frac{\eta_{10}^2}{8.5}\,, && (1.32)
\end{aligned}
$$

where $\eta_{10} = 10^{10}\eta_B$ is the rescaled baryon to photon ratio. Fig. 1.3 shows the primordial abundance and mass fractions of several light elements as a function of η_{10}. The red-shaded band indicates a concordant value of baryon number

$$\eta_B = 5.7 \pm 0.4 \times 10^{-10}\,. \tag{1.33}$$

1.3.1.b Cosmic Microwave Background

The most accurate measurement of baryon asymmetry n_b/n_γ so far is provided by the Wilkinson Microwave Anisotropy Probe (WMAP), which detects tiny fluctuations in the cosmic microwave background (CMB) radiation. The CMB photon comes from decoupling from scattering with matter. When the temperature drops to ~ 0.25 eV, the major thermal scattering for photons is Thomson scattering

$$\gamma + e^- \leftrightarrow e^- + \gamma\,, \tag{1.34}$$

with a reaction rate $\Gamma_{\rm Th} = n_e \sigma_{\rm Th}$. n_e is the electron number density and $\sigma_{\rm Th}$ is the Thomson scattering cross section

$$\sigma_{\rm Th} = 1.71 \times 10^3\,{\rm GeV}^{-2}\,. \tag{1.35}$$

When the Hubble parameter[11] drops to $H \sim \Gamma_{\rm Th}$, the scattering of photons deviates from equilibrium and the photon becomes a free streaming particle. This is called the

[11] The definition and the expression of the Hubble parameter can be found in Appendix (E.1).

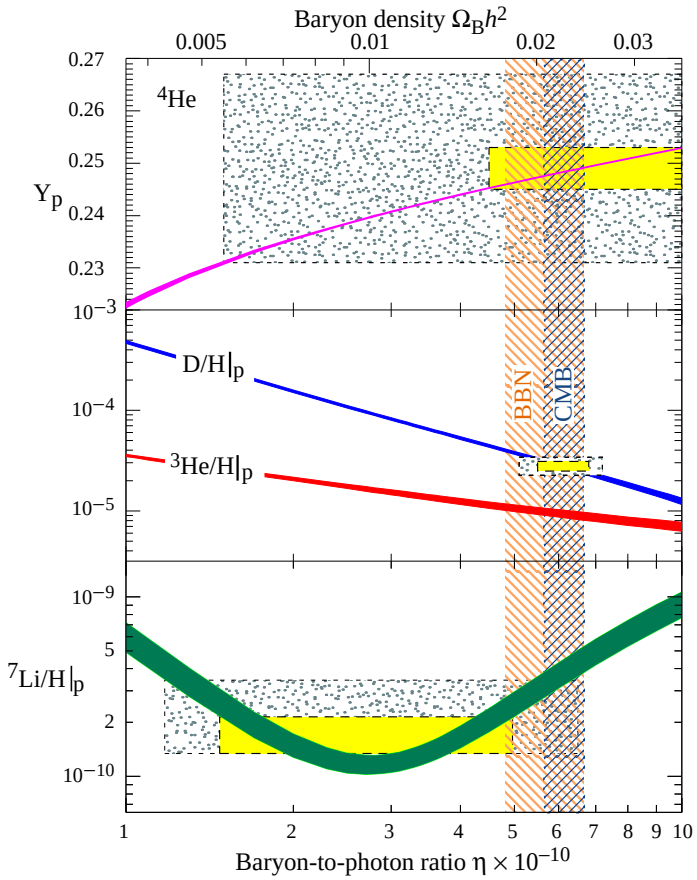

Figure 1.3: The number densities of BBN products, as a function of baryon-photon ratio. Figure is taken from [69]

last scattering and photon decoupling. One finds that photon decoupling happens at $T \simeq 0.26\,\mathrm{eV}$, corresponding the present CMB temperature $T_{\mathrm{CMB}} = 2.73\,K$. One finds the distribution of the temperature field is not homogeneous. Tiny angular distributions of CMB anisotropies, which is assumed come from the quantum fluctuation during inflation (exponential expansion of the Universe driven by the negative pressure of vacuum energy, which happened before Nucleosynthesis), are observed by COBE [70]-[72] and WMAP [49]. The distribution is described by

$$\frac{\Delta T(\theta,\phi)}{T_{\mathrm{mean}}} = \frac{T(\theta,\phi) - T_{\mathrm{mean}}}{T_{\mathrm{mean}}}\,, \tag{1.36}$$

and it can be expressed in spherical harmonics

$$\frac{\Delta T(\theta,\phi)}{T_{\rm mean}} = \sum_{\ell=1}^{\infty}\sum_{m=-\ell}^{\ell} a_{\ell m} Y_m^{\ell}(\theta,\phi)\,. \tag{1.37}$$

Here $a_{\ell m}$ are the coefficents for spherical harmonics functions $Y_m^{\ell}(\theta\,,\phi)$. The spectrum is sensitive to some cosmological parameters, including decoupling time $t_{\rm d}$ (the time when the Universe cools down to the moment the photons decoupled from electrons), matter density $\Omega_{\rm m}h^2$, baryonic matter density $\Omega_{\rm b}h^2$ and energy density Ωh^2 ($\Omega \equiv \rho/\rho_c$, where $\rho_{\rm c} = 3H^2/8\pi G_N$.). Fig. 1.4 shows how the spectrum varies with different values of $\Omega_{\rm b}h^2$. The matter content in the Universe plays a role in the evolution of anisotropies of the CMB spectrum. One uses Boltzmann Equations and Euler fuild equations to describe the temperature perturbation, and find that this can determine the matter content of the Universe. For the details of how $\Omega_{\rm b}$ effects the spectrum, we refer the reader to [73] and [74]. How the variation of matter density changes the temperature angular spectrum is illustrated in Fig. 1.4. One finds the baryon asymmetry [49]

$$\eta_B = 6.225 \pm 0.17 \times 10^{-10}\,. \tag{1.38}$$

1.3.1.c Sakharov's three conditions

In 1960's, Sakharov proposed three conditions that are critical to explain the baryon asymmetry of the universe [76].

(i) There must be a process violating baryon number.

(ii) There must be a process violating C and CP.

(iii) The process must be out-of-thermal equilibrium.

The first condition ensures that a net baryon number can be generated. The second condition ensures that the process generating baryon number and the process generating anti-baryon number have different rates, and therefore a net baryon number can be

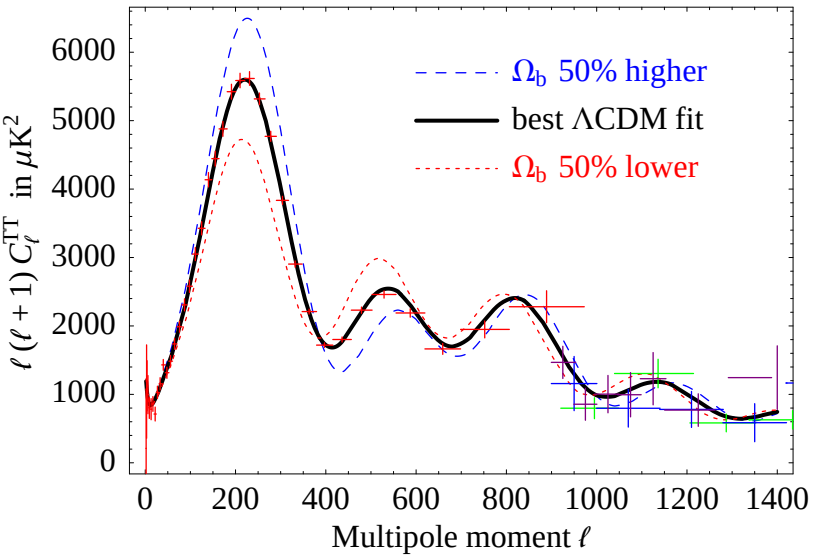

Figure 1.4: Temperature angular spectrum with different $\Omega_{\rm b}$ varying near its central value. Figure is taken from [75]

maintained. The third condition means the process can not be inverted. So the generated baryon number would not be totally erased by the time reversed processes.

1.3.2 Sphaleron Process

One of the successes of the SM is a natural explanation of baryon and lepton number conservation law. However, baryon and lepton number violation exists via quantum tunnelling between topologically different vacua (the *instanton process*) [77][78]. At low temperature, the transition is strongly suppressed by a factor

$$e^{-(4\pi/\alpha_W)} \sim 10^{-160}\,, \tag{1.39}$$

where $\alpha_W \simeq 1/29$ in the electroweak theory.

The classical baryon current and lepton current

$$j^\mu_B = \frac{1}{N_c}\sum_{i,a}\bar{q}^a_i\gamma^\mu q^a_i\,, \quad j^\mu_L = \sum_i \bar{\ell}_i\gamma^\mu\ell_i\,, \tag{1.40}$$

where i and a are the flavour index and colour index respectively, are conserved due to the B and L symmetry naturally induced by the Standard Model. However at high temperatures, a nonperturbative topological transition becomes active. One can find that both baryon number and lepton number are violated by the triangle anomaly

$$\partial_\mu j_B^\mu = \frac{3}{8\pi^2}\,\mathrm{Tr}(F_{\mu\nu}\widetilde{F}^{\mu\nu})\,, \tag{1.41}$$

where $F_{\mu\nu} = \partial_\mu A_\nu - \partial_\nu A_\mu + [A_\mu, A_\nu]$ is the $SU(2)$ gauge field strength. Similarly we find the lepton current j_L^μ satisfies

$$\partial_\mu j_L^\mu = \frac{3}{8\pi^2}\,\mathrm{Tr}(F_{\mu\nu}\widetilde{F}^{\mu\nu})\,. \tag{1.42}$$

One can see the current $j_B^\mu - j_L^\mu$ is conserved from Eq.(1.41) and Eq.(1.42)

$$\partial_\mu(j_B^\mu - j_L^\mu) = 0\,. \tag{1.43}$$

And $j_B^\mu + j_L^\mu$ is violated:

$$\int \mathrm{d}^4x \partial^\mu(j_B^\mu + j_L^\mu) = \int \mathrm{d}^4x \frac{3}{4\pi^2}\,\mathrm{Tr}(F_{\mu\nu}\widetilde{F}^{\mu\nu})\,. \tag{1.44}$$

The RHS of Eq.(1.44) is the divergence of the topological current. We define

$$\mathrm{Tr}(F_{\mu\nu}\widetilde{F}^{\mu\nu}) = \partial_\mu K^\mu\,, \tag{1.45}$$

which could be non-zero. One introduces the *Chern-Simons* number when we integrate K^0 over space

$$n_{CS} \equiv \frac{1}{16\pi^2}\int d^3x K^0\,. \tag{1.46}$$

Different vacua configurations have different *Chern-Simons* numbers $n_{CS} = 0,\ \pm1,\ \pm2\ \cdots$ but the same energy. And a change in the *Chern-Simons* number $\delta n_{CS} = 1$ would lead to an effective 12-fermion interaction

$$\mathbf{O}_{B+L} = \prod_{i=1,2,3}(q_{L_i}q_{L_i}q_{L_i}\ell_{L_i})\,, \tag{1.47}$$

This allows the $\Delta B = \Delta L = \pm 3$ process, like

$$u^c + d^c + c^c \leftrightarrow d + 2s + 2b + t + \nu_e + \nu_\mu + \nu_\tau \,, \tag{1.48}$$

where all the components are left-handed. Notice that this process conserves color and hyper/electric charge. This means both B and L number can be generated via the sphaleron process. And if leptons (baryons) are generated by some mechanism, the electroweak sphaleron process can convert them into left anti-baryons (anti-leptons). However, the electroweak sphaleron process always keep $B + L$ number vanishing in the hot plasma, so the number of leptons (baryons) and anti-baryons (anti-leptons) will be balanced, and only a part of leptons will be transited into baryons. It is clear that in order to generated a positive baryon number in the Universe via sphaleron process, we need to have a negative lepton asymmetry.

Electroweak sphaleron process is exponetially suppressed at zero temperature, but at temperature $T \sim E_{sph}$, where E_{sph} is of order of the electroweak scale, one finds that the tunnelling probability $P \propto e^{-\frac{E_{sph}}{T}}$. And when the temperature $T \gg E_{sph}$, the rate of the process is proportional to T^4. So it is clear that when the temperature approaches the electroweak scale, the transition between different vacua can be substantial, leading to the violation of B, L and $B + L$ numbers. We can compare Γ_{sph} with the Hubble parameter at temperature T (When $\Gamma_{sph} > H(T)$, electroweak sphaleron process is in thermal equilibrium), and find that the electroweak sphaleron process can be substantial when [79]

$$100\,\mathrm{GeV} < T < 10^{12}\,\mathrm{GeV}\,. \tag{1.49}$$

The sphaleron process has two important consequences for Baryogenesis: *(a)* It generates baryon number (Electroweak Baryogenesis) *(b)* It converts lepton number into baryon number (Leptogenesis and Affleck-Dine mechanism).

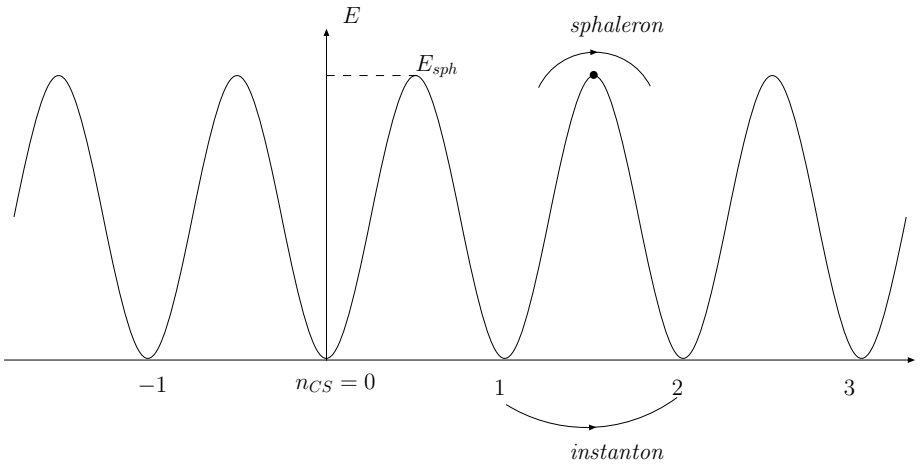

Figure 1.5: The transition between different vacua

1.3.2.a The rate of B-L Transition

At high temperature, the sphaleron processes have reaction densities much larger than the Hubble expansion rate, which makes the relevant particles in equilibrium. In addition, Yukawa interactions of leptons and quarks are also in thermal equilibrium at certain temperatures. In this thesis, we will be working in the range of temperature where all Yukawa interactions of leptons/quarks (also exotic particles in Beyond Standard Model) are in equilibrium. The ratios of particle densities n_X of species X, can be calculated via chemical potentials μ_X via the equilibrium conditions of sphaleron processes and Yukawa interactions.

At high temperature $T \ll m$, the chemical potentials are related to number densities of particles differently for bosons and fermions:

$$\begin{aligned} n_X - n_{\bar{X}} &= \frac{g_X T^3}{6} \cdot \mu_X/T + \mathcal{O}\left(\frac{\mu^3}{T^3}\right) \quad \text{for fermions} \\ n_X - n_{\bar{X}} &= \frac{g_X T^3}{6} \cdot 2\mu_X/T + \mathcal{O}\left(\frac{\mu^3}{T^3}\right) \quad \text{for bosons} \end{aligned} \tag{1.50}$$

In this section, we firstly consider the non-supersymmetric case. The ratio of particles in equilibrium depends on the reactions involved. In a model with $N_{\rm f}$ flavours quark and lepton, we need to know the relations of number densities of left-handed quark Q, right-handed up and down type quark u and d, left-handed lepton ℓ, right-handed charged

lepton e, Higgs field H. They have chemical potentials μ_Q, μ_u, μ_d, μ_ℓ, μ_e and μ_H respectively, The relations comes from:

(a) The electroweak sphaleron process conserves $B - L$ number:

$$3\mu_Q + \mu_\ell = 0\,, \tag{1.51}$$

where the factor 3 comes from the colour degrees of freedom of quarks.

(b) The QCD sphaleron process balances left-handed quarks and right-handed quarks

$$2\mu_Q - \mu_u - \mu_d = 0\,. \tag{1.52}$$

(c) The total hypercharge in the plasma should be neutral

$$\sum_{flavour} (n_Q + 2n_u - n_d - n_l - n_e) + n_H = 0\,, \tag{1.53}$$

or in the form of chemical potentials:

$$\sum_{flavour} (\mu_Q + 2\mu_u - \mu_d - \mu_l - \mu_e) + 2\mu_H = 0\,. \tag{1.54}$$

The coefficient in front of μ_H comes from the difference of chemical potential for bosons and fermions Eq.(1.50).

(d) The Yukawa couplings for quarks are in equilibrium[12]

$$\mu_Q - \mu_H - \mu_d = 0, \quad \mu_Q + \mu_H - \mu_u = 0\,. \tag{1.55}$$

Notice that one of these two equations is redundant.

(e) When the temperature of the Univere drops to $T \sim 10^{4-5}\,\mathrm{GeV}$, the Yukawa interaction rate $\sim h_e^2 T$ is comparable to the Univere expanding rate H, the electron Yukawa interactions comes into equilibrium.

$$\mu_l - \mu_H - \mu_e = 0\,. \tag{1.56}$$

[12]The Yukawa interactions come into equilibrium when the reaction rate $\Gamma \sim h^2 T$ is comparable with the Hubble expansion rate H.

One should notice that when the temperature is higher than $10^{4-5}\,\mathrm{GeV}$, the chemical potential for the RH electron is zero. And the relations of chemical potentials change slightly. Using Eq.(1.51)-(1.56), the ratio of leptons and up-type quarks in the plasma can be obtained

$$\mu_u = \frac{2N_f - 1}{6N_f + 3}\,\mu_l\,, \tag{1.57}$$

We are interested in the ratio of n_B to $n_B - n_L$

$$n_B = C(n_B - n_L)\,, \tag{1.58}$$

where C can be given by

$$C = \frac{8N_f + 4}{22N_f + 13}\,. \tag{1.59}$$

In the SM, $N_f = 3$, one finds $C = 28/79$. The coefficient of C stands for that once one unit of $B - L$ number is generated in the plasma of the early universe, 28/79 of it will stay in the form of baryon.

1.3.3 Leptogenesis

In this section, we introduce the canonical Leptogenesis mechanism from thermally produced RH neutrino decays [80][13]. We will discuss the CP violation of RH neutrino decay in the Standard Model with three additional generations of RH neutrinos. And we will briefly introduce the form of Boltzmann Equations of lepton asymmetry. However, the details of Leptogenesis can be found in Chapter 3 and (4).

1.3.3.a Lepton Asymmetric decay of RH neutrino

If RH neutrinos have large Majorana masses, lepton number violating processes likely happen at the energy scale of their masses. These processes include decay, inverse decay

[13]For reviews, we refer the reader to [81] [82].

and scattering. RH neutrino decay is the most intriguing process, since it is naturally out-of-thermal equilibrium as the universe cools down. However, significant lepton asymmetries can also be produced by scatterings [83].

The minimal necessary extension of the Standard Model should include three families of gauge singlet RH neutrinos with Majorana masses. In addition, these RH neutrinos should couple to the Standard Model lepton doublets and Higgs doublets via Yukawa couplings. In the RH neutrino mass-eigenstate basis, the additional Lagrangian is

$$\mathcal{L} = -\frac{1}{2} M_i N_i^c N_i - h_{ij} H_u L_j N_i^c + \text{h.c.}\,. \tag{1.60}$$

Due to the Majorana nature, the RH neutrinos can decay into leptons and Higgs also anti-leptons and anti-Higgs through the Yukawa couplings. At tree level the decay width reads

$$\Gamma_{N_i}^{tot} = \Gamma(N_i \to H_u + \ell) + \Gamma(N_i \to H_u^* + \bar{\ell}) = \frac{1}{8\pi}(hh^\dagger)_{ii} M_i\,, \tag{1.61}$$

Since the Yukawa couplings could be complex in principle, one could expect CP violation in this decay. The amount of CP violation can be defined as

$$\varepsilon_{i,j} \equiv \frac{\Gamma_{N_i \to \ell_j + H} - \Gamma_{N_i \to \bar{\ell_j} + H^*}}{\Gamma_{N_i \to \ell_j + H} + \Gamma_{N_i \to \bar{\ell_j} + H^*}}\,, \tag{1.62}$$

where the index i stands for the three generations of RH neutrinos, and $j = e, \mu, \tau$ is the lepton flavor index. In the case of strongly hierarchical RH neutrinos $M_1 \ll M_{2,3}$, only the lepton asymmetries from N_1 decays need to be taken into account. This is because $N_{2,3}$, being heavier particles, decay earlier than N_1 and the lepton asymmetries produced by $N_{2,3}$ would be washed out by N_1 mediated scattering processes. However, in some special case of Yukawa couplings, the lepton asymmetry produced by N_2 decay may exist in a certain direction (a combination of lepton flavours), which has small Yukawa couplings, preventing the lepton asymmetries from being washed-out. This scenario is called N_2 Leptogenesis [84]. However, we do not consider this scenario in this thesis. This first order CP asymmetry can be calculated from the interference terms of the tree level diagram and one loop diagrams, in Fig. 1.6.

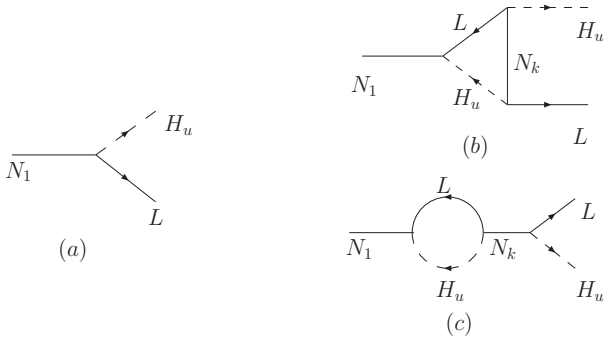

Figure 1.6: RH neutrino decay at tree level (a) and one loop, given by the vertex correction (b) and the self-energy correction (c).

In the framework of the Standard Model with right-handed neutrinos, it reads [85, 86] [87]

$$\varepsilon_{1,i} = \frac{1}{16\pi} \frac{1}{[hh^\dagger]_{ii}} \sum_{j \neq i} \mathrm{Im}\left\{[hh^\dagger]^2_{ij}\right\} \left[f_V\left(\frac{M_j^2}{M_i^2}\right) + f_S\left(\frac{M_j^2}{M_i^2}\right)\right], \tag{1.63}$$

where the functions from the vertex correction and the self-energy correction are given by

$$f_V(x) = \sqrt{x}\left[1 - (1+x)\ln\left(\frac{1+x}{x}\right)\right] \quad \text{and} \quad f_S(x) = \frac{\sqrt{x}}{1-x}\,. \tag{1.64}$$

In the limit $M_1 \ll M_{2,3}$, we have

$$\varepsilon_{1,j} \simeq -\frac{3}{16\pi} \frac{\mathrm{Im}\left[(hh^\dagger)^2_{1j}\right]}{(hh^\dagger)_{11}} \frac{M_1}{M_j}\,. \tag{1.65}$$

Leptogenesis is indirectly dependent on light neutrino masses, because the Yukawa couplings linking RH neutrinos to leptons and the RH neutrino mass both leed into the light left-handed neutrino masses, which are known to be $< 0.1 - 1\,\mathrm{eV}$. An upper bound on the CP asymmetry is derived [88]. Under this condition, to achieve successful Leptogenesis, $M_1 > 10^9\,\mathrm{GeV}$ is required. This leads to an gravitino-over-production problem, which will be discussed in Section (1.3.3.d). And, an extension to the canonical picture is required.

1.3.3.b Boltzmann Equations

In this section, we briefly review the Boltzmann Equations (BE) for the evolution of the thermally produced lightest RH neutrino and the lepton asymmetry (in one flavour approximation). The full details of the Boltzmann Equations will be given in Chapter 4.

Boltzmann Equations are a set of differential equations that describe the dynamical evolution of RH neutrinos and lepton/baryon number. The third Sakharov condition is reflected in the BEs: the processes of generating lepton number are out-of-thermal equilibrium.

Possible particles involved in generating baryon number in the universe are RH neutrino, leptons (both left-handed and right-handed) and quarks, which are converted from LH lepton by the electroweak sphaleron process. Since the electroweak sphaleron process conserves $B-L$ number, we write the coupled Boltzmann equations for RH neutrino number and $B-L$ number (in single flavour):

$$\frac{\mathrm{d}Y_{N_1}}{\mathrm{d}z} = -\frac{1}{sHz}(\gamma_D+\gamma_{\rm S})\left(\frac{Y_{N_1}}{Y_{N_1}^{\rm eq}}-1\right), \tag{1.66}$$

$$\frac{\mathrm{d}Y_{\ell}}{\mathrm{d}z} = -\frac{1}{sHz}\left[\varepsilon(\gamma_D+\gamma_{\rm S})\left(\frac{Y_{N_1}}{Y_{N_1}^{\rm eq}}-1\right)-\gamma_{\rm W,\Delta L=1}\frac{Y_{\ell}}{Y_{\ell}^{\rm eq}}\right], \tag{1.67}$$

where $z\equiv M_1/T$ is a dimensionless parameter with T the temperature of the hot plasma in the universe. γ_D, γ_S and γ_W are the reaction densities of decaying, scattering and wash-out process respectively. H is the Hubble expansion rate. $Y_{N_1}\equiv n_{N_1}/s$ is the abundance of lightest RH neutrino, normalised by the entropy density of the Universe. $Y_{B-L}\equiv(n_B-b_L)/s$ is the abundance of $B-L$. $Y_{N_1}^{\rm eq}$ and $Y_{B-L}^{\rm eq}$ are the abundances in equilibrium of N_1 and $B-L$ respectively. We have

$$Y_{B-L}^{\rm eq}=Y_Q^{\rm eq}=Y_{\ell}^{\rm eq}\simeq\frac{45}{\pi^4 g_*}, \quad Y_{N_1}^{\rm eq}\simeq\frac{45}{2\pi^4 g_*}z^2K_2(z). \tag{1.68}$$

Here, $K_2(z)$ is the second modified Bessel function. The details of the Boltzmann Equations can be found in Chapter 4.

Fig. 1.7 shows a typical numerical solution of Boltzmann Equations, where the initial

conditions are set to be $Y_{N_1}(z \ll 1) = Y_\ell(z \ll 1) = 0$ at $z \ll 1$. In this case, we assume all the right-handed neutrinos are produced thermally (via scatterings and inverse decays) after the inflation and reheating. Alternatively, the initial condition can be $Y_{N_1}(z \ll 1) = Y_{N_1}^{\rm eq}$ or $Y_{N_1}(z \ll 1) = \infty$ corresponding to the RH neutrinos are produced from the inflaton decay in some certain inflation models. However, as we will discuss the initial conditions in Section (4.3), the initial condition would not change the final $B-L$ number density about 1 to 2 orders of magnitude. In this thesis, we constraint ourselves to the scenario of thermally produced RH neutrino after inflation.

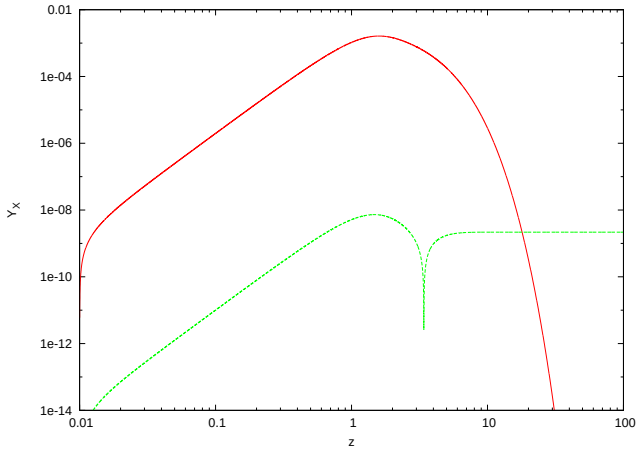

Figure 1.7: Evolution of Y_{N_1} abundance (the red line) and $Y_{|B-L|}$ asymmetry (the green line) for $M_1 = 10^{11}\,\text{GeV}$, $\varepsilon_1 = 4.6 \times 10^{-6}$ and $K = 2.3$

The reader may notice that there is a 'tail' for the $Y_{|B-L|}$ line. The reason is the $B-L$ number shifts from negative to positive during the evolution. The result from numerical calculation leads to the tail in the log-log plot.

1.3.3.c The Davidson-Ibarra Bound

An intriguing part of Leptogenesis is that the lepton asymmetry $\varepsilon_{i,\alpha}$ is constrained measurable light neutrino masses [88].

The total decay width of the first generation of RH neutrinos is proportional to modulus squared of the Yukawa couplings of the lightest RH neutrino, according to Eq.(1.61).

We introduce a mass parameter

$$\widetilde{m}_1 = (hh^\dagger)_{11}\frac{\langle H\rangle^2}{M_1}\,, \tag{1.69}$$

as above $\langle H\rangle = v$ is the vacuum expectation value of the Higgs field. The Yukawa couplings in the seesaw model satisfy $m_\nu = h^T M^{-1} h v^2$, and we can write them in the form

$$h = \frac{1}{v} D_{\sqrt{M}}\, R\, D_{\sqrt{M}}\, U^\dagger\,, \tag{1.70}$$

where $D_{\sqrt{M}} \equiv \mathrm{diag}(\sqrt{M_1}, \sqrt{M_2}, \sqrt{M_3}\,)$ when we work in the basis of the RH neutrino mass eigenstates, R is a orthogonal matrix, and U is the PMNS matrix. Inserting Eq.(1.70) into Eq.(1.65), we have

$$\varepsilon_1 = -\frac{3}{8\pi}\frac{M_1}{v^2}\frac{\sum_j m_j^2\,\mathrm{Im}(R_{1j}^2)}{\sum_j m_j |R_{1j}|^2}\,. \tag{1.71}$$

Using the orthogonal condition $\sum_j R_{1j}^2 = 1$, we can arrive at a upper limit of the CP asymmetry

$$|\varepsilon_1| \leq \frac{3}{8\pi}\frac{M_1}{v^2}(m_3 - m_1)\,. \tag{1.72}$$

The final baryon number Y_B needs to be calculated by Boltzmann Equations, which is linked to the lepton asymmetry of RH neutrino decays by $Y_{B-L} = \eta_{\mathrm{eff}}\varepsilon_1$, where $\eta_{\mathrm{eff}} \lesssim 10^{-(2-3)}$ is the efficiency factor. Taking the vacuum expectation value of the Higgs field $v = 246\,\mathrm{GeV}$ and the observed baryon asymmetry $n_B \simeq 10^{-10}$, one finds a lower limit for the RH neutrino mass, $M_1 \gtrsim 10^{8-9}\,\mathrm{GeV}$.

1.3.3.d The Gravitino-over-production Problem

In this section, we present the cosmological gravitino over production problem [89], showing the result of the bound on the reheating temperature. This bound is important for Leptogenesis where the RH neutrino is produced by thermal scattering. In this case, the reheating temperature $T_R \simeq M_1$ is required.

The gravitino is the supersymmetric partner of the graviton in a supergravity theory. The exact scale of the gravitino mass and its main decaying channel vary in different scenarios. There are also several schemes of how supersymmetry is broken and how the universe inflates. We briefly discuss the bounds from the gravitino in different scenarios. For a early review of the gravitino in the Universe, see [90].

- In gravity mediated SUSY breaking models, gravitinos are unstable particles with mass $m_{3/2} \sim \mathcal{O}(100\,\mathrm{GeV} - 10\,\mathrm{TeV})$ [91]. In this scenario, the gravitino decays after Nucleosynthesis ($t_{\mathrm{BBN}} \sim 100$ sec) with a lifetime [63]

$$\tau_{3/2} \simeq 4 \times 10^5 \left(\frac{m_{3/2}}{1\,\mathrm{TeV}}\right) \mathrm{sec}\,, \tag{1.73}$$

  unless the gravitino is relatively heavy: $m_{3/2} \sim 10\mathrm{TeV}$. The decay of gravitino (Gravitinos majorly decay into photons and photinos $\tilde{g} \to \gamma\tilde{\gamma}$ or neutrinos and sneutrinos $\tilde{g} \to \nu\tilde{\nu}$) would dilute the abundance of light element (D, ^{3}He, ^{4}He, ^{7}Li ...) produced in Nucleosynthesis. In Ref.([90]), the bounds on reheating temperature is given by [62]

$$T_R < 10^6 - 10^8 \mathrm{GeV}\,. \tag{1.74}$$

- If gravitinos are stable, *e.g.* in the gauge mediated SUSY breaking model, we have $m_{3/2} < \mathcal{O}(10)\,\mathrm{GeV}$. In this scenario gravitino is the lightest supersymmetric particle (LSP), and therefore a candidate of dark matter (DM) particle [92]. The bound on the reheating temperature comes from the density of the gravitino, which can not exceed the density of DM. One can derive the bound on the reheating temperature [62]

$$T_R < \mathcal{O}(10^7)\,\mathrm{GeV}\,, \tag{1.75}$$

  for $m_{3/2} > 100$ keV.

In Leptogenesis, if the RH neutrinos are produced thermally, one requires $M_1 \simeq T_R$. One can compare with the Davidson-Ibarra bound in the last section and find the condition

for reheating temperature is not satisfied, so canonical Leptogenesis must be modified in some way. Apart from inflation models, one interesting solution is resonant Leptogenesis [93] [94] [95], where at least two of the three RH neutrino are mass degenerate. The lepton asymmetry ε_1 can be enhanced drastically even in the small mass case $M_1 \sim M_2 \sim 10^7\,\mathrm{GeV}$. However, one has to impose a mechanism to explain why the RH neutrino masses are degenerate. In this thesis, we do not investigate this situation.

1.3.4 Affleck-Dine Leptogenesis

In the previous two sections, we have discussed the mechanism of baryon asymmetry produced from the RH neutrino's out-of-thermal equilibrium decay. However, this is not the only scenario of Baryogenesis. An alternative mechanism is proposed by Affleck and Dine [96] based on the framework of SUSY, neutrino masses in effective theories and inflation.

In the supersymmetric model, quarks and leptons have supersymmetric scalar partners, which also carry lepton and baryon number. These Supersymmetric particle/condensate may exist in the early universe, but we should not worry about these particles being present in our visible universe. The supersymmetric particles, which contains baryon number and lepton number, decay into baryons and leptons in the SM via baryon number/lepton number conserved processes. So the baryon and lepton number is converted without any loss.

In supersymmetric models some special combinations of scalars, lying along flat-directions in the potential, can have arbitrarily large vacuum expectation value during the inflation of the universe.

In the MSSM, the most interesting flat-direction for the Affleck-Dine mechanism is the combination of scalar lepton field and Higgs field, which is defined as

$$\phi_i^2 = \widetilde{L}_i H_u \,, \tag{1.76}$$

where $\widetilde{L}_i$ are the scalar lepton doublet fields with family index $i = 1, 2, 3$. The flat-direction is lifted by higher order non-renormalizable operators in the superpotential

$$W = \frac{\lambda_i^2}{2\, M_{\text{eff}}}(L_i H_u)(L_i H_u)\,, \tag{1.77}$$

where λ_i describe the spectrum of flavours and M_{eff} is a heavy scale in an effective theory. Notice that we work in the basis of left-handed neutrino mass eigenstates rather than flavour eigenstates. Since this operator also gives left-handed neutrino masses, we can rewrite it as

$$W = \frac{m_i}{2\,\langle H_u\rangle^2}(L_i H_u)(L_i H_u)\,, \tag{1.78}$$

where $\langle H_u\rangle$ is the vev of up-type Higgs field. It is effective to just investigate one flat direction. The reason is, as we will see, in the case of $L_i H_u$ flat direction, the successful baryon asymmetry is generated only in one flavour, which corresponds to the lightest left-handed neutrino. We denote this previously flat direction as ϕ and therefore the potential reads

$$V = \frac{m_i^2}{4\,\langle H_u\rangle^4}|\phi|^6\,. \tag{1.79}$$

In addition, the flat direction field obtains soft mass terms from supersymmetry breaking

$$\delta V = m_\phi^2|\phi|^2 + \frac{m_{3/2}}{8\, M_{\text{eff}}}(a_m\phi^4 + \text{h.c.})\,. \tag{1.80}$$

Here m_ϕ and $m_{3/2} \simeq 1$ TeVare SUSY breaking parameters. The flat direction field also gains a Hubble mass term

$$\delta V = -c_H H_{inf}^2|\phi|^2 + \frac{H_{inf}}{8\, M_{\text{eff}}}\left(a_H\phi^4 + \text{h.c.}\right)\,, \tag{1.81}$$

where H_{inf} is the Hubble parameter during the inflation, and $c_H \simeq |a_H| \simeq 1$.

The evolution of the scalar field is described by equation

$$\frac{\partial^2\phi}{\partial t^2} + 3H\,\frac{\partial\phi}{\partial t} + \frac{\partial V_{total}}{\partial\phi^*} = 0\,, \tag{1.82}$$

where V_{total} is the summation of all possible potentials related to ϕ. And the number density of scalar is

$$n = i\left(\frac{\partial\phi^*}{\partial t}\phi - \phi^*\frac{\partial\phi}{\partial t}\right)\,. \tag{1.83}$$

The lepton number density is related to the scalar number density by $n_{\rm L} = \frac{1}{2}n$. If we write the scalar field in the form of $\phi(t) = |\phi(t)|\, e^{-i\,\theta(t)}$, the number density of scalar reads

$$n_{\rm L} = -|\phi|^2\, \frac{\partial\theta}{\partial t}\,, \tag{1.84}$$

from which we can clearly see that the number of scalars depends on the angular momentum of the flat-direction.

After inflation, the flat-direction field begins oscillating and it has the value

$$|\phi| \simeq \sqrt{M_{\rm eff}\, H}\,, \tag{1.85}$$

The effective CP violation comes from the relative phase of a_m and a_H and the evolution of the lepton number can be described by the equation derived from Eq.(1.82) and (1.83)

$$\dot{n}_L + 3\,H\,n_L \;=\; \frac{m_{3/2}}{M_{\rm eff}}{\rm Im}\left(a_m\phi^4\right) \;+\; \frac{H}{2\,M_{\rm eff}}{\rm Im}\left(a_H\phi^4\right)\,. \tag{1.86}$$

According to the above equation, one can obtain the final net lepton number normalised to the entropy density, which reads

$$\frac{n_L}{s} \;=\; \frac{3T_R}{4M_G}\frac{v^2}{6m_\nu M_{pl}^2}\,, \tag{1.87}$$

where T_R is the reheating temperature. Again the sphaleron process plays the role of converting part of lepton number into baryon number, and one finds that the baryon asymmetry $n_B/s \sim 10^{-10}$ requires the corresponding neutrino mass to be $m_\nu \sim 10^{-9}\,{\rm eV}$ for $T_R \sim 10^6$ GeV. This implies that the neutrino mass pattern should be a normal hierarchy, which can be tested in neutrinoless double beta decay experiments.

The Affleck-Dine mechanism can naturally explain why the amount of baryonic matter and dark matter in the universe are of the same order. This problem arises if baryonic matter is generated by CP violating RH neutrino decay whereas the amount of dark matter is decided by the decoupling of the dark matter particle. In the Affleck-Dine mechanism, the scalar condensate develops into baryons and baryonic Q-balls (a type of non-topological soliton). If baryonic Q-balls are unstable, they decay into baryons and dark matter, whereas if they are stable, they play the role of dark matter. In either situation, one can straightforwardly arrive at the conclusion of $\Omega_{\rm b} \sim \Omega_{\rm DM}$.

1.3.5 Electroweak Baryogenesis

The SM itself contains all three of Sakharov's conditions: CP violation exists in the CKM matrix and QCD process, electroweak sphaleron process violates B number, thermal processes depart from equilibrium due to the expansion of the universe. In fact, net baryon number is generated in the framework of the Standard Model, and this scenario is called "Electroweak Baryogenesis" [97] [98].

Electroweak Baryogenesis happens when the temperature of the universe reaches $\sim$ 246 GeV where the electroweak phase transition takes place. If the electroweak phase transition is at first order, degenerate vacua, including regions with the broken phase and regions where EW symmetry is conserved coexist in the universe. When the temperature continues to drop, the regions with the broken phase expand. This process is called "bubble nucleation". When fermions pass the border of the unbroken phase region and the broken phase region, baryon number is produced due to the sphaleron process and the CP violation from the CKM matrix. To avoid the generated baryon number from being washed out, one requires that the rate of the sphaleron process be smaller than the Hubble parameter, the rate of expansion of the universe.

However, in the SM, Electroweak Baryogenesis is not sufficient. Numerically calculation finds that the generated baryon number from bubble nucleation is much smaller than the observed baryon number in the universe. In addition, the electroweak phase transition at first order requires the Higgs mass $m_{\mathrm{H}} < 40$ GeV. However the lower bound of Higgs particle in SM from LEP is $m_{\mathrm{H}} > 114$ GeV.

The most compelling solution is supersymmetry, where extra CP violation sources are provided and a first order phase transition is available. We do not discuss details of the electroweak Baryogenesis here; for a review and recent development, we refer readers to [99][100].

Chapter 2

The Exceptional Supersymmetric Standard Model

In this chapter, we present the motivation, theory background, and phenomenology of the Exceptional Supersymmetric Standard Model (E_6SSM) [102] [101] [113] [103], in which we will discuss Leptogenesis in the next chapter. The feature of E_6SSM includes the light Higgs mass, gauge unification, neutrino mass and the signals from LHC.

2.1 Motivations of E_6SSM

From the top-down point of view, the Exceptional Supersymmetry Standard Model is inspired by $E_8 \times E_8'$ string theory [104]. The gauge symmetry E_8 breaks down into its subgroup E_6 by the compactification of extra dimensions, whereas E_8' represents the hidden sector in charge of the spontaneous breaking of SuperGravity. The E_6 in the observable sector has subgroups including $SO(10)$ and $SU(5)$ which are commonly used gauge groups for Grand Unification Theories (GUT) [105]. From the bottom-up point of view, some problems in the MSSM need physics of larger gauge symmetries.

2.1.1 The Down-up Approach: μ Problem and Domain Wall Problem

In the simplest realisation of Supersymmetry, the Minimal Supersymmetric Standard Model (MSSM), an extra up Higgs H_u distinguished from the down Higgs field H_d is introduced, since the Supersymmetry forbids H_d to give mass to the down type quarks and leptons. There is a bilinear term of the up Higgs and down Higgs, called μ term: $\mu\hat{H}_u\hat{H}_d$. One could naively expect it to be zero or the Plank scale M_{pl}. However, if $\mu = 0$ at some scale Q, the mixing between the two Higgs fields vanish, and leads to $\langle H_d \rangle = 0$ below the scale of Q. In this case, no mass for down type quarks and charged leptons can be generated via the Higgs mechanism. On the other hand, if μ is at Plank scale, it leads to a contribution $\sim \mu^2$ to the Higgs mass and the electroweak symmetry breaking can not happen. Then, it is believed that there must be a mechanism as the source of the μ term.

In the Next-to-Minimal Supersymmetric Standard Model (NMSSM) [106] [107], the μ arise automatically in the Giudice-Masiero mechanism [108], where the μ term comes from the general couplings of broken supergravity. In this model, a singlet field S which couples to the Higgs fields is proposed. The extra terms in the NMSSM superpotential reads $\lambda\hat{S}(\hat{H}_d\hat{H}_u) + \frac{1}{3}\kappa\hat{S}^3$. The S field develops a vev and generates an effective μ term, when the additional $U(1)_{PQ}$ global symmetry is broken into a discrete Z_3 symmetry. However, the different regions in the early universe may have different vacua, which are separated by domain walls [109] formed by discrete symmetries. The domain walls would finally evolve into large anisotropies in the Cosmic Microwave Background, which conflicts with the observation of COBE and WMAP. To break the undesirable Z_3 discrete symmetry, one can introduce operators, which are suppressed by powers of the Plank scale. However, these operators would lead to quadratically divergent tadpoles, and therefore destablize the mass hierarchy once again.

2.1.2 The Top-down Approach from SuperString Theory

The supergravity theory, which partially unifies SM interactions and the gravitational interaction in the context of supersymmetry is a non-renormalisable theory. Therefore one has to consider it as a low-energy effective theory. A ten-dimensional heterotic $E_8 \times E_8'$ SuperString model [104] is a candidate of "beyond supergravity" theory. The strong interaction is determined by the eleven-dimensional SUGRA (M-theory), where the string scale is compatible with the unification scale M_{GUT}. When the compactication of extra dimensions happens, the E_8 may break into E_6 or its subgroups which describe the observable sector, whereas E_8' describes the sector which only couples to the E_6 sector via the gravitational force. Hence, E_8' plays the role of a hidden sector and leads to the breakdown of supergravity. At low energy scales, the E_8' decouples from the visible sector but the breaking of supersymmetry is transmitted to the visible sector.

2.2 The E_6SSM

The low energy scale physics of the E_6SSM is inspired by the E_6 symmetry. The particle content forms three families of the fundamental 27_i representation of E_6, where i is the index for the family. At the string scale, the E_6 group breaks into its subgroup $SO(10)$

$$E_6 \;\; \rightarrow \;\; SO(10) \times U(1)_\psi \,, \tag{2.1}$$

and the $SO(10)$ breaks via

$$SO(10) \;\; \rightarrow \;\; SU(5) \times U(1)_\chi \,. \tag{2.2}$$

The $SU(5)$ further breaks to $SU(3)_C \times SU(2)_W \times U(1)_Y \times U(1)_\psi \times U(1)_\chi$ resulting in $SU(3)_C \times SU(2)_W \times U(1)_Y \times U(1)_\psi \times U(1)_\chi$, which is simply the SM gauge symmetry with two extra $U(1)$ gauges. One can write the two $U(1)$ gauges in a form of linear combination

$$U(1)_N = U(1)_\psi \, \sin\theta \times U(1)_\chi \, \cos\theta \tag{2.3}$$

Since the see-saw model which generates light neutrino mass is widely accepted, we need the RH neutrinos to be neutral in a certain combination of $U(1)_\psi$ and $U(1)_\chi$. This corresponds to $\theta = \arctan\sqrt{15}$. So the $U(1)_\psi \times U(1)_\chi$ guage is reduced to $U(1)_N$ gauge. The other combination of $U(1)_\psi$ and $U(1)_\chi$ breaks at the higher scale, leading to non-renormalizable terms, *e.g.* Eq.(2.10) which will be discussed later. In this case, the RH neutrino can be arbitrarily heavy so that it can play a role in the seesaw model, where particles as heavy as $\mathcal{O}(10^{15}\,\mathrm{GeV})$ is needed to suppress the LH neutrino masses in the case of Yukawa coupling ~ 1.

The three families of 27_i representation of E_6 break into $SU(5) \times U(1)_N$

$$\begin{aligned} 27_i \to \left(10, \frac{1}{\sqrt{40}}\right)_i + \left(5^*, \frac{2}{\sqrt{40}}\right)_i + \left(5^*, -\frac{3}{\sqrt{40}}\right)_i + \left(5, -\frac{2}{\sqrt{40}}\right)_i \\ + \left(1, \frac{5}{\sqrt{40}}\right)_i + (1,0)_i \,, \end{aligned} \tag{2.4}$$

where the second elements in each brackets are the charge of $U(1)_N$. $\left(10, \frac{1}{\sqrt{40}}\right)_i + \left(5^*, \frac{2}{\sqrt{40}}\right)_i$ contains left-handed quark and lepton doublets Q_i and L_i, the right-handed quark and lepton singlet u_i^c, d_i^c and e_i^c of the SM and the last term, $(1,0)_i$ represents the RH neutrino N_i^c.

The first term in the second line of Eq. (2.4), $\left(1, \frac{5}{\sqrt{40}}\right)_i$ represents another singlet field S_i which carries non-zero $U(1)_N$ charge and therefore survive to the electro-weak scale. Two pairs of $SU(2)_W$-doublets with three families (H_{1i} and H_{2i}) that are contained in the third and forth term of Eq. (2.4) $\left(5^*, -\frac{3}{\sqrt{40}}\right)_i$ and $\left(5, -\frac{2}{\sqrt{40}}\right)_i$ behave as Higgs doublets. The other components of the $SU(5)$ multiplets form colour triplets of exotic quarks $\overline{D}_i$ and D_i with electric charges $-1/3$ and $+1/3$ respectively. They carry a $B-L$ charge $\pm 2/3$. Therefore in phenomenologically viable E_6 inspired models they can be either diquarks, with 2/3 baryon number (model I) or leptoquarks with one lepton number and $-1/3$ baryon number (model II). The breaking of $U(1)_N$ gauge leads to an extra Z' gauge boson at low energy scale. The phenomenology of a Z' gauge boson together with exotic quarks of the LHC is discussed in [110]. In E$_6$SSM, an extra pair of L_4 and $\bar{L}_4$

is introduced[1], which exist in another 27 and $\overline{27}$ representation, to help unify the gauge couplings. L_4 and $\bar{L}_4$ behave like a forth generation of lepton in the Yukawa couplings as they couples to ordinary leptons via Yukawa couplings. Furthermore, one should notice that they are $SU(2)_W$ doublets and participate the electro-weak interaction at the low energy scale.

The flavour changing neutral currents (*e.g.* $b \to s + \gamma$, $\mu^- \to e^- + e^- + e^+$) and proton decay ($p \to \pi + e^+$) are strongly suppressed experimentally, which yields a strong constraint on Grand Unification Models. To suppress these processes, a Z_2^H symmetry is imposed to forbid the lepton and baryon number violating operators. Under this discrete symmetry, all superfields are odd except the third generation of up-type and down-type Higgs field $H_{1,3}$, $H_{2,3}$ together with a SM singlet field ($S \equiv S_3$), which are even. The first two generations of Higgs field are called "inert Higgs", since they do not develop a vacuum expectation value. The third generation of Higgs $H_{1,3} \equiv H_u$, $H_{2,3} \equiv H_d$ are the Higgs field of the MSSM, which give mass to quark and lepton fields after the breaking of electro-weak symmetry. The singlet field S_3 couples to the Higgs doublet via the term $\lambda_{332} H_u H_d S$, and the breaking of $U(1)_N$ results in a natural μ term in the MSSM at the TeVscale.

The Z_2^H symmetry forbids non-diagonal flavour transitions in the Yukawa couplings, but meanwhile induces charged stable particles, which is ruled out by experiments and cosmological observation [112]. Therefore the Z_2^H symmetry can not be exact and has to break at some scale. Since the operator leading to proton decay violates both L number and B number, we only need to keep one of them conserved. After the breaking of Z_2^H, we can impose an exact Z_2^L discrete symmetry, under which all fields except leptons are even (called Model I) or Z_2^B symmetry, under which lepton and exotic quark superfields are odd whereas all other fields are even (called Model II). In the case where Z_2^L is exact, the baryon number is conserved and the exotic quarks are diquarks (with baryon number $B_D = -2/3$ and $B_{\bar{D}} = 2/3$). In the case where Z_2^B symmetry is unbroken, the exotic

[1] L_4 is also denoted as H' and $4'$ in some literature.

quarks are leptoquarks (with baryon number $B_D = 1/3$ and $B_{\bar{D}} = -1/3$).

The renormalisable superpotential allowed by the $SU(3) \times SU(2) \times U(1)_Y \times U(1)_N$ gauge symmetry can be written in the following form:

$$W_{\text{total}} = W_0 + W_1 + W_2 + W_{\not{E}_6}\,, \tag{2.5}$$

The first term in Eq. (2.5) is the most general superpotential allowed by the E_6 symmetry. W_1 and W_2 are the superpotentials for models I and model II respectively. W_0, W_1 and W_2 are expressed as

$$\begin{aligned}
W_0 &= \lambda_{ijk} S_i (H_{1j} H_{2k}) + \kappa_{ijk} S_i (D_j \overline{D}_k) + h^N_{ijk} N^c_i (H_{2j} L_k) + h^U_{ijk} u^c_i (H_{2j} Q_k) + \\
&\quad + h^D_{ijk} d^c_i (H_{1j} Q_k) + h^E_{ijk} e^c_i (H_{1j} L_k)\,, \\
W_1 &= g^Q_{ijk} D_i (Q_j Q_k) + g^q_{ijk} \overline{D}_i d^c_j u^c_k\,, \\
W_2 &= g^N_{ijk} N^c_i D_j d^c_k + g^E_{ijk} e^c_i D_j u^c_k + g^D_{ijk} (Q_i L_j) \overline{D}_k\,.
\end{aligned} \tag{2.6}$$

Notice that we drop the colour index for the SM quarks and exotic quarks. There are three colour degrees of freedom for one generation of leptoquark and 9 colour degrees of freedom for one diquark.

The first three terms in the superpotential in Eq.(2.5) come from the $27 \times 27 \times 27$ decomposition of the E_6 fundamental representation. It possesses a global $U(1)$ symmetry that can be associated with $B - L$ number conservation. This global symmetry has to be broken explicitly, therefore the last term of the superpotential (2.5) violating $B - L$ is imposed:

$$W_{\not{E}_6} = \frac{1}{2} M_{ij} N^c_i N^c_j + W'_0 + W'_1 + W'_2\,, \tag{2.7}$$

where

$$\begin{aligned}
W'_0 &= \mu'_i (\overline{L}_4 L_i) + \mu'_4 (L_4 \overline{L}_4) + h_{ij} N^c_i (H_{2j} L_4) + h^{H'}_{ij} e^c_i (H_{1j} L_4)\,, \\
W'_1 &= \tfrac{\sigma_{ijk}}{3} N^c_i N^c_j N^c_k + \Lambda_k N^c_k + \lambda_{ij} S_i (H_{1j} \overline{L}_4) + g^N_{ij} N^c_i (\overline{L}_4 L_j) \\
&\quad + g^N_i N^c_i (\overline{L}_4 L_4) + g^U_{ij} u^c_i (\overline{L_4} Q_j) + \mu_{ij} (H_{2i} L_j) + \mu_i (H_{2i} L_4) + \mu_{ij} D_i d^c_j\,, \\
W'_2 &= g^{H'}_{ij} (Q_i L_4) \overline{D}_j\,, \qquad\qquad i, j, k = 1, 2, 3\,.
\end{aligned} \tag{2.8}$$

Similarly, W_1' is associated with model I and W_2' is associated with model II.

In model II, the Z_2^H symmetry forbids W_1'. We can summarise the superpotential for E_6SSM in model I and model II:

$$\begin{aligned} W_{\rm ESSM,I} &= W_0 + W_1 + \frac{1}{2}M_{ij}N_i^c N_j^c + W_0', \\ W_{\rm ESSM,II} &= W_0 + W_2 + \frac{1}{2}M_{ij}N_i^c N_j^c + W_0' + W_2'. \end{aligned} \tag{2.9}$$

2.2.1 Bilinear Terms in E_6SSM

We can rotate and redefine the representation of $27'$, so that only one L_4 interacts with $\overline{L}_4$. In this case, the mixing between the SM leptons and L_4 (the term $\mu_i'(L_4 L_i)$, $i = 1, 2, 3$) vanishes. Therefore only two bilinear terms in the superpotential are left. One is the mass term for the RH neutrino $\frac{1}{2}M_{i,j}N_i^c N_j^c$, with masses of RH neutrinos set to be at the intermediate scale. The other is the mass term for L_4, $\mu' L_4\overline{L_4}$, where μ' has to be ~ 1 TeV, in order to unify the gauge couplings.

In SUGRA models, $\mu' L_4\overline{L}_4$ can arise when the local supersymmetry breaks from an extra term $Z(L_4\overline{L_4}) + \text{h.c.}$ in the Kähler potential (a potential K related to the metric by $h_{ij} = 2\partial^2 K/\partial\phi_i\partial\bar{\phi}_j$, with ϕ_i, $\bar{\phi}_j$ being the superfields [111]), where Z is a generic function of ϕ_i and $\bar{\phi}_j$. This mechanism is similar to that in NMSSM solving the μ problem. However, the bilinear term of up-type Higgs and down-type Higgs are not allowed in either superpotential and Kähler potential due to the E_6 symmetry.

The RH neutrino mass terms can be induced from the non-renormalisation term of 27 and $\overline{27}$, $\frac{\kappa_{\alpha\beta}}{M_{\rm pl}}(27_\alpha\overline{27}_\beta)^2$. When N^c and $\overline{N}^c$ from the extra 27 and $\overline{27}$ representation develops a vev along a flat-direction $\langle N_H^c\rangle = \langle\overline{N}_H^c\rangle$, the two $U(1)_\phi$ and $U(1)_\chi$ reduce to $U(1)_N$. The RH neutrino mass term is generated via the coupling of 27plet to ordinary 27plet

$$\delta W = \frac{\kappa_{ij}}{M_{\rm pl}}(\overline{27}_H 27_i)(\overline{27}_H 27_j)\,. \tag{2.10}$$

The mass for RH neutrino therefore is $M_{ij} = \frac{\kappa_{ij}}{M_{\rm pl}}\langle\overline{N}_H^c\rangle^2$. In order to generate light left-handed neutrino masses at the 1eV scale, the $U(1)_\phi$ and $U(1)_\chi$ symmetry should break

into $U(1)_N$ at an intermediate scale of order $10^{14}\,\mathrm{GeV}$, assuming the Yukawa couplings ~ 1.

2.2.2 The Right-handed Neutrino Yukawa couplings in E_6SSM

The RH neutrinos are neutral under the gauge transformation of SM and $U(1)_N$, and they couple to the exotic quarks after the breaking of the Z_2^H symmetry. The additional superpotential corresponding to RH neutrinos reads:

$$\Delta W = \xi_{\alpha ij}(H_{2\alpha}L_i)N_j^c + \xi_{\alpha 4j}(H_{2\alpha}L_4)N_j^c + g_{kij}^N D_k d_i^c N_j^c \,. \tag{2.11}$$

Here $\alpha = 1, 2$ are the family indices for inert Higgs and $i, j, k = 1, 2, 3$ are family indices for RH neutrino, leptons, quarks and exotic quarks. The last term in this superpotential exists only in Model II, where the exotic quarks are leptoquarks. This superpotential has to be suppressed strongly and the major constraints are from the rare decay of muon *e.g.* $\mu \to e^- e^+ e^-$ and $K^0 - \overline{K}^0$ mixing [39].

2.3 Neutrino Masses

In section (1.2.5), we discussed the canonical scenario of the seesaw model, where only the RH neutrinos contribute to the masses of light neutrinos. However, from the theoretical point of view, exotic particles/physics beside RH neutrinos may also contribute to the mass of light neutrinos. In some models, there may be multiple sources of light neutrino masses. In this section, we firstly review the type II and type III seesaw model, and then present the neutrino mass from E_6SSM, showing the contribution from the exotic lepton L_4.

2.3.1 Type II Seesaw Model

In the classical seesaw model (Type I), the masses of left-handed neutrino come from integrating out the RH neutrinos with heavy Majorana masses. However, in some Grand Unification models, that is not the only source of light neutrino mass. One possible scenario is $SU(2)_L$ triplet Higgs superfields $\hat{\Delta}$ and $\bar{\hat{\Delta}}$ with hypercharge 1 and -1 respectively, representing the triplets as matrices [119]

$$\hat{\Delta} = \begin{pmatrix} \hat{\Delta}^{+} & \hat{\Delta}^{++} \\ \hat{\Delta}^{0} & -\hat{\Delta}^{+} \end{pmatrix}, \quad \bar{\hat{\Delta}} = \begin{pmatrix} \bar{\hat{\Delta}}^{+} & \bar{\hat{\Delta}}^{++} \\ \bar{\hat{\Delta}}^{0} & -\bar{\hat{\Delta}}^{+} \end{pmatrix}. \tag{2.12}$$

The triplet couples to lepton fields via

$$\mathcal{L} = \frac{1}{2} \left(Y_{\Delta}^{+}\right)_{fg} \hat{L}^{Tf}\, i\, \sigma_2\, \hat{\Delta}\, \hat{L}^{g}\,, \tag{2.13}$$

where Y_{Δ}^{+} is the coupling constant and f, g are the family indices for the lepton doublets and σ_2 is the second Pauli matrix. The scalar potential for Δ reads

$$V = M_{\Delta} \lambda_u H_u^T\, i\sigma_2 \Delta^* H_u + M_{\Delta}^2 \mathrm{Tr}(\Delta^* \Delta) + \mathrm{h.c.} \tag{2.14}$$

After electro-weak symmetry breaking, the neutral component of $\hat{\Delta}$, $\hat{\Delta}^0$ develops a vev

$$v_{\Delta} \simeq \frac{\lambda_u\, v_u^2}{M_{\Delta}}\,. \tag{2.15}$$

Giving a contribution to the light neutrino mass

$$m^{\mathrm{II}} = Y_{\Delta}\, v_{\Delta}\,. \tag{2.16}$$

The total mass of light neutrino then reads

$$m_{\nu} = m^{\mathrm{II}} + m^{\mathrm{I}} = Y_{\Delta}\, v_{\Delta} - v_u^2\, Y_{\nu}\, M_N^{-1} Y_{\nu}^T\,, \tag{2.17}$$

where $m^{\mathrm{I}} = v_u^2\, Y_{\nu}\, M_N^{-1} Y_{\nu}^T$ is the contribution from the type I seesaw, where the heavy RH neutrinos with mass M_N are integrated out.

2.3.2 Type III Seesaw Model

In some grand unification theories, for example, the left-right symmetric model based on $SU(3)_C \times SU(2)_L \times SU(2)_R \times U(1)_{B-L}$ gauge symmetry, a fermion triplet with three families is introduced. The left and right handed components are

$$\rho_L = \frac{1}{2}\begin{pmatrix} \rho_L^0 & \sqrt{2}\rho_L^+ \\ \sqrt{2}\rho_L^- & -\rho_L^0 \end{pmatrix}, \quad \rho_R = \frac{1}{2}\begin{pmatrix} \rho_R^0 & \sqrt{2}\rho_R^+ \\ \sqrt{2}\rho_R^- & -\rho_R^0 \end{pmatrix}, \tag{2.18}$$

respectively [120][121][122]. The left and right handed Higgs field belong to the $SU(2)_L$ and $SU(2)_R$, and they are

$$H_L = \begin{pmatrix} \phi_L^+ \\ \frac{\phi_L^0 \, + \, i \, A_L^0}{\sqrt{2}} \end{pmatrix} \quad H_R = \begin{pmatrix} \phi_R^+ \\ \frac{\phi_R^0 \, + \, i \, G_R^0}{\sqrt{2}} \end{pmatrix} \tag{2.19}$$

The corresponding Lagrangian is

$$\begin{aligned} \mathcal{L}_\nu^{III} &= \mathcal{L}_l + Y_5 \left(l_L^T \, C \, i\sigma_2 \, \rho_L H_L + \; l_R^T \, C \, i\sigma_2 \rho_R H_R \right) \\ &+ M_\rho \mathrm{Tr} \left(\rho_L^T \, C \, \rho_L + \rho_R^T \, C \, \rho_R \right) + \mathrm{h.c.} \end{aligned} \tag{2.20}$$

The left-handed Higgs H_L and right handed Higgs H_R acquire vevs v_L and v_R respectively when $SU(2)_L$ and $SU(2)_R$ are broken spontaneously. The C is the charge conjugate defined in Appendix (A). The resulting mass matrix in the basis of left-handed neutrino, RH neutrino, fermion triplet $\left((\nu^C)_R, \; \nu_R, \; \rho_R^0 \right)$ can be written as

$$M_\nu^{III} = \begin{pmatrix} 0 & M_\nu^D & 0 \\ (M_\nu^D)^T & 0 & -\frac{Y_5 v_R}{2\sqrt{2}} \\ 0 & -\frac{Y_5^T v_R}{2\sqrt{2}} & M_\rho \end{pmatrix}. \tag{2.21}$$

In the limit of $M_\rho \gg Y_5 v_R / 2\sqrt{2} \gg M_\nu^D$ one finds the mass for the light neutrino

$$M_{(\nu^C)_R} = M_\nu^D \; M_{\nu_R}^{-1} \; \left(M_\nu^D \right)^T, \tag{2.22}$$

where M_{ν_R} is the effective mass for the RH neutrino,

$$M_{\nu_R} = \frac{v_R^2}{8} \; Y_5 \; (M_\rho)^{-1} \; Y_5^T. \tag{2.23}$$

In type III seesaw models, the light neutrino mass is proportional to the fermion triplet mass M_ρ. Thus is also called the double seesaw model. Note that the fermioin triplet mass M_ρ can be $\sim 1\,\mathrm{TeV}$, so it can be interesting for LHC.

2.3.3 Neutrino Masses from the E_6SSM

To consider the light neutrino mass in the E_6SSM, one has to take into account all particles with which the left-handed neutrinos have bilinear terms below electro-weak scale. As discussed in the last section, we have to consider the neutral component of the exotic lepton doublets L_4 and $\overline{L}_4$ and the RH neutrinos N. The bilinear term $\mu'_i(\overline{L}_4 L_i)$ mixes the left-handed neutrino with exotic lepton L_4. Here, we drop the family index and re-denote it as $\mu''(\overline{L}_4 L_i)$. Also the Yukawa coupling between left-handed neutrino, exotic lepton $\overline{L}_4$ and RH neutrino $h^N_{4j}(H_u L_4)N^c_j$ and $h^N_{ij}(H_u L_i)N^c_j$ turns into a mixing term after the electro-weak symmetry breaking. The mixing between left-handed neutrinos and right-handed neutrinos is of order $v = 246$ GeV provided the corresponding Yukawa couplings are of order unity. In addition, there are bilinear mass terms for L_4, $\mu'(L_4\overline{L}_4)$, where $\mu' \sim 1$ TeV and heavy Majorana mass terms for RH neutrinos $M_{ij}N^c_i N^c_j$ with $M_{ij} \sim 10^{15}$ GeV.

Then the mass matrix in the basis of $(\nu,\, L_4,\, \bar{L}_4\, N)$ reads

$$M = \begin{pmatrix} 0 & 0 & \mu'' & v' \\ 0 & 0 & \mu'_4 & v^T \\ \mu''^T & \mu'_4 & 0 & 0 \\ v'^T & v & 0 & M \end{pmatrix}. \tag{2.24}$$

Note that there are three families of ν and N, but only one family for the exotic lepton L_4. Therefore μ'' and v are 3×1 column vectors, v' and M are 3×3 matrices, and μ'_4 is just a number.

In the E_6SSM, M is at an intermediate scale to the Plank scale; μ'_4, the Dirac mass for L_4 should be at TeV scale; v and v' come from the breaking of electro-weak symmetry, so we have $v \sim v' \sim \mathcal{O}(100\,\mathrm{GeV})$. We may therefore assume $v\,, \mu''\,, \mu'_4 \ll M$. In addition, the mixing between light neutrinos and L_4 has to be small. This constraint comes from the requirement that violation of unitarity of the PMNS matrix small, which otherwise would lead to unwanted consequences including lepton flavour violating processes at low energy. Hence we assume $\mu'' \ll \mu'_4$. By diagonalising this matrix we can derive the

effective mass for the light neutrino, ignoring the flavour structure

$$m_\nu \simeq \frac{v'^2}{M}\left(1+\frac{v}{v'}\frac{\mu''}{\mu'_4}+\left(\frac{v}{v'}\frac{\mu''}{\mu'_4}\right)^2\right). \tag{2.25}$$

From the effective light neutrino mass given above, we find the first order contribution is identical to that of the type I seesaw, where only the RH neutrino is added. The second and third terms depend on the mixing of the exotic lepton and the SM leptons μ'', which is small. And therefore the contribution from L_4 is negligible.

2.4 Light Higgs Mass in the E$_6$SSM

One of the important consequences of the E$_6$SSM is the light Higgs mass, which plays an important role in Supersymmetric theories. In E$_6$SSM, all extra contribution to the lightest CP-even Higgs mass at tree-level comes from extra $U(1)_N$ D term. The approximate upper-bound reads

$$m^2_{h_1} \lesssim \frac{\lambda^2}{2}v^2\sin^2 2\beta + M_Z^2\cos^2 2\beta + \left(\frac{M_Z}{2}\right)^2(1+\frac{1}{4}\cos 2\beta)^2, \tag{2.26}$$

where λ is the Higgs coupling constant. The second term is the usual upper bound as that in the MSSM, while the first term is a combination from the effective μ-term, analogous to that found in the Next-to-Minimal Supersymmetric Standard Model. The last term is the extra $U(1)_N$ D term, particular to the E$_6$SSM. One finds that the upper bound of the lightest Higgs mass is around 140 GeV at $\tan\beta \sim 1-2$, in comparison to the upper bound in the MSSM and NMSSM of 120 GeV and 130 GeV respectively.

One loop and two loop upper bounds are calculated in [101]. The upper bound of the lightest Higgs mass in the leading approxiamation is given by

$$m^2_{h1} \lesssim \frac{\lambda^2}{2}v^2\sin^2 2\beta + M_Z^2\cos^2 2\beta + \frac{M_Z^2}{4}\left(1+\frac{1}{4}\cos 2\beta\right)^2 + \Delta^t_{11} + \Delta^D_{11}, \tag{2.27}$$

where Δ^t_{11} and Δ^D_{11} are one-loop corrections from the top-quark and D-quark supermultiplets. When $m^2_{D_i} = m^2_{\bar{D}_i} = M_S^2$, the contribution from the D-quark reads

$$\Delta^D_{11} = \sum_{i=1,2,3}\frac{3\lambda^2\kappa_i^2 v^2}{32\pi^2}\sin^2\beta\ln\left[\frac{m_{D_{1,i}}m_{D_{2,i}}}{Q^2}\right], \tag{2.28}$$

With this correction, the upper bound for lightest Higgs mass can be 155 GeV when $\tan\beta \sim 1-2$.

2.5 Signals of E_6SSM on Colliders

The existence of an extra $U(1)$ symmetry leads to a Z' gauge boson in the E_6SSM. At tree level, the mass for Z' boson is determined by the vev of the singlet field S, so is constrained only by fine turning arguments to be of order the electroweak scale. However, collider experiments gives stringent constraints on the Z' mass and $Z-Z'$ mixing. The major constraint comes from $p\bar{p} \to Z' \to \ell^+\ell^-$ at Tevatron [114], which gives a lower bound on the Z' mass of 500-600 GeV, and $Z-Z'$ mixing $\lesssim (2-3)\times 10^{-3}$ [115]. In Ref. [116], an upper bound of $Z-Z'$ mixing $\sin\theta_{ZZ'}$ can be $\sim 10^{-2}$. For exotic quarks, the Tevatron, HERA and LEP exclude leptoquarks with mass $< 290\,\mathrm{GeV}$ [117] whereas CDF and D0 exclude diquark with mass $< 420\,\mathrm{GeV}$ [118].

In the E_6SSM, exotic squarks and non-Higgs (inert Higgs) masses are generated via SUSY breaking and therefore they are expected to be heavy (at the SUSY breaking scale). Exotic fermions, including exotic quarks and non-Higgsinos (the super-partner of non-Higgs) have masses associated with Yukawa couplings, hence they may be relatively lighter. So, we are interested in the signals of exotic fermions at colliders, which are expected to be lighter than Z'. We assume further that the mixing of $Z-Z'$ is smaller than the upper bound given in [116] in order to reduce the contribution to observables in the SM.

The presence of the Z' leads to a resonance in the differential distribution of lepton pair $\ell^+\ell^-$ production at the LHC. For exotic quarks, in the case of Z_H^2 symmetry is broken, the decay of exotic quarks are observable:

$$\begin{aligned} &\overline{D} \to t+\tilde{b} \quad \overline{D} \to b+\tilde{t} && \text{diquark}\,, \\ D \to t+\tilde{\tau} \quad D \to \tau+\tilde{t} \quad D \to b+\tilde{\nu_\tau} \quad D \to \nu_\tau+\tilde{b} \quad &&\text{leptoquark}\,. \end{aligned} \tag{2.29}$$

In addition, exotic quarks can enhance the cross section of $pp \to t\bar{t}b\bar{b} + X$ and $pp \to b\bar{b}b\bar{b} + X$. Non-Higgsinos decays similar to Higgsino: they decay majorly into the third generation of quarks and squarks or leptons and sleptons.

$$\begin{aligned} &\tilde{H}^0 \to t + \tilde{\bar{t}}\,, \qquad \tilde{H}^0 \to \bar{t} + \tilde{t}\,, \qquad \tilde{H}^0 \to b + \tilde{\bar{b}}\,, \qquad \tilde{H}^0 \to \bar{b} + \tilde{b}\,, \\ &\tilde{H}^0 \to \tau + \tilde{\bar{\tau}}\,, \qquad \tilde{H}^0 \to \bar{\tau} + \tilde{\tau}\,, \qquad \tilde{H}^- \to b + \tilde{\bar{t}}\,, \qquad \tilde{H}^- \to \bar{t} + \tilde{b}\,, \\ &\qquad\qquad \tilde{H}^- \to \tau + \tilde{\bar{\nu}}_\tau\,, \qquad \tilde{H}^- \to \bar{\nu}_\tau + \tilde{\tau}\,. \end{aligned} \tag{2.30}$$

Moreover, the non-Higgsinos also enhance the cross section of the production of $Q\bar{Q}Q'\bar{Q}'$ and $Q\bar{Q}\tau^+\tau^-$, where Q is a heavy quark. This would lead to an excess in the b, t and exotic D quark pair production cross section at LHC.

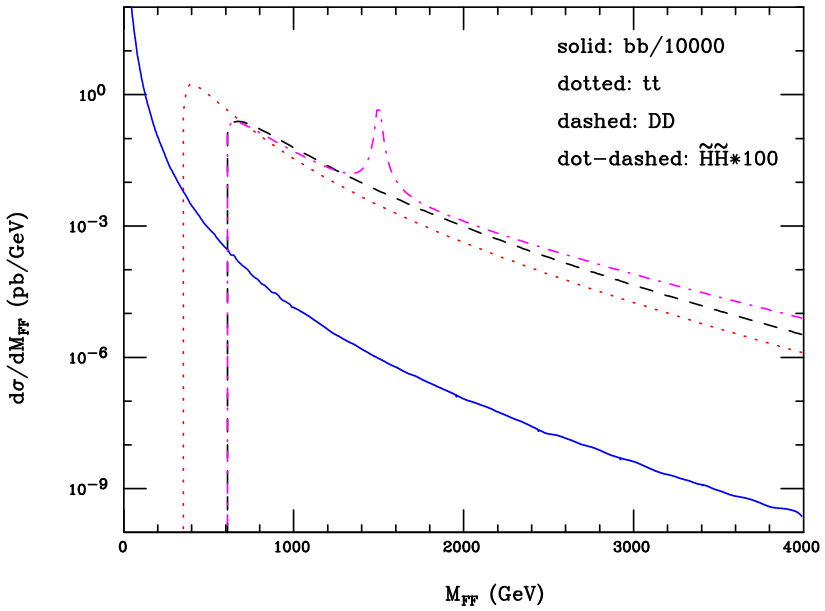

Figure 2.1: Differential cross section at the LHC for pair production of b-, t- and exotic D-quarks, for $\mu_{Di} = \mu_{Hi} = 300\,\text{GeV}$and $M_{Z'} = 1.5$ TeV. Figure is taken from [101].

Chapter 3

The Lepton Asymmetries in E_6SSM

In the E_6SSM, exotic particles couple to the RH neutrino via Yukawa couplings. They can play the role of final states of the RH neutrino decays and contribute the CP asymmetry of RH neutrino decay via one-loop Feynman diagrams. As discussed in Chapter 1, we need to extend the canonical model to avoid the Davidson-Ibarra bound. Previous work in this field includes: *e.g.* Leptogenesis with an additional Higgs triplet [123], Leptogenesis in NMSSM [124], Leptogenesis in an E_6 model [125], Leptogenesis in the right-handed sector [126], Leptogenesis with a fourth generation lepton [127], post-sphaleron Baryogenesis [128] and Leptogenesis from triplet Higgs [129] [130] [131], soft leptogenesis [132], resonant leptogenesis [133] and leptogenesis with additional particle [134].

In this chapter, we calculate the flavoured CP asymmetries of the lightest RH neutrino decay in three scenarios of the E_6SSM, *(a)* the case of unbroken Z_2^H symmetry, *(b)* model I with broken Z_2^H *(a)* model II with broken Z_2^H symmetry. The dependence of CP asymmetries on exotic Yukawa couplings are illustrated in linear and countour plots. We find that the CP asymmmetries can be enhancecd drastically if the exotic Yukawa couplings are relatively large.

3.1 Flavoured Lepton Asymmetries

In Chapter 1, the decay asymmetry of RH neutrinos was written as a summation over all flavours ε. However, to calculate the final baryon asymmetry more precisely, one should consider "flavoured lepton asymmetries" [135] of RH neutrino decays for two reasons. The first is the Yukawa interaction may be in equilibrium for some flavours whereas not in equilibrium for other flavours. This results in left-handed lepton doublets with different flavours may not have equal number density, and therefore the reaction densities for wash-out processes vary for different flavours. The second is when scatterings as wash-out processes are taken into account, the reaction densities for scatterings are also different. However, in Section (4.5), we will discuss the scenario where the soft SUSY breaking mass terms may lead to the flavour transition between leptons and quarks in equilibrium. In this case, Boltzmann Equations with the total lepton asymmetry are used.

3.2 CP asymmetries for Model I

In this section, we discuss the CP asymmetries of RH neutrino decays in Model I, where an additional inert Higgs fields and the "forth generation" lepton are involved. We calculate the flavoured lepton asymmetries of RH neutrino decays and show the lepton asymmetries can be enhanced drastically.

The terms related to RH neutrino decay can be found in Eqs. (2.8) and (2.11). We summarise it as

$$W_N = h^N_{kxj}(H^u_k L_x)N^c_j\,, \tag{3.1}$$

where h^N_{kxj} is the Yukawa couplings for RH neutrinos. The family indices run over $x = 1,2,3,4$ and $k,i,j = 1,2,3$, with $x = 4$ corresponding to the exotic lepton L_4.

The CP asymmetry can be defined as

$$\varepsilon_{1,\,\ell_k} \equiv \frac{\Gamma_{N_1\ell_k} - \Gamma_{N_1\bar{\ell}_k}}{\sum_m \left(\Gamma_{N_1\ell_m} + \Gamma_{N_1\bar{\ell}_m}\right)}\,. \tag{3.2}$$

where $\Gamma_{N_1\ell_k}$ and $\Gamma_{N_1\bar{\ell}_k}$ are respectively the partial decaying widths of $N_1 \to L_k + H_{1,3}$ and $N_1 \to \overline{L}_k + H^*_{1,3}$ with $k, m = 1, 2, 3$. At tree level, we have $\Gamma_{N_1\ell_k} = \Gamma_{N_1\bar{\ell}_k}$ for all flavours and the lepton asymmetries are zero. Small CP asymmetries arise at one-loop if the Yukawa couplings are complex with CP phases.

In supersymmetric models, RH neutrinos are allowed to decay into sleptons $\widetilde{L}_k$ and Higgsino $\widetilde{H}_u$, therefore the decay width of RH neutrinos is doubled due to the extra channel sharing the same Yukawa coupling. When considering the CP asymmetries in supersymmetric models, one should treat sleptons in the final state in the same way as leptons, as the sleptons are unstable particles, which decay into leptons and gauginos at a later stage. The corresponding flavour CP asymmetries are defined as:

$$\varepsilon_{1,\widetilde{\ell}_k} = \frac{\Gamma_{N_1\widetilde{\ell}_k} - \Gamma_{N_1\widetilde{\ell}^*_k}}{\sum_m \left(\Gamma_{N_1\widetilde{\ell}_m} + \Gamma_{N_1\widetilde{\ell}^*_m}\right)} \,. \tag{3.3}$$

In addition, Supersymmetry leads to an extra source of lepton asymmetries: the scalar partner of the RH neutrino, the RH sneutrino $\widetilde{N}_1$. Sneutrinos decay into lepton and Higgsino and into slepton and Higgs. The CP asymmetries for the RH sneutrino decay are also defined as the lepton number produced per $\widetilde{N}_1$ decay:

$$\varepsilon_{\widetilde{1},\ell_k} = \frac{\Gamma_{\widetilde{N}^*_1\ell_k} - \Gamma_{\widetilde{N}_1\bar{\ell}_k}}{\sum_m \left(\Gamma_{\widetilde{N}^*_1\ell_m} + \Gamma_{\widetilde{N}_1\bar{\ell}_m}\right)} \,, \qquad \varepsilon_{\widetilde{1},\widetilde{\ell}_k} = \frac{\Gamma_{\widetilde{N}_1\widetilde{\ell}_k} - \Gamma_{\widetilde{N}^*_1\widetilde{\ell}^*_k}}{\sum_m \left(\Gamma_{\widetilde{N}_1\widetilde{\ell}_m} + \Gamma_{\widetilde{N}^*_1\widetilde{\ell}^*_m}\right)} \,. \tag{3.4}$$

In SUSY models one finds the relation between CP asymmetries of RH neutrino decays and RH sneutrino decays:

$$\varepsilon_{1,\ell_k} = \varepsilon_{1,\widetilde{\ell}_k} = \varepsilon_{\widetilde{1},\ell_k} = \varepsilon_{\widetilde{1},\widetilde{\ell}_k} \,. \tag{3.5}$$

In the Exceptional SUSY model, extra particles are introduced, which result in the new channels of the decays of RH (s)neutrino. Effectively, we consider them as extra flavours and the definitions of CP asymmetries of RH neutrino decay is intact. In the E_6SSM Model I, only inert Higgs superfield and the exotic lepton superfield L_4 are allowed to have non-zero Yukawa couplings to the RH neutrino superfields (see Eq. (2.8)). At the scale of temperature of Leptogenesis ($T \sim M_{N_1}$), the extra inert Higgs remains massless

and the "fourth family" of the vector like lepton has a mass of order of TeV, which is much smaller than RH (s)neutrino masses. Then, the decay of RH (s)neutrino into inert Higgs and L_4 is allowed. The complete set of decay channels of the RH (s)neutrino includes

$$N_1 \to L_x + H_k^u, \qquad N_1 \to \widetilde{L}_x + \widetilde{H}_k^u, \qquad \widetilde{N}_1 \to \bar{L}_x + \overline{\widetilde{H}}_k^{\,u}, \qquad \widetilde{N}_1 \to \widetilde{L}_x + H_k^u. \tag{3.6}$$

The family index $x = 1, 2, 3, 4$, where 4 stands for the exotic lepton. The decay width of N_1 and $\widetilde{N}_1$ are determined by the Yukawa couplings h^N_{kx1} and the mass of the lightest RH neutrino N_1. Supersymmetry implies that

$$\Gamma^k_{N_1\ell_x} + \Gamma^k_{N_1\bar{\ell}_x} = \Gamma^k_{N_1\widetilde{\ell}_x} + \Gamma^k_{N_1\widetilde{\ell}^*_x} = \Gamma^k_{\widetilde{N}^*_1\ell_x} = \Gamma^k_{\widetilde{N}_1\bar{\ell}_x} = \Gamma^k_{\widetilde{N}_1\widetilde{\ell}_x} = \Gamma^k_{\widetilde{N}^*_1\widetilde{\ell}^*_x} = \frac{|h^N_{kx1}|^2}{8\pi}\, M_1\,, \tag{3.7}$$

where the superscript $k = 3$ represents either "active" Higgs or Higgsino and $k = 1, 2$ stands for inert Higgs or Higgsino in the final state. We work in a framework where the charged lepton Yukawa matrix and mass matrix of the RH neutrinos are both diagonal. We also make the assumption of supersymmetry breaking at the TeVscale, which is negligibly small compared with M_1, and therefore all soft SUSY breaking terms can be safely neglected in the calculation of decaying rates and CP asymmetries. Also when the Leptogenesis occurs, SUSY is exact and therefore there is no supersymmetric contribution to the RH sneutrino mass. The lightest RH neutrino mass is equal to the lightest RH sneutrino mass.

Each decay channel (3.2) corresponds to a CP asymmetry that contributes to the generation of lepton/baryon asymmetry. In the E_6SSM Model I, the CP asymmetries (3.2) of the decays of the lightest RH neutrino can be generalised as

$$\varepsilon^k_{1,\,f} \;=\; \frac{\Gamma^k_{N_1 f} - \Gamma^k_{N_1 \bar{f}}}{\sum_{m,\,f'}\left(\Gamma^m_{N_1 f'} + \Gamma^m_{N_1 \bar{f}'}\right)}\,, \tag{3.8}$$

where f and f' could be either ℓ_x or $\widetilde{\ell}_x$ while $\bar{f}$ and $\bar{f}'$ are the corresponding anti-particle fields $\bar{\ell}_x$ or $\widetilde{\ell}^*_x$. Here, $\varepsilon^3_{1,\,\ell_n}$ and $\varepsilon^3_{1,\,\widetilde{\ell}_n}$ $(n = 1, 2, 3)$ are flavour CP asymmetries that stem from the decays of the lightest RH neutrino into (s)leptons and (the neutral component of) the H_u (Higgsino $\widetilde{H}_u$), while $\varepsilon^3_{1,\,\ell_4}$, $\varepsilon^3_{1,\,\widetilde{\ell}_4}$, $\varepsilon^1_{1,\,f}$ and $\varepsilon^2_{1,\,f}$ are extra CP asymmetries result from N_1 decays into exotic lepton L_4 and inert Higgs. The denominators of Eq. (3.8) is

the total decay widths of the lightest RH neutrino. For $\varepsilon^{k}_{1,\,\ell_x}$ the total width includes all partial widths of N_1 decays into final state involving SM leptons and fermionic components of L_4. The expressions for $\varepsilon^{k}_{1,\,\widetilde{\ell}_x}$ contain in the denominator a sum of partial decay widths of N_1 over all possible decay modes that have either slepton or scalar components of L_4 in the final state. The CP asymmetries caused by the decays of the lightest RH sneutrino $\varepsilon^{k}_{\widetilde{1},\,f}$ can be defined similarly to the neutrino ones. In this case the RH neutrino field in Eqs. (3.8) ought to be replaced by either $\widetilde{N}_1$ or $\widetilde{N}^{*}_1$.

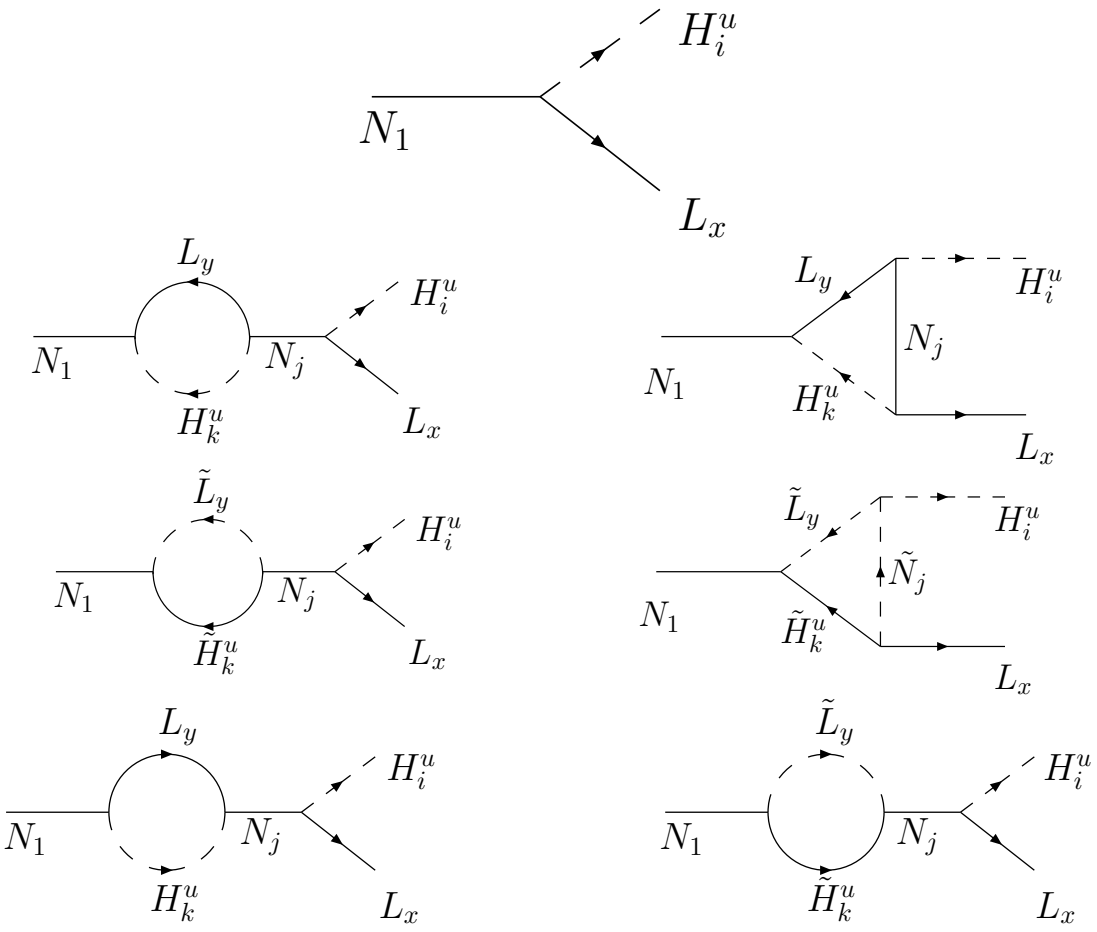

Figure 3.1: Diagrams that give contribution to the CP asymmetries in the E_6SSM Model I, including the presence of two extra inert Higgs doublets, and the fourth family lepton doublet.

As in the SM and MSSM, the CP asymmetries of the E_6SSM Model I stem from the interference between the tree-level amplitudes of the lightest RH neutrino decays and one-loop corrections to them, including self-energy and vertex diagrams. The corresponding tree-level and one-loop diagrams are shown in Fig. 3.1 - 3.2. The calculation to one-loop

yields

$$\begin{aligned}\varepsilon^{k}_{1,\,\ell_x} &= \varepsilon^{k}_{1,\,\widetilde{\ell}_x} = \varepsilon^{k}_{\widetilde{1},\,\ell_x} = \varepsilon^{k}_{\widetilde{1},\,\widetilde{\ell}_x} = \frac{1}{4\pi A_1}\sum\nolimits_{j=2,3}\mathrm{Im}\Big\{A_j h^{N*}_{kx1}h^{N}_{kxj} f^{S}\left(\frac{M_j^2}{M_1^2}\right) \\ &+ \sum\nolimits_{m,\,y} h^{N*}_{my1}h^{N}_{mxj}h^{N}_{kyj}h^{N*}_{kx1}\, f^{V}\left(\frac{M_j^2}{M_1^2}\right)\Big\},\end{aligned} \tag{3.9}$$

where,

$$A_j = \sum\nolimits_{m,y}\left(h^{N*}_{my1}h^{N}_{myj} + \frac{M_1}{M_j}h^{N}_{my1}h^{N*}_{myj}\right),$$
$$f^{S}(z) = \frac{2\sqrt{z}}{1-z}, \qquad f^{V}(z) = -\sqrt{z}\,\ln\left(\frac{1+z}{z}\right),$$

with $k, m = 1, 2, 3$ and $x, y = 1, 2, 3, 4$. In the right-hand side of Eq. (3.9), the terms in the first line are induced by the self-energy diagrams while terms in the second line come from vertex corrections. It is worth to notice here that the coefficients in front of $f^S(x)$ and $f^V(x)$ are not the same, in contrast to the realisations of Leptogenesis in the SM and MSSM. It means that in general vertex and self-energy contributions to $\varepsilon_{1,\,f}$ and $\varepsilon_{\widetilde{1},\,f}$ are not related to each other in the considered model. This is a common feature of the models in which right-handed Majorana neutrinos interact with a few lepton doublets and with doublets that have quantum numbers of Higgs fields.

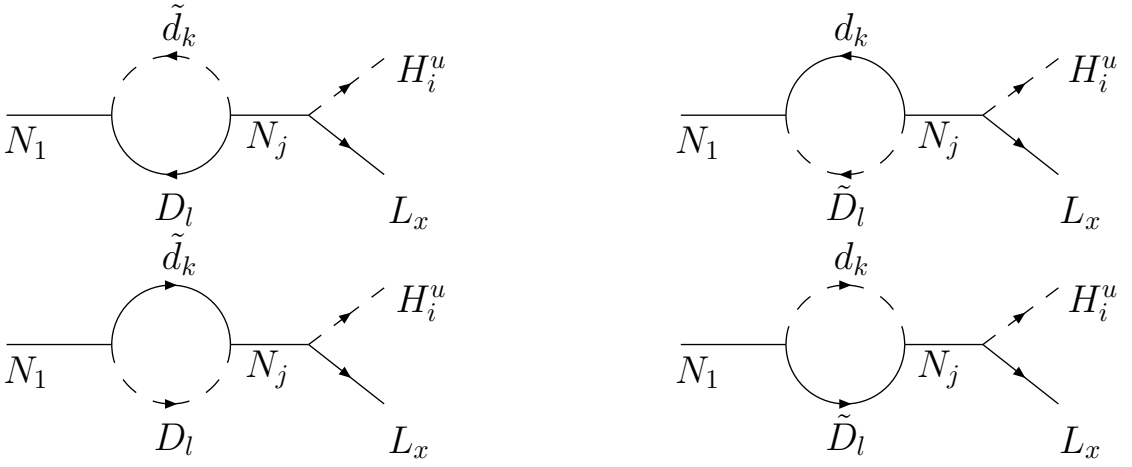

Figure 3.2: Extra one–loop diagrams involving internal leptoquarks D that contribute to the CP asymmetries associated with the decays $N_1 \to L_x + H_k^u$ in the E_6SSM Model II.

Since inert Higgs and inert Higgsino fields do not carry lepton number, they are not variables in the Boltzmann Equation, which describe the evolution of lepton/baryon

number densities in the universe. It is useful to define the overall CP asymmetries which are associated with each flavour, i.e.

$$\varepsilon^{tot}_{1,\,f} = \sum_k \varepsilon^k_{1,\,f}\,, \qquad\qquad \varepsilon^{tot}_{\widetilde{1},\,f} = \sum_k \varepsilon^k_{\widetilde{1},\,f}\,. \tag{3.10}$$

These overall decay asymmetries represent the total net lepton number produced from one unit RH neutrino decay, irrespective of which Higgs field the corresponding lepton is associated with. The CP asymmetries (3.9) can then be rewritten in a compact form

$$\varepsilon^{tot}_{1,\,f} = \varepsilon^{tot}_{\widetilde{1},\,f} = \frac{1}{8\pi(\mathrm{Tr}\Pi^1)}\sum_{j=2,3}\mathrm{Im}\left\{A_j\Pi^j_{ff}f^S\left(\frac{M_j^2}{M_1^2}\right) + (\Pi^j)^2_{ff}f^V\left(\frac{M_j^2}{M_1^2}\right)\right\}, \tag{3.11}$$

where

$$\Pi^j_{\ell_y\ell_x} = \Pi^j_{\tilde{\ell}_y\tilde{\ell}_x} = \sum_m h^{N*}_{my1}h^N_{mxj}\,, \tag{3.12}$$

are three 4×4 matrices and $A_j = \mathrm{Tr}\,\Pi^j + \dfrac{M_1}{M_j}\mathrm{Tr}\,\Pi^{j*}$. Eqs. (3.11)-(3.12) indicate that despite a large number of new couplings appearing due to the breakdown of the Z_H^2 symmetry, only some combinations contribute to the generation of lepton asymmetries. The parametrisation of the overall flavour CP asymmetries presented above can be used in any model in which the lightest right-handed neutrino can decay into lepton multiplets and $SU(2)_W$ doublets that have quantum numbers of Higgs fields.

In the case of unbroken Z_2^H symmetry, the analytic expressions for the decay asymmetries (3.9) and (3.11) are simplified dramatically. In particular, CP asymmetries $\varepsilon^1_{1,\,f}$ and $\varepsilon^2_{1,\,f}$ which are associated with the decays of N_1 into either the scalar or fermion components of inert Higgs superfields $H_{2\alpha}$ vanish. The analytical expressions for the other decay asymmetries reduce to

$$\varepsilon^3_{1,\,\ell_x} = \varepsilon^3_{1,\,\widetilde{\ell}_x} = \varepsilon^3_{\widetilde{1},\,\ell_x} = \varepsilon^3_{\widetilde{1},\,\widetilde{\ell}_x} = \frac{1}{8\pi}\frac{\sum_{j=2,3}\mathrm{Im}\left[h^{N*}_{3x1}B_{1j}h^N_{3xj}\right]}{\sum_y |h^N_{3y1}|^2}\,, \tag{3.13}$$

where

$$B_{1j} = \sum_y\left\{h^{N*}_{3y1}h^N_{3yj}g\left(\frac{M_j^2}{M_1^2}\right) + \frac{M_1}{M_j}h^N_{3y1}h^{N*}_{3yj}f^S\left(\frac{M_j^2}{M_1^2}\right)\right\}, \tag{3.14}$$

and

$$g(z) = f^V(z) + f^S(z) = \sqrt{z}\left[\frac{2}{1-z} - \ln\left(\frac{1+z}{z}\right)\right], \tag{3.15}$$

where x and y vary from 1 to 4. If the second lightest and heaviest right-handed neutrinos are significantly heavier than the lightest one, i.e. M_2, $M_3 \gg M_1$, the formulae for the CP asymmetries (3.13) are simplified even further

$$\varepsilon^3_{1,\ell_x} \simeq -\frac{3}{8\pi}\sum\nolimits_{j=2,3} \frac{\mathrm{Im}\left[(h^{N\dagger}h^N)_{1j}h^{N*}_{3x1}h^N_{3xj}\right]}{(h^{N\dagger}h^N)_{11}}\,\frac{M_1}{M_j}\,, \tag{3.16}$$

where $(h^{N\dagger}h^N)_{1j} = \sum_y h^{N*}_{3y1}h^N_{3yj}$. From Eq. (3.13-3.15) one can see that in this case the self-energy contribution to the flavour CP asymmetries is twice as large as the vertex contribution.

The analytic expressions for the CP asymmetries (3.13)-(3.16) are very similar to the MSSM ones. Moreover in the limit $h^N_{34j} \to 0$ the extra CP asymmetries induced by the decays

$$N_1 \to L_4 + H_u, \qquad N_1 \to \widetilde{L}_4 + \widetilde{H}_u, \qquad \widetilde{N}_1 \to \bar{L}_4 + \overline{\widetilde{H}}_u, \qquad \widetilde{N}_1 \to \widetilde{L}_4 + H_u, \tag{3.17}$$

vanish and the MSSM results for the flavoured lepton decay asymmetries are reproduced. However if h^N_{34j} have non-zero values, the generation of lepton asymmetry in the MSSM and E$_6$SSM with unbroken Z_2^H can be entirely different due to the presence of superfields L_4 in the E$_6$SSM. Indeed, since h^N_{34j} can be of the order of, or even larger than, the Yukawa couplings of the ordinary lepton superfields to the Higgs doublet H_u, the decay rates and CP asymmetries associated with the decays (3.17) can be substantially larger than other decay rates and asymmetries. The fermion and scalar components of the supermultiplet L_4 being produced in the decays of the lightest right-handed neutrino and sneutrino sequentially decay either to the leptons or to the sleptons, changing the induced lepton number asymmetries.

3.2.1 CP asymmetries for the Model II

In the E_6SSM Model II there are, in addition to the states in Model I, exotic leptoquarks which carry baryon and lepton numbers simultaneously. In this case quark-lepton couplings of $\overline{D}_i$ and D_i in the superpotential do not violate either baryon or lepton $U(1)$ global symmetries so that these interactions are allowed from the phenomenological point of view. On the other hand these couplings violate Z_2^H symmetry and therefore the corresponding interactions should be rather weak.

The non-zero complex Yukawa couplings of the leptoquarks to the right-handed Majorana neutrinos (see Eq.(2.8)) give rise to extra contributions to the CP asymmetries which correspond to different lepton flavours. These contributions come from the one-loop self-energy diagrams shown in Fig. 3.3 that contain virtual (possibly exotic) quarks and squarks. Since Yukawa couplings of the leptoquarks do not induce any one-loop vertex corrections to the amplitude of the decay of the lightest right-handed neutrino, lepton decay asymmetries can be described by Eqs. (3.8) in which A_2 and A_3 should be replaced by $\widetilde{A}_2$ and $\widetilde{A}_3$ where

$$\widetilde{A}_j = A_j + \frac{3}{2}\sum_{m,n}\left(g^{N*}_{mn1}g^{N}_{mnj} + \frac{M_1}{M_j}g^{N}_{mn1}g^{N*}_{mnj}\right). \tag{3.18}$$

At the same time, the interactions of D_i and $\overline{D}_i$ with N_1 and quark superfields give rise to the new channels of the lightest right-handed neutrino and sneutrino decays

$$N_1 \to D_k + \widetilde{d^c}_i, \quad N_1 \to \widetilde{D}_k + d^c_i, \quad \widetilde{N}_1 \to \overline{D}_k + d_i, \quad \widetilde{N}_1 \to \widetilde{D}_k + \widetilde{d^c}_i, \tag{3.19}$$

where D_k and $\widetilde{D}_k$ are fermion and scalar components of leptoquark superfields while d_i and $\widetilde{d}_i$ are right-handed down type quarks and their superpartners. When the supersymmetry breaking scale lies considerably lower than the lightest right-handed neutrino mass M_1, the corresponding partial decay widths are determined by the Z_2^H symmetry violating Yukawa couplings g^N_{ki1} only, i.e.

$$\begin{aligned}\Gamma^i_{N_1 D_k} + \Gamma^i_{N_1 \bar{D}_k} = \Gamma^i_{N_1 \widetilde{D}_k} + \Gamma^i_{N_1 \widetilde{D}^*_k} = \Gamma^i_{\widetilde{N}^*_1 D_k} = \Gamma^i_{\widetilde{N}_1 \bar{D}_k} \\ = \Gamma^i_{\widetilde{N}_1 \widetilde{D}_k} = \Gamma^i_{\widetilde{N}^*_1 \widetilde{D}^*_k} = \frac{3|g^N_{ki1}|^2}{16\pi} M_1 \,.\end{aligned} \tag{3.20}$$

New channels of the decays of the lightest right-handed neutrino (or sneutrino) contribute to the generation of lepton asymmetry via the sequential decay of leptoquarks and their superpartners at low energies. Due to the lepton number conservation, each D_k and $\widetilde{D}_k$ produce a lepton in the final state whereas the decay of their antiparticles leads to the appearance of an anti-lepton. As a consequence one can calculate lepton CP asymmetries associated with each additional channel of the lightest right-handed neutrino (or sneutrino) decay (3.19). We define the CP asymmetries caused by the decays of N_1 into the exotic quarks (squarks) as follows

$$\varepsilon^{i}_{1,\,q_k} = \frac{\Gamma^{i}_{N_1 q_k} - \Gamma^{i}_{N_1 \bar{q}_k}}{\sum_{j,\,m}\left(\Gamma^{j}_{N_1 q_m} + \Gamma^{j}_{N_1 \bar{q}_m}\right)}\,. \tag{3.21}$$

In Eq. (3.21) q_k can be either leptoquark fermion fields D_k or their scalar superpartners $\widetilde{D}_k$ whereas $\bar{q}_k$ represents charge conjugate states $\overline{D}_k$ or $\widetilde{D}^{*}_{k}$. The superscripts i and j indicate the generation number of the down type quark or its superpartner in the final state. In the denominator of Eq. (3.21) we sum over possible partial widths of the decays of N_1 either into exotic quark and right-handed down type squark if $\varepsilon^{i}_{1,\,q_k} = \varepsilon^{i}_{1,\,D_k}$ or into exotic squark and ordinary d-quark if $\varepsilon^{i}_{1,\,q_k} = \varepsilon^{i}_{1,\,\widetilde{D}_k}$. The CP asymmetries $\varepsilon^{i}_{\widetilde{1},\,q_k}$ which originate from the decays of the lightest right-handed sneutrino into the exotic quark (squark) can be defined in a similar way replacing N_1 in Eq. (3.21) by either $\widetilde{N}_1$ or $\widetilde{N}^{*}_{1}$. It is worth noticing that here we treat the CP asymmetries for the right-handed neutrino (sneutrino) decays to leptons and leptoquarks separately. In other words we do not combine together all possible partial widths of the decays of N_1 into exotic quarks (squark) and leptons (sleptons) in the denominator of Eq. (3.21) because leptoquarks and lepton fields carry different quantum numbers.

In the tree level approximation, the CP asymmetries which are associated with the new decay modes of N_1 and $\widetilde{N}_1$ (3.19) vanish. The non-zero values of $\varepsilon^{i}_{1,\,q_k}$ are induced after the inclusion of one-loop vertex and self-energy corrections to the decay amplitudes of N_1 and $\widetilde{N}_1$ if some of the Yukawa couplings of the right-handed Majorana neutrinos to leptons and quarks are complex. The tree-level and one-loop diagrams that contribute to the decay asymmetries (3.21) are presented in Fig. 3.3. The interference of the corresponding

tree-level decay amplitude with the one-loop corrections yields

$$\begin{aligned}\varepsilon^{i}_{1,\,D_k} &= \varepsilon^{i}_{1,\,\widetilde{D}_k} = \varepsilon^{i}_{\widetilde{1},\,D_k} = \varepsilon^{i}_{\widetilde{1},\,\widetilde{D}_k} = \frac{1}{8\pi A_0}\sum\nolimits_{j=2,3}\mathrm{Im}\Biggl\{\widetilde{A}_j g^{N}_{kij} g^{N*}_{ki1} f^{S}\left(\frac{M_j^2}{M_1^2}\right) \\ &+ \sum\nolimits_{m,\,n} g^{N*}_{mn1} g^{N}_{mij} g^{N}_{knj} g^{N*}_{ki1} f^{V}\left(\frac{M_j^2}{M_1^2}\right)\Biggr\},\end{aligned} \tag{3.22}$$

where $A_0 = \sum_{k,\,i} g^{N}_{ki1} g^{N*}_{ki1}$. As before, supersymmetry ensures that the CP asymmetries originating from the decays of the lightest right-handed neutrino and sneutrino are equal. As in the case of the lepton decay asymmetries (3.13) the terms in the right-hand side of Eqs. (3.22) involving $\widetilde{A}_j$ stem from the self-energy diagrams while all other terms represent vertex corrections. Again the coefficients in front of $f^{S}(x)$ and $f^{V}(x)$ are not equal unlike the simplest realisations of Fukugita-Yanagida mechanism [80]. From Eq. (3.22) it follows that the decay asymmetries induced by the additional decay modes (3.19) depend not only on the Yukawa couplings of exotic quarks and squarks to the right-handed neutrino but also on the couplings of the right-handed neutrino to leptons and sleptons. Extra CP asymmetries (3.22) tend to zero when the Z_2^H symmetry violating Yukawa couplings g^{N}_{kij} vanish.

We can also define the overall decay asymmetries which are associated with each generation of exotic quarks, i.e.

$$\varepsilon^{tot}_{1,\,q_k} = \sum_{i}\varepsilon^{i}_{1,\,q_k}\,, \qquad\qquad \varepsilon^{tot}_{\widetilde{1},\,q_k} = \sum_{i}\varepsilon^{i}_{\widetilde{1},\,q_k}\,. \tag{3.23}$$

The overall decay asymmetries that stem from the decays of the lightest right-handed neutrino and sneutrino can be presented in the following form

$$\begin{aligned}\varepsilon^{tot}_{1,\,f} &= \frac{1}{8\pi(\mathrm{Tr}\Pi^{1})}\sum\nolimits_{j=2,3}\mathrm{Im}\Biggl\{\widetilde{A}_j\Pi^{j}_{ff} f^{S}\left(\frac{M_j^2}{M_1^2}\right) + (\Pi^{j})^2_{ff} f^{V}\left(\frac{M_j^2}{M_1^2}\right)\Biggr\}, \\ \varepsilon^{tot}_{1,\,k} &= \frac{1}{8\pi(\mathrm{Tr}\Omega^{1})}\sum\nolimits_{j=2,3}\mathrm{Im}\Biggl\{\widetilde{A}_j\Omega^{j}_{kk} f^{S}\left(\frac{M_j^2}{M_1^2}\right) + (\Omega^{j})^2_{kk} f^{V}\left(\frac{M_j^2}{M_1^2}\right)\Biggr\}, \\ \widetilde{A}_j &= \mathrm{Tr}\Pi^{j} + \frac{M_1}{M_j}\mathrm{Tr}\Pi^{j*} + \frac{3}{2}\left(\mathrm{Tr}\Omega^{j} + \frac{M_1}{M_j}\mathrm{Tr}\Omega^{j*}\right),\end{aligned} \tag{3.24}$$

where we set $\varepsilon^{tot}_{1,\,D_k} = \varepsilon^{tot}_{1,\,\widetilde{D}_k} = \varepsilon^{tot}_{\widetilde{1},\,D_k} = \varepsilon^{tot}_{\widetilde{1},\,\widetilde{D}_k} = \varepsilon^{tot}_{1,\,k}$, $\Omega^{j}_{ki} = \sum_m g^{N*}_{km1} g^{N}_{imj}$ while Π^{j}_{mn} are given by Eqs. (3.12). Compact parametrisation of the overall CP asymmetries (3.24) allows elimination of a number of parameters on which total lepton asymmetry does not depend.

3.3 Numerical Results and Discussions

We now consider the impact of new particles and interactions appearing in the E_6SSM on the numerical values of the lepton CP asymmetries originating from the decays of the lightest right-handed neutrino and sneutrino. These decay asymmetries depend on all Yukawa couplings of neutrino superfields. Since the purpose of our studies here is to reveal the impact of extra couplings on the CP asymmetries we shall fix the Yukawa couplings of the lightest right-handed neutrino and sneutrino to lepton and Higgs superfields so that the observed pattern of neutrino masses and mixing angles is reproduced.

Here, as an example, we concentrate on the see-saw models [136] with sequential dominance (SD) of right-handed neutrinos [137]-[139] which lead to the appropriate neutrino spectrum in a technically natural way, i.e. small perturbations in the high energy input parameters do not change substantially the neutrino mass splittings at low energies. This means that small neutrino mass splittings are preserved in the presence of radiative corrections[1].

3.3.1 Constrained Sequential Dominance

To review how sequential dominance works we begin by writing the right-handed neutrino Majorana mass matrix in a diagonal basis as

$$M_{RR} = \begin{pmatrix} M_1 & 0 & 0 \\ 0 & M_2 & 0 \\ 0 & 0 & M_3 \end{pmatrix} \tag{3.25}$$

[1]In general the radiative corrections in see-saw models may be sufficient to destroy (or create) the cancellations necessary to achieve the desired mass hierarchy [140].

and the matrix of Yukawa couplings of the right-handed neutrino to lepton and Higgs fields h^N_{ij} in terms of (1, 3) column vectors A_i, B_i and C_i as

$$h^N_{ij} = (A \quad B \quad C) = \begin{pmatrix} d & a & a' \\ e & b & b' \\ f & c & c' \end{pmatrix}. \tag{3.26}$$

In sequential dominance, we assume

$$\frac{A_i A_j}{M_1} \gg \frac{B_i B_j}{M_2} \gg \frac{C_i C_j}{M_3}\,, \tag{3.27}$$

which is supported by the strong hierarchy in RH neutrino masses $M_1 \ll M_2 \ll M_3$. In addition, we assume that $|d| \ll |e| \sim |f|$. The breakdown of electroweak symmetry induces Majorana mass terms for the left-handed neutrinos via the Yukawa interactions of the neutrino with the Higgs fields. After the integrating out the right-handed neutrinos we get

$$\mathcal{L}^{\nu}_{mass} = \frac{(\nu_i^T A_i)(A_j^T \nu_j)}{M_1} v_2^2 + \frac{(\nu_i^T B_i)(B_j^T \nu_j)}{M_2} v_2^2 + \frac{(\nu_i^T C_i)(C_j^T \nu_j)}{M_3} v_2^2\,, \tag{3.28}$$

where v_2 is a VEV of the Higgs doublet H_u. We can see that the dominant contribution to the neutrino masses is the first term of Eq.(3.27). The 3×3 mass matrix of the left-handed neutrino induced by $\mathcal{L}^{\nu}_{mass}$ can be diagonalised by means of a unitary transformation, the PMNS matrix in Eq. 1.8. The CHOOZ experiment sets a stringent constraint on the value of $\theta_{13} \lesssim 0.2$ [16]. We will assume that $\theta_{13} \ll 1$.

The sequential dominance implies that the first term in Eq. (3.28) gives a dominant contribution to the mass matrix of the left-handed neutrino, the second term is sub-dominant whereas the contribution of the last term in Eq. (3.28) is negligible [137]-[139]. This structure of the mass terms guarantees that the mass of the heaviest light neutrino m_3 is much larger than the mass of the second lightest one. If the heaviest left-handed neutrino is denoted ν_3 then sequential dominance results in the physical neutrino eigenstate $\nu_3 \simeq d\,\nu_e + e\,\nu_\mu + f\,\nu_\tau$ with the mass [138]

$$|m_3| \simeq (|d|^2 + |e|^2 + |f|^2) v_2^2 / M_1\,. \tag{3.29}$$

m_3 is associated with the atmospheric neutrino mass $\sqrt{\Delta m^2_{\rm atm}}$. Two other orthogonal combinations of neutrinos remain massless in the leading approximation. The requirement of a small angle θ^ν_{13} implies that $|d| \ll |e|, |f|$. Then the atmospheric angle θ_{23} is given by [138]

$$\tan\theta_{23} \approx \tan\theta^\nu_{23} \approx \frac{|e|}{|f|} \approx \frac{1}{\sqrt{2}}\,. \tag{3.30}$$

Although the leading approximation allows us to get an appropriate description of atmospheric neutrino data, we need to go beyond it to account for the data of other neutrino experiments. The contribution of the sub-leading right-handed neutrino does not substantially change the mass of the heaviest left-handed neutrino state (3.29) and atmospheric angle (3.30). However it gives rise to non-zero second lightest neutrino mass. The sub-leading contributions to the left-handed neutrino mass matrix also induce mixing between the heaviest and other left-handed neutrino states. The neutrino mass matrix can be reduced to the block diagonal form by means of unitary transformations U_{13} if

$$\theta^\nu_{13} \approx e^{i(\tilde\phi+\phi_a-\phi_e)}\frac{|a|(e^*b+f^*c)}{(|e|^2+|f|^2)^{3/2}}\frac{M_1}{M_2} + e^{i(\tilde\phi+\phi_d-\phi_e)}\frac{|d|}{\sqrt{|e|^2+|f|^2}}\,, \tag{3.31}$$

where ϕ_x are the phases of Yukawa couplings, i.e. $x = |x|e^{i\phi_x}$. The relative phase $\phi_e - \phi_f$ is chosen so that the angle θ^ν_{23} is real. The phase $\tilde\phi$ is fixed by the requirement that the angle θ_{13} is real and positive. When $d = 0$ we get

$$\tilde\phi = \phi_e - \phi_a - \zeta\,, \qquad\qquad \zeta = \arg(e^*b + f^*c)\,. \tag{3.32}$$

It is worth to notice here that the angle θ^ν_{13} is automatically small in the considered approximation.

Finally, the left-handed neutrino mass matrix can be completely diagonalised by the R_{12} rotation. Then the second lightest left-handed neutrino gets mass [138]

$$|m_2| \simeq \frac{|a|^2 v_2^2}{M_2 \sin^2\theta^\nu_{12}}\,, \tag{3.33}$$

while the solar angle is given by [138]

$$\begin{gathered}\tan\theta_{12} \approx \tan\theta^\nu_{12} \simeq \frac{a}{b\cos\theta_{23} - ce^{i(\phi_e-\phi_f)}\sin\theta_{23}} = \frac{|a|}{|b|c_{23}\cos\phi'_b - |c|s_{23}\cos\phi'_c}\,, \\ \phi'_b = \phi_b - \phi_a - \tilde\phi - \delta\,, \qquad \phi'_c = \phi_c - \phi_a + \phi_e - \phi_f - \tilde\phi - \delta\,.\end{gathered} \tag{3.34}$$

Once again the phases can be chosen so that $\tan\theta_{12}^{\nu}$ is real and positive. This can be achieved if phases ϕ_b' and ϕ_c' satisfy the condition

$$|b|c_{23}\sin\phi_b' \approx |c|s_{23}\sin\phi_c' \,. \tag{3.35}$$

Note that in contrast with θ_{13}^{ν} the solar angle (3.34) is completely determined by the sub-leading couplings due to a natural cancellation of the leading contributions. Therefore this angle should be relatively large. The lightest left-handed neutrino state remains massless in the considered approximation. Its mass is generated by the sub-sub-leading couplings of the heaviest right-handed neutrino, i.e.

$$|m_1| \simeq O\left(\frac{|C|^2 v_2^2}{M_3}\right) \,. \tag{3.36}$$

Thus sequential dominance results in a full neutrino mass hierarchy $m_1 \ll m_2 \ll m_3$. Because SD does not require any fine tuning the contribution of radiative corrections to the neutrino masses and mixing angles is expected to be quite small, at the level of a few per cent [142].

Current neutrino oscillation data point strongly to a specific form for the lepton mixing matrix with effective bi-maximal mixing of ν_μ and ν_τ at the atmospheric scale and effective trimaximal mixing for ν_e, ν_μ and ν_τ at solar scale (tri-bimaximal mixing [143]). In the tri-bimaximal mixing scenario the PMNS matrix takes a form in Eq.(1.23). Comparing matrix (1.23) with the general parametrisation of the neutrino mixing matrix (1.8) one can easily establish that tri-bimaximal mixing scenario corresponds to $\theta_{13} = 0$, $\sin\theta_{12} = 1/\sqrt{3}$ and $\theta_{23} = \pi/4$. Within the framework of sequential dominance the vanishing of the mixing angle θ_{13} can be naturally achieved when

$$d \simeq 0 \,, \qquad\qquad e^* b + f^* c = (A^\dagger B) \simeq 0 \,. \tag{3.37}$$

Since in this case the bimaximal mixing between ν_μ and ν_τ implies that $|e| = |f|$ the conditions (3.37) constrain the Yukawa couplings of the second lightest right-handed neutrino. In particular, from Eq. (3.37) it follows that $|b| = |c|$. Taking into account that tri-bimaximal mixing also requires $\sin\theta_{12} = 1/\sqrt{3}$ one can show that within the sequential dominance the Yukawa couplings of the lightest and second lightest right-handed

neutrinos which correspond to the tri-bimaximal mixing scenario can be always chosen so that

$$d \simeq 0\,, \qquad f = -e = |A|e^{i\phi_A}\,, \qquad a = b = c = |B|e^{i\phi_B}\,. \tag{3.38}$$

This is so-called constrained sequential dominance (CSD) [144]. Note that CSD does not constrain the Yukawa couplings of the heaviest right-handed neutrino a', b' and c' because they only give sub-sub-dominant contribution to the neutrino mass matrix. Additional issues concerning the Leptogenesis in the neutrino models based on the seesaw mechanism and sequential right-handed neutrino dominance were discussed in [139], [145].

3.3.2 Results of numerical analysis

3.3.2.a E_6SSM with unbroken Z_H^2 symmetry

With the assumption of the constrained sequential dominance we calculate the values of the decay asymmetries in the E_6SSM. According to CSD one can ignore the contribution of the heaviest right-handed neutrino so that the analytical expressions for the CP asymmetries derived in Section 3 are considerably simplified. We start our analysis from the E_6SSM with exact Z_H^2 symmetry. In this case there is only one extra CP asymmetry associated with the decay of the lightest right-handed neutrino into scalar (fermion) components of the fourth lepton doublet superfield L_4 and Higgsinos (Higgs bosons). Substituting the pattern of Yukawa couplings that corresponds to the constrained sequential dominance into Eqs. (3.16) and neglecting the contribution of the heaviest right-handed neutrino to the CP asymmetries we get

$$\begin{aligned}
\varepsilon^3_{1,\,L_4} &\simeq \frac{3}{8\pi}\frac{|h^N_{H_3^u L_4 N_1}|^2|h^N_{H_3^u L_4 N_2}|^2\sin\phi_L}{2|A|^2+|h^N_{H_3^u L_4 N_1}|^2}\,\frac{M_1}{M_2}\,, \qquad \varepsilon^3_{1,\,e}=0\,,\\
\varepsilon^3_{1,\,\tau} &\simeq -\varepsilon^3_{1,\,\mu} \simeq \frac{3}{8\pi}\frac{|h^N_{H_3^u L_4 N_1}||h^N_{H_3^u L_4 N_2}||A||B|\sin\phi_{\mu\tau}}{2|A|^2+|h^N_{H_3^u L_4 N_1}|^2}\,\frac{M_1}{M_2}\,,\\
\phi_{\mu\tau} &= \phi_{41}+\phi_A-\phi_{42}-\phi_B\,, \qquad \phi_L = 2(\phi_{41}-\phi_{42})\,,
\end{aligned} \tag{3.39}$$

where $h^N_{H_3^u L_4 N_1} \equiv h^N_{341} = h^N_{41}$, $h^N_{H_3^u L_4 N_2} \equiv h^N_{342} = h^N_{42}$, $h^N_{H_3^u L_4 N_1} = |h^N_{H_3^u L_4 N_1}|e^{i\phi_{41}}$ and $h^N_{H_3^u L_4 N_2} = |h^N_{H_3^u L_4 N_2}|e^{i\phi_{42}}$. Note that in the limit when $h^N_{H_3^u L_4 N_1}$ and $h^N_{H_3^u L_4 N_2}$ go to zero all

CP asymmetries vanish. This is not an accident. When Yukawa couplings $h^N_{H^u_3 L_4 N_1}$ and $h^N_{H^u_3 L_4 N_2}$ tend to zero the interactions of the right-handed neutrinos with the Higgs and lepton superfields are exactly the same as in the MSSM. At the same time the conditions (3.37) which result in the natural realisation of the tri-bimaximal mixing scenario in the framework of sequential dominance ensure the vanishing of all decay asymmetries within the SM and the MSSM. Thus the induced values of the lepton decay asymmetries (3.39) are entirely caused by the new particles and interactions appearing in the E_6SSM.

The CP asymmetries (3.39) also vanish when all Yukawa couplings are real, i.e. CP invariance in the lepton sector is preserved. The decay asymmetries $\varepsilon^3_{1,\,L_4}$ and $\varepsilon^3_{1,\,\tau} = -\varepsilon^3_{1,\,\mu}$ attain their maximum absolute values when $\sin\phi_L$ and $\sin\phi_{\mu\tau}$ are equal to ± 1 respectively. The maximum absolute values of the CP asymmetries (3.39) are given by

$$\begin{aligned} |\varepsilon^3_{1,\,L_4}| &\simeq \frac{3}{8\pi}\frac{|h^N_{H^u_3 L_4 N_1}|^2 |h^N_{H^u_3 L_4 N_2}|^2}{2|A|^2 + |h^N_{H^u_3 L_4 N_1}|^2}\,\frac{M_1}{M_2}\,, \\ |\varepsilon^3_{1,\,\tau}| &= |\varepsilon^3_{1,\,\mu}| \simeq \frac{3}{8\pi}\frac{|h^N_{H^u_3 L_4 N_1}||h^N_{H^u_3 L_4 N_2}||A||B|}{2|A|^2 + |h^N_{H^u_3 L_4 N_1}|^2}\,\frac{M_1}{M_2}\,. \end{aligned} \tag{3.40}$$

The dependence of the maximum values of $|\varepsilon^3_{1,\,L_4}|$ and $|\varepsilon^3_{1,\,\tau}| = |\varepsilon^3_{1,\,\mu}|$ on the absolute values of the additional Yukawa couplings $|h^N_{H^u_3 L_4 N_1}|$ and $|h^N_{H^u_3 L_4 N_2}|$ is examined in Fig. 3.4, where we fix $(M_2/M_1) = 10$. To avoid problems related with the overproduction of gravitinos we assume that the mass of the lightest right-handed neutrino is relatively small $M_1 \simeq 10^7\,\mathrm{GeV}$. We also set $v_2 = v \simeq 246\,\mathrm{GeV}$ that corresponds to large values of $\tan\beta$ and choose parameters $|A|$ and $|B|$ so that the observed neutrino mass-squared differences are reproduced (see, for example, [46]). Here we have taken $|A| = 2.0 \times 10^{-5}$ and $|B| = 3.8 \times 10^{-5}$. In Figs. 3.4a and 3.4b the dependence of the maximum value of $|\varepsilon^3_{1,\,\tau}| = |\varepsilon^3_{1,\,\mu}|$ on $|h^N_{H^u_3 L_4 N_1}|$ and $|h^N_{H^u_3 L_4 N_2}|$ is studied whereas in Figs. 3.4c and 3.4d we plot the maximum value of $|\varepsilon^3_{1,\,L_4}|$ as a function of new Yukawa couplings. From Eqs.(3.40) and Figs. 3.4a and 3.4c it follows that both maximum absolute values of the CP asymmetries (3.40) grow monotonically with increasing of $|h^N_{H^u_3 L_4 N_2}|$. The dependence of $|\varepsilon^3_{1,\,L_4}|$ and $|\varepsilon^3_{1,\,\tau}| = |\varepsilon^3_{1,\,\mu}|$ on $|h^N_{H^u_3 L_4 N_1}|$ is more complicated. At small values of $|h^N_{H^u_3 L_4 N_1}|$ these decay asymmetries are small and increase when $|h^N_{H^u_3 L_4 N_1}|$ becomes larger. However if $|h^N_{H^u_3 L_4 N_1}|$ is much larger than $|A|$ the maximum absolute values of $|\varepsilon^3_{1,\,\tau}| = |\varepsilon^3_{1,\,\mu}|$ are

inversely proportional to $|h^N_{H^u_3 L_4 N_1}|$ and therefore diminish with increasing $|h^N_{H^u_3 L_4 N_1}|$ (See Fig. 3.4b). In contrast, the dependence on $|h^N_{H^u_3 L_4 N_1}|$ in $|\varepsilon^3_{1,\,L_4}|$ cancels between numerator and denominator making the dependence flat (See Fig. 3.4d). The CP asymmetries $|\varepsilon^3_{1,\,\tau}| = |\varepsilon^3_{1,\,\mu}|$ attain their maximal possible value at $|h^N_{H^u_3 L_4 N_1}| \simeq \sqrt{2}|A|$. Thus we establish the following theoretical restrictions on the values of decay asymmetries

$$|\varepsilon^3_{1,\,L_4}| \lesssim \frac{3M_1}{8\pi M_2}|h^N_{H^u_3 L_4 N_2}|^2\,, \qquad\qquad |\varepsilon^3_{1,\,\tau}| = |\varepsilon^3_{1,\,\mu}| \lesssim \frac{3\sqrt{2}M_1}{32\pi M_2}|h^N_{H^u_3 L_4 N_2}||B|\,. \tag{3.41}$$

One can easily see that the theoretical upper bounds on the absolute values of the CP asymmetries (3.41) are determined by the Yukawa couplings of the second lightest right-handed neutrino and do not depend on the Yukawa couplings of the lightest right-handed neutrino. In general the maximal absolute values of decay asymmetries diminish when the couplings $|h^N_{H^u_3 L_4 N_1}|$ and $|h^N_{H^u_3 L_4 N_2}|$ decrease (see Fig. 3.5).

There is also another general tendency that should be mentioned here. When $M_1 \ll 10^{13} - 10^{14}\,\mathrm{GeV}$ the absolute value of the CP asymmetry associated with the decay $N_1 \to L_4 + H_u$ tends to be considerably larger than lepton decay asymmetries $\varepsilon^3_{1,\,\mu}$ and $\varepsilon^3_{1,\,\tau}$ (see Figs. 3.4-3.5). This happens because lower masses of the right-handed neutrinos require smaller values of the Yukawa couplings of the Higgs doublet H_u to leptons. Otherwise the observed neutrino mass-squared differences can not be reproduced within the framework of sequential dominance. From Eqs. (3.29) and (3.33) it follows that $|A| \propto \sqrt{M_1|m_3|/v^2}$ while $|B| \propto \sqrt{M_2|m_2|/v^2}$. Thus for a fixed ratio M_1/M_2 the maximal possible values of the decay asymmetries $|\varepsilon^3_{1,\,\mu}|$ and $|\varepsilon^3_{1,\,\tau}|$ (3.41) diminishes as $\sqrt{M_1}$ when M_1 decreases. In fact, the decrease of lepton CP asymmetries with the mass of the lightest right-handed neutrino is a common feature of most see-saw models. This results in the lower bound on the lightest right-handed neutrino mass: $M_1 \gtrsim 10^9\,\mathrm{GeV}$ [146]. At the same time the results of our analysis presented in Figs. 3.5 demonstrate that within the E$_6$SSM with unbroken Z_2^H it is possible to generate an appreciable value of the CP asymmetry $|\varepsilon^3_{1,\,L_4}| = 10^{-6} - 10^{-4}$ even for $M_1 = 10^7\,\mathrm{GeV}$. This can be achieved if the Yukawa couplings of the fourth lepton doublet L_4 to the Higgs fields H_u vary from 0.01 to 0.1. At low energies the induced lepton asymmetry is transferred to the ordinary

lepton asymmetries via the decays of heavy L_4 and $\tilde{L}_4$ into leptons (sleptons) and Higgs fields H_d (Higgsinos $\tilde{H}_d$).

3.3.2.b E_6SSM Model I

In the case of the E_6SSM Model I two generations of inert-Higgs superfields H^u_α ($\alpha = 1,2$) contribute to ε_{1,ℓ_x} through loop diagrams and give rise to a set of extra decay asymmetries $\varepsilon^{\alpha}_{1,\ell_x}$ defined by Eq. (3.8). Because the Yukawa couplings of H^u_α to the quarks and leptons of the first two generation are expected to be rather small in order to avoid non-diagonal flavour transitions we assume that inert Higgs fields couple to the third generation fermions only. To simplify our analysis further we also assume that only one inert Higgs doublet H^u_2 has non-zero couplings with the doublet of leptons of the third generation and right-handed neutrinos. Then the analytic expression (3.13) for the overall CP asymmetries reduces to

$$\begin{aligned}
\varepsilon^{tot}_{1,\mu} &\simeq \frac{1}{4\pi}\frac{|h^N_{H^u_2 L_3 N_1}||h^N_{H^u_2 L_3 N_2}||A||B|\sin\phi_\mu}{2|A|^2+|h^N_{H^u_2 L_3 N_1}|^2}\,\frac{M_1}{M_2}\,, \qquad \varepsilon^{tot}_{1,e}=0\,,\\
\varepsilon^{tot}_{1,\tau} &\simeq \frac{\left(4|h^N_{H^u_2 L_3 N_1}||h^N_{H^u_2 L_3 N_2}||A||B|\sin\phi_\mu+3|h^N_{H^u_2 L_3 N_1}|^2|h^N_{H^u_2 L_3 N_2}|^2\sin\phi_\tau\right)}{8\pi(2|A|^2+|h^N_{H^u_2 L_3 N_1}|^2)}\,\frac{M_1}{M_2}\,,\\
\phi_\mu &= \phi_{231}+\phi_A-\phi_{232}-\phi_B\,, \qquad \phi_\tau = 2(\phi_{231}-\phi_{232})\,,
\end{aligned} \tag{3.42}$$

where $h^N_{H^u_2 L_3 N_1} \equiv h^N_{231}$, $h^N_{H^u_2 L_3 N_2} \equiv h^N_{232}$, $h^N_{H^u_2 L_3 N_1} = |h^N_{H^u_2 L_3 N_1}|e^{i\phi_{231}}$ and $h^N_{H^u_2 L_3 N_2} = |h^N_{H^u_2 L_3 N_2}|e^{i\phi_{232}}$. Here, to clarify the contribution of the inert-Higgs doublet, we set all Yukawa couplings of L_4 to the right-handed neutrinos to be zero.

As before the overall CP asymmetries (3.42) vanish in the MSSM limit of the E_6SSM when $h^N_{H^u_2 L_3 N_1}$ and $h^N_{H^u_2 L_3 N_2}$ go to zero. The decay asymmetries (3.42) also tend to zero if CP invariance is preserved in the lepton sector, i.e. phases of all Yukawa couplings vanish. Once again $\varepsilon^{tot}_{1,\mu}$ and $\varepsilon^{tot}_{1,\tau}$ reach their maximum absolute values when $\sin\phi_\mu$ and $\sin\phi_\tau$ are equal to ± 1. The corresponding maximum absolute values of the overall CP asymmetries

(3.42) can be written as

$$
\begin{aligned}
|\varepsilon^{tot}_{1,\mu}| &\simeq \frac{1}{4\pi}\frac{|h^N_{H^u_2 L_3 N_1}||h^N_{H^u_2 L_3 N_2}||A||B|}{2|A|^2+|h^N_{H^u_2 L_3 N_1}|^2}\,\frac{M_1}{M_2}\,, \\
|\varepsilon^{tot}_{1,\tau}| &\simeq \frac{\left(4|h^N_{H^u_2 L_3 N_1}||h^N_{H^u_2 L_3 N_2}||A||B|+3|h^N_{H^u_2 L_3 N_1}|^2|h^N_{H^u_2 L_3 N_2}|^2\right)}{8\pi\,(2|A|^2+|h^N_{H^u_2 L_3 N_1}|^2)}\,\frac{M_1}{M_2}\,.
\end{aligned}
\tag{3.43}
$$

In Figs. 3.6-3.7 we present the results of our numerical analysis of the decay asymmetries in the E_6SSM Model I. The dependence of the maximum values of $|\varepsilon^{tot}_{1,\mu}|$ and $|\varepsilon^{tot}_{1,\tau}|$ on $|h^N_{H^u_2 L_3 N_1}|$ and $|h^N_{H^u_2 L_3 N_2}|$ is studied in Fig. 3.6. As before we set $(M_2/M_1)=10$, $M_1\simeq 10^6\,\mathrm{GeV}$, $v_2\simeq v\simeq 246\,\mathrm{GeV}$ and adjust parameters $|A|$ and $|B|$ to reproduce the observed neutrino mass-squared differences. In Figs. 3.6a and 3.6b we plot the maximum value of $|\varepsilon^{tot}_{1,\mu}|$ as a function of $|h^N_{H^u_2 L_3 N_1}|$ and $|h^N_{H^u_2 L_3 N_2}|$ while the dependence of the maximum value of $|\varepsilon^{tot}_{1,\tau}|$ on these new Yukawa couplings is explored in Figs. 3.6c and 3.6d. From Eq. (3.43) one can see that at very small values of new Yukawa couplings ($|h^N_{H^u_2 L_3 N_1}|$, $|h^N_{H^u_2 L_3 N_2}| \ll |A|$ and $|B|$) the maximum absolute values of the overall CP asymmetry are proportional to $|h^N_{H^u_2 L_3 N_1}|\cdot|h^N_{H^u_2 L_3 N_2}|$. At so small values of $|h^N_{H^u_2 L_3 N_1}|$ and $|h^N_{H^u_2 L_3 N_2}|$ the maximum absolute value of the overall CP asymmetry associated with the decay of N_1 into τ-lepton is twice as large as the maximum value of $|\varepsilon^{tot}_{1,\mu}|$. The maximum values of $|\varepsilon^{tot}_{1,\mu}|$ and $|\varepsilon^{tot}_{1,\tau}|$ rise with increasing of $|h^N_{H^u_2 L_3 N_2}|$ (see Fig. 3.6a and 3.6c). When $|h^N_{H^u_2 L_3 N_2}| \gg |A|$, $|B|$ the value of $|\varepsilon^{tot}_{1,\tau}|$ tends to be much larger than $|\varepsilon^{tot}_{1,\mu}|$.

At small values of $|h^N_{H^u_2 L_3 N_1}|$ the maximum absolute values of both decay asymmetries also grow with increasing of $|h^N_{H^u_2 L_3 N_1}|$ independently of $|h^N_{H^u_2 L_3 N_2}|$ (see Fig. 3.7b and 3.7d). But $|\varepsilon^{tot}_{1,\mu}|$ attains its maximum possible value at $|h^N_{H^u_2 L_3 N_1}|=\sqrt{2}|A|$ whereas $|\varepsilon^{tot}_{1,\tau}|$ approach its upper bound at large values of $|h^N_{H^u_2 L_3 N_1}| \gg |A|$, $|B|$. When $|h^N_{H^u_2 L_3 N_1}|$ is significantly larger than $|A|$ and $|B|$ the maximum value of $|\varepsilon^{t}_{1,\mu}|$ is inversely proportional to $|h^N_{H^u_2 L_3 N_1}|$ while $|\varepsilon^{tot}_{1,\tau}|$ is almost independent of $|h^N_{H^u_2 L_3 N_1}|$. In the considered case the

theoretical upper bounds on $|\varepsilon^{tot}_{1,\mu}|$ and $|\varepsilon^{tot}_{1,\tau}|$ are given by

$$\begin{aligned} |\varepsilon^{tot}_{1,\tau}| &\lesssim \frac{M_1}{8\pi M_2}|h^N_{H_2^u L_3 N_2}|^2\left[3+\frac{4x}{12+\sqrt{8x+9}}\right], \qquad x=\frac{|B|^2}{|h^N_{H_2^u L_3 N_2}|^2}, \\ |\varepsilon^{tot}_{1,\mu}| &\lesssim \frac{\sqrt{2}M_1}{16\pi M_2}|h^N_{H_2^u L_3 N_2}||B|. \end{aligned} \tag{3.44}$$

As before the theoretical restrictions on the absolute values of CP asymmetries (3.44) are set by the Yukawa couplings of the second lightest right-handed neutrino and independent of the Yukawa couplings of the lightest right-handed neutrino. Because for a fixed ratio M_1/M_2 the values of $|A|$ and $|B| \propto \sqrt{M_1}$ the maximum possible value of $|\varepsilon^{tot}_{1,\mu}|$ decreases when M_1 becomes smaller while the theoretical upper bound on $|\varepsilon^{tot}_{1,\tau}|$ does not change much. As a consequence $|\varepsilon^{tot}_{1,\tau}|$ tends to dominate over $|\varepsilon^{tot}_{1,\mu}|$ at low masses of the lightest right-handed neutrino $M_1 \ll 10^{13}-10^{14}\,\mathrm{GeV}$ (see Figs. 3.6-3.7). Since the maximum possible value of $|\varepsilon^{tot}_{1,\tau}|$ is determined mainly by $|h^N_{H_2^u L_3 N_2}|$, which is not constrained by the neutrino oscillation data, an appreciable CP asymmetry within the E$_6$SSM Model I can be induced even when M_1 is relatively low. Fig. 3.7 demonstrates that for $M_1 \simeq 10^6\,\mathrm{GeV}$ the decay asymmetry $|\varepsilon^{tot}_{1,\tau}| = 10^{-6}-10^{-4}$ can be generated if $|h^N_{H_2^u L_3 N_2}|$ varies from 0.01 to 0.1.

3.3.2.c E$_6$SSM Model II

Within the E$_6$SSM Model II the lightest right-handed neutrino may decay into the leptoquarks (squarks) and down-type squarks (down-type quarks). New decay modes of the lightest right-handed neutrino lead to the set of extra CP asymmetries ε^i_{1,D_k} (3.21) which appear in addition to those arising in the E$_6$SSM Model I. Leptoquarks also give a substantial contribution to ε^k_{1,ℓ_x}, through loop diagrams if the corresponding Yukawa couplings g^N_{kij} are large enough. By construction the exotic quarks and squarks in the E$_6$SSM couple predominantly to the the quark and lepton superfields of the third generation. Therefore in our analysis we neglect the Yukawa couplings of the exotic quarks and squarks to the first and second generation particles. Moreover for simplicity we assume that only the third generation exotic quarks and squarks have appreciable couplings to the bosons and

fermions of the third generation and the Yukawa couplings of L_4 and H^u_α to the right-handed neutrinos vanish. In this approximation for the maximum absolute values of the CP asymmetries $|\varepsilon^3_{1,\tau}| = |\varepsilon^3_{1,\mu}|$ and $|\varepsilon^3_{1,D_3}|$ one obtains

$$|\varepsilon^3_{1,\tau}| = |\varepsilon^3_{1,\mu}| \simeq \frac{3|B|M_1}{16\pi|A|M_2}|g^N_{D_3d_3N_1}||g^N_{D_3d_3N_2}|\,, \qquad |\varepsilon^3_{1,D_3}| \simeq \frac{3M_1}{2\pi M_2}|g^N_{D_3d_3N_2}|^2\,, \quad (3.45)$$

where $g^N_{D_3d_3N_1} \equiv g^N_{331}$ and $g^N_{D_3d_3N_2} = g^N_{332}$. All other decay asymmetries vanish in the considered approximation. As before the maximum absolute values of the CP asymmetries (3.45) tend to zero if $g^N_{D_3d_3N_1} \to 0$ and $g^N_{D_3d_3N_2} \to 0$. However in contrast with the scenarios considered before the absolute values of the CP asymmetries $|\varepsilon^3_{1,\mu}|$ and $|\varepsilon^3_{1,\tau}|$ do not change when the lightest right-handed neutrino mass varies while M_1/M_2 remains intact. Indeed, according to the Eqs. (3.29) and (3.33) the ratio $|A|/|B|$ is proportional to $\sqrt{M_1/M_2}$. As a result the explicit dependence of the lepton decay asymmetries on the right-handed neutrino mass scale in Eq. (3.45) is partially cancelled. The maximum absolute values of the CP asymmetries (3.45) are determined by $|g^N_{D_3d_3N_1}|$ and $|g^N_{D_3d_3N_2}|$.

The dependence of the maximum values of $|\varepsilon^3_{1,\tau}| = |\varepsilon^3_{1,\mu}|$ and $|\varepsilon^3_{1,D_3}|$ on the Yukawa couplings $g^N_{D_3d_3N_1}$ and $g^N_{D_3d_3N_2}$ is examined in Fig. 3.8. Once again we fix $(M_2/M_1) = 10$, $v_2 \simeq 246\,\text{GeV}$ and choose $|A|$ and $|B|$ so that the phenomenologically acceptable pattern of the neutrino mass spectrum is reproduced. From Eq. (3.45) and Fig. 3.9 one can see that the decay asymmetries $|\varepsilon^3_{1,\tau}| = |\varepsilon^3_{1,\mu}|$ and $|\varepsilon^3_{1,D_3}|$ rise monotonically with increasing of $|g^N_{D_3d_3N_2}|$. The maximum absolute values of the lepton CP asymmetries also grow when $|g^N_{D_3d_3N_1}|$ increases. At the same time $|\varepsilon^3_{1,D_3}|$ does not depend on $|g^N_{D_3d_3N_1}|$. When $|g^N_{D_3d_3N_2}| \gg |g^N_{D_3d_3N_1}|$ the decay asymmetry $|\varepsilon^3_{1,D_3}|$ tends to be considerably larger than lepton decay asymmetries. At low energies the induced lepton asymmetry in the exotic quark sector is converted into the ordinary lepton asymmetries via the decays of leptoquarks into leptons (sleptons) and ordinary quarks (squarks). In the opposite limit $|g^N_{D_3d_3N_2}| \ll |g^N_{D_3d_3N_1}|$ lepton decay asymmetries dominate over $|\varepsilon^3_{1,D_3}|$. If $|g^N_{D_3d_3N_1}| \sim |g^N_{D_3d_3N_2}|$ these CP asymmetries are comparable. From Fig. 3.9 one can see that appreciable values of the decay asymmetries $\varepsilon^3_{1,\mu}$, $\varepsilon^3_{1,\tau}$ and $\varepsilon^3_{1,D_3} \sim 10^{-6} - 10^{-4}$ can be induced if $|g^N_{D_3d_3N_1}|$, $|g^N_{D_3d_3N_2}| \gtrsim 0.01 - 0.1$.

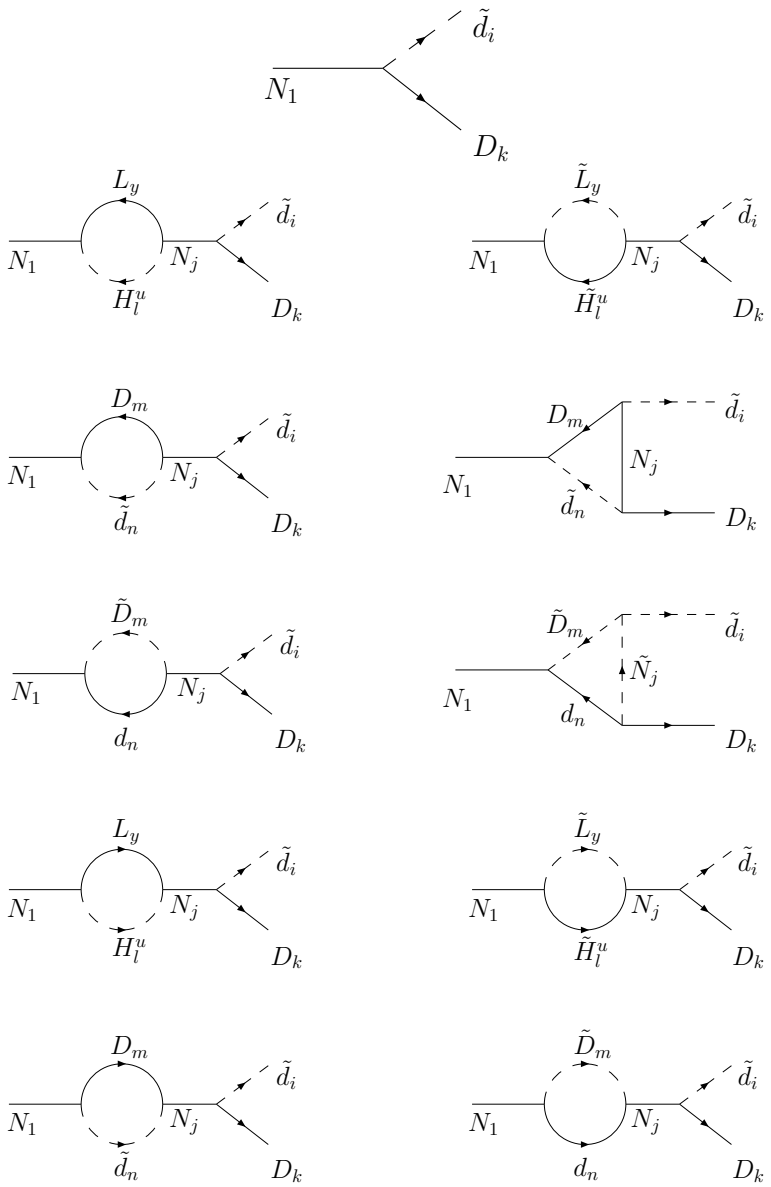

Figure 3.3: Tree-level and one-loop diagrams that give contribution to the CP asymmetries associated with the decays $N_1 \to D_k + d_i$ involving final state leptoquarks D in the E_6SSM Model II.

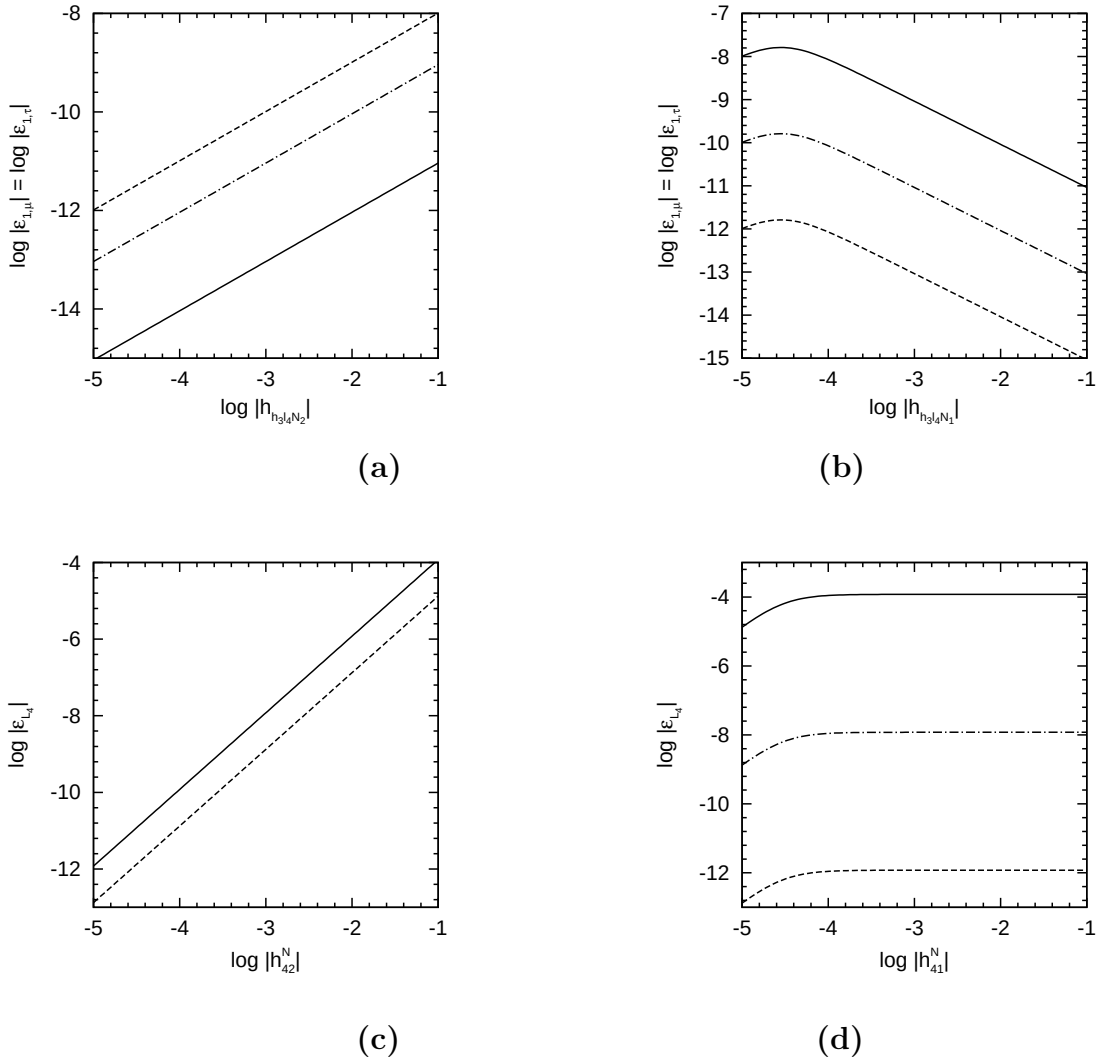

Figure 3.4: Maximal absolute values of *(a)-(b)* $|\varepsilon^3_{1,\mu}| = |\varepsilon^3_{1,\tau}|$ and *(c)-(d)* $|\varepsilon^3_{1,L_4}|$ in the E$_6$SSM with unbroken Z_H^2 symmetry versus $|h^N_{H_3^u L_4 N_1}|$ and $|h^N_{H_3^u L_4 N_2}|$ for $M_1 = 10^6\,\text{GeV}$, $M_2 = 10 \cdot M_1$. The solid, dash-dotted and dashed lines in figures *(a)* and *(c)* represent the maximal absolute values of the decay asymmetries for $|h^N_{H_3^u L_4 N_1}| = 0.1$, 10^{-3} and 10^{-5} while solid, dash-dotted and dashed lines in figures *(b)* and *(d)* correspond to $|h^N_{H_3^u L_4 N_2}| = 0.1$, 10^{-3} and 10^{-5} respectively.

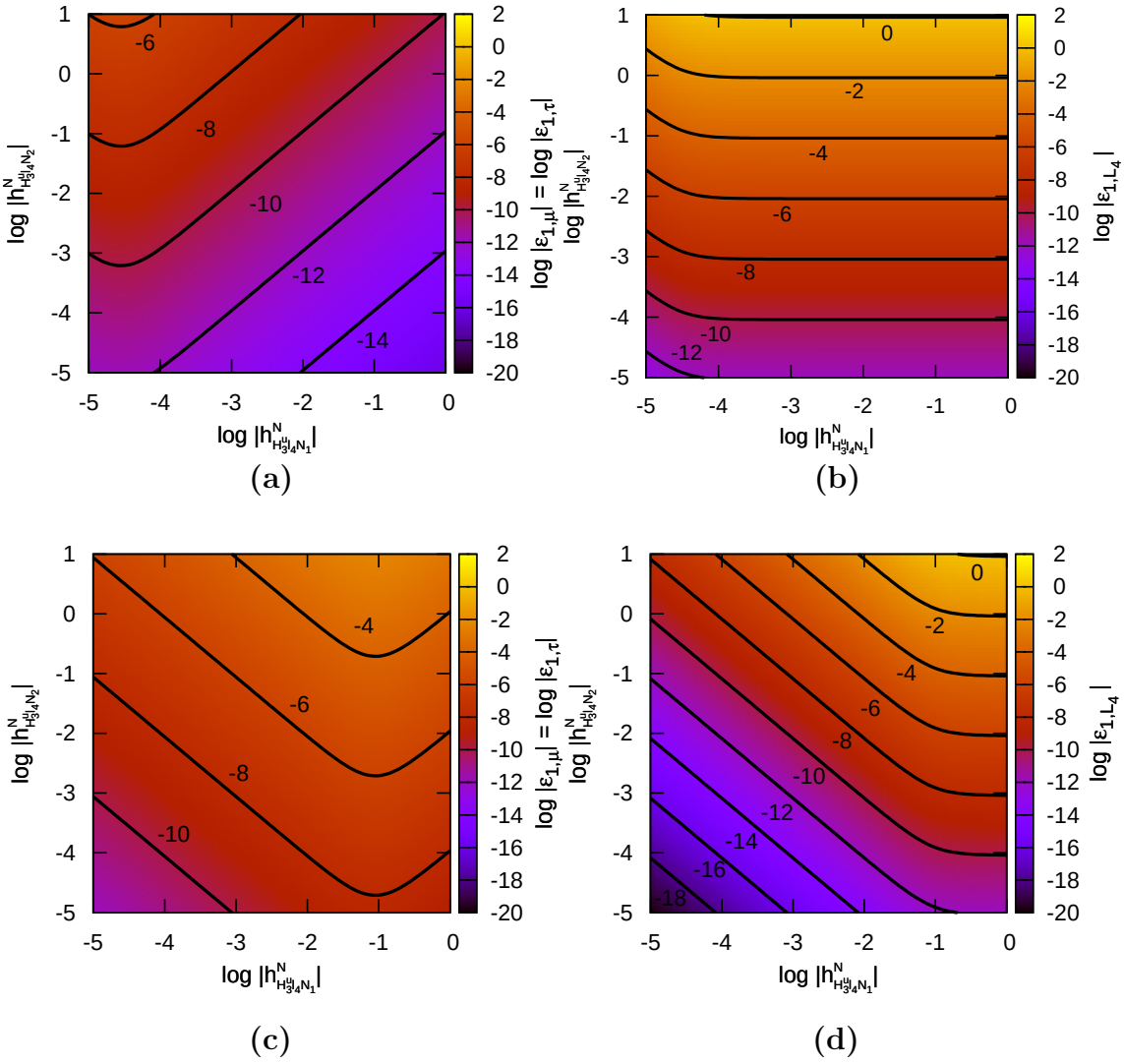

Figure 3.5: Logarithm (base 10) of the maximal values of $|\varepsilon^3_{1,\mu}| = |\varepsilon^3_{1,\tau}|$ (a, c) and $|\varepsilon^3_{1,L_4}|$ (b, d) in the E$_6$SSM with unbroken Z_H^2 symmetry versus $\log|h^N_{H_3^u L_4 N_1}|$ and $\log|h^N_{H_3^u L_4 N_2}|$ for $M_1 = 10^6\,\text{GeV}$ (a, b), $M_1 = 10^{13}\,\text{GeV}$ (c, d), and $M_2 = 10\,M_1$. The solid contour lines show steps of 2 in the logarithm (base 10) of the asymmetries.

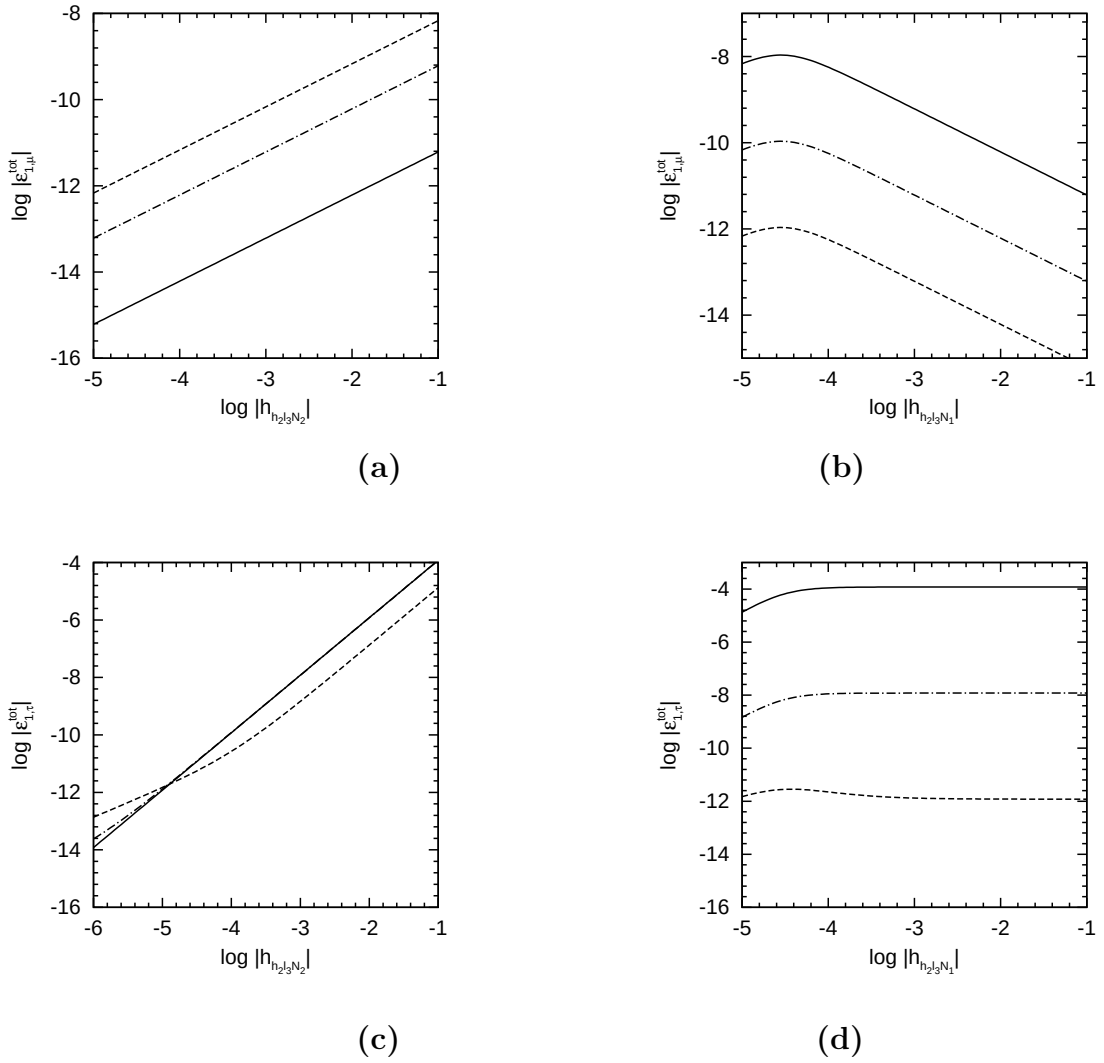

Figure 3.6: Maximal absolute values of *(a)-(b)* $|\varepsilon^{tot}_{1,\mu}|$ and *(c)-(d)* $|\varepsilon^{tot}_{1,\tau}|$ in the E_6SSM Model I versus $|h^N_{H_2^u L_3 N_2}|$ and $|h^N_{H_2^u L_3 N_1}|$ for $M_1 = 10^6$ GeV and $M_2 = 10 \cdot M_1$. All couplings $|h^N_{H_k^u L_4 N_j}|$ are set to zero. The solid, dash-dotted and dashed lines in figures *(a)* and *(c)* represent the maximal absolute values of the decay asymmetries for $|h^N_{H_2^u L_3 N_1}| = 0.1$, 10^{-3} and 10^{-5} while solid, dash-dotted and dashed lines in figures *(b)* and *(d)* correspond to $|h^N_{H_2^u L_3 N_2}| = 0.1$, 10^{-3} and 10^{-5} respectively.

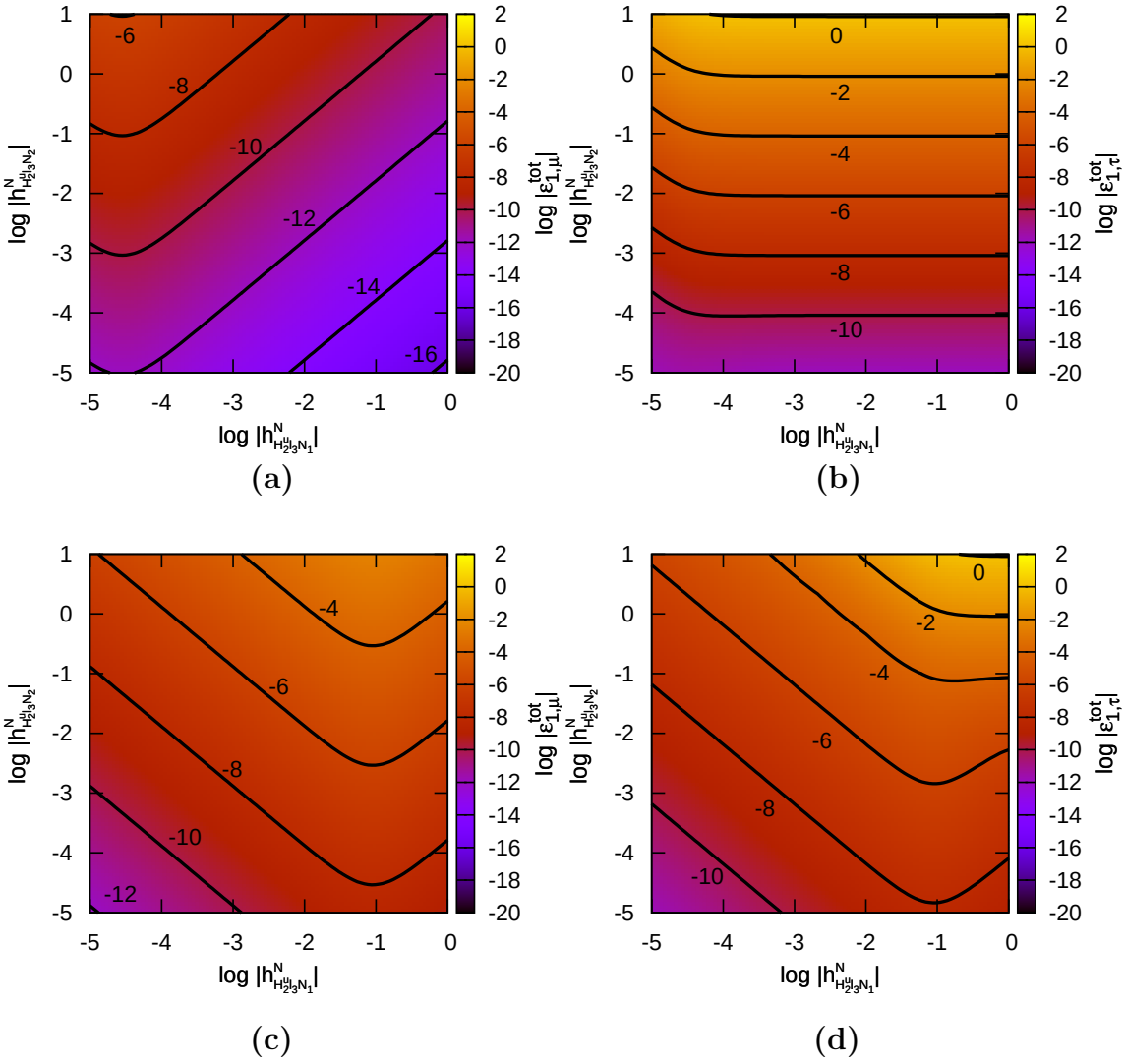

Figure 3.7: Logarithm (base 10) of the maximal values of $|\varepsilon^{tot}_{1,\mu}|$ (a, c) and $|\varepsilon^{tot}_{1,\tau}|$ (b, d) in the E$_6$SSM Model I versus $\log|h^N_{H^u_2 L_3 N_2}|$ and $\log|h^N_{H^u_2 L_3 N_1}|$ for $M_1 = 10^6\,\text{GeV}$ (a, b), $M_1 = 10^{13}\,\text{GeV}$ (c, d), and $M_2 = 10\,M_1$. All couplings $|h^N_{H^u_k L_4 N_j}|$ are set to zero. The solid contour lines show steps of 2 in the logarithm (base 10) of the asymmetries.

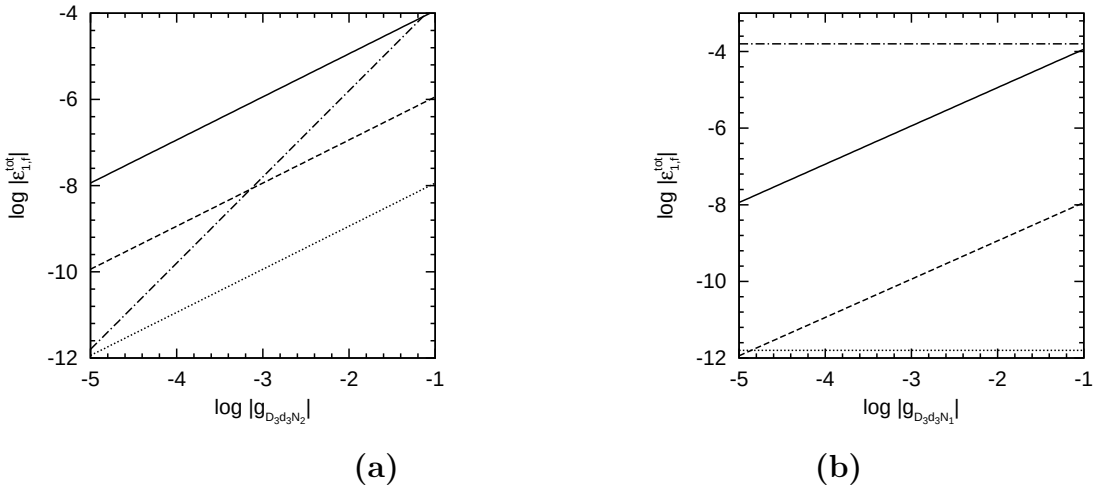

Figure 3.8: Maximal absolute values of the CP asymmetries in the E$_6$SSM Model II as a function of *(a)* $|g^N_{D_3 d_3 N_2}|$ and *(b)* $|g^N_{D_3 d_3 N_1}|$ for $M_1 = 10^6$ GeV and $M_2 = 10 \cdot M_1$. All couplings $|h^N_{H^u_k L_4 N_j}|$ and $|h^N_{H^u_\alpha L_x N_j}|$ ($\alpha = 1, 2$) are set to zero. The solid, dashed and dotted lines in figure *(a)* represent $|\varepsilon^3_{1,\mu}| = |\varepsilon^3_{1,\tau}|$ computed for $|g^N_{D_3 d_3 N_1}| = 0.1$, 10^{-3} and 10^{-5} while the dash-dotted line corresponds to $|\varepsilon^3_{1,D_3}|$. The solid and dashed lines in figure *(b)* show the dependence of $|\varepsilon^3_{1,\mu}| = |\varepsilon^3_{1,\tau}|$ on $|g^N_{D_3 d_3 N_1}|$ for $|g^N_{D_3 d_3 N_2}| = 0.1$ and 10^{-5} while the dash-dotted and dotted lines correspond to $|\varepsilon^3_{1,D_3}|$ calculated for $|g^N_{D_3 d_3 N_2}| = 0.1$ and 10^{-5} respectively.

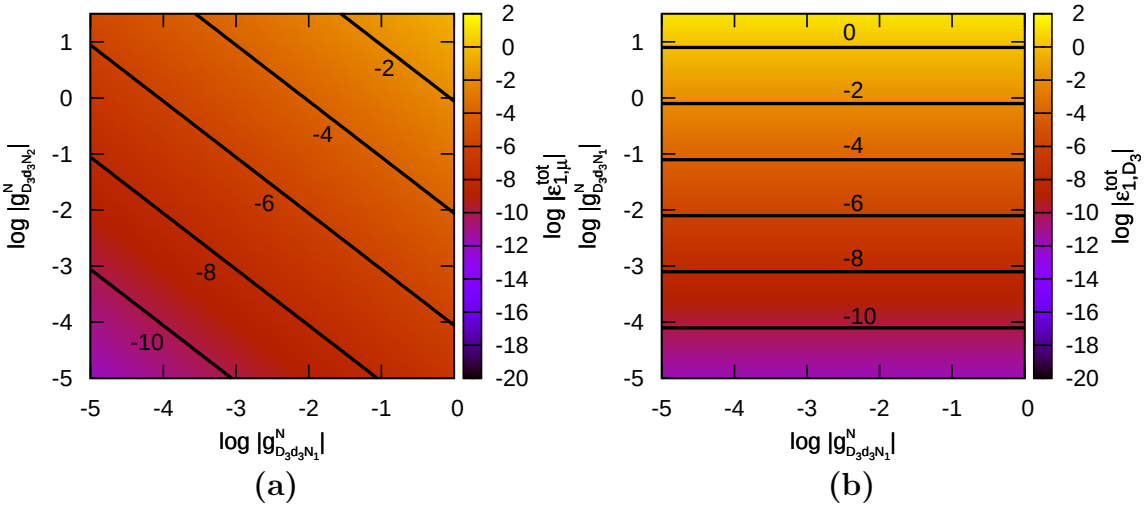

Figure 3.9: Logarithm (base 10) of the maximal values of $|\varepsilon^3_{1,\mu}| = |\varepsilon^3_{1,\tau}|$ (*a*) and $|\varepsilon^3_{1,D_3}|$ (*b*) in the E$_6$SSM Model II versus $\log|g^N_{D_3 d_3 N_2}|$ and $\log|g^N_{D_3 d_3 N_1}|$ for $M_2 = 10\, M_1$ (fixing the ratio M_1/M_2 these asymmetries become independent of M_1). All couplings $|h^N_{H^u_k L_4 N_j}|$ and $|h^N_{H^u_\alpha L_x N_j}|$ ($\alpha = 1, 2$) are set to zero. The solid contour lines show steps of 2 in the logarithm (base 10) of the asymmetries.

Chapter 4

The Evolution of Lepton/Baryon Asymmetries

Lepton asymmetries discussed in the last chapter describe how much net lepton is produced per RH neutrino decay. To ensure that the produced leptons remain in the present universe, the process of RH neutrino decay should happen out-of-thermal equilibrium. To calculate the number densities of lepton/baryon in the present universe, one have to solve the Boltzmann Equations, involving all relevant processes. These processes include: the RH neutrino decays/inverse decays, lepton number changing scatterings, sphaleron processes, and Yukawa interactions. The rates of these processes are functions of the temperature of the universe at that time, particle number densities and the rate of the corresponding interaction at zero temperature. We do not consider Quantum Boltzmann Equations, where correlation functions are used instead of particle number density [147]-[152]. Also we do not consider the case where the decays and inverse decays can not thermalise the heavy (s)neutrino distribution function [153].

We will begin with unflavoured Boltzmann Equations in the non-supersymmetric case, where the sum of lepton asymmetries is used and analyse the rate of corresponding processes. Then, to get a quantitatively accurate result, we consider full flavoured Boltzmann

Equations in two approaches. In the first approach, the asymmetries of each lepton flavour are considered as separate variables. The reason to distinguish lepton flavours is that the wash-out terms, which are functions of number density of each lepton are different for each flavour. One introduces the flavour transition matrix to describe the Yukawa interactions and sphaleron processes. In the second approach, the number density relations of corresponding particles are calculated, and the Boltzmann Equations are used to describe the evolution of the total $B-L$ number instead of three individual left-handed lepton flavours.

We will extend the Boltzmann Equations to the context of supersymmetry and the E_6SSM with the second approach. We discuss the case *(a)* E_6SSM with conserved Z_2^H symmetry (with only the L_4 and $\bar{L}_4$ added), *(b)* E_6SSM model I (with the inert Higgs added) and *(c)* E_6SSM model II (with leptoquarks added). We then show that the right amount of baryon number can be achieved in both of these cases by numerical calculation.

4.1 The Set-up of Boltzmann Equations

In this section, we discuss the basic ingredients of the Boltzmann Equations for Leptogenesis. Boltzmann Equations are widely used in particle cosmology to calculate the abundance of light elements from nucleosynthesis, the density of dark matter and the generation of lepton/baryon number in Leptogenesis. The Boltzmann Equations are a set of differential equations, the right hand side of which are the rates of increasing or decreasing the corresponding component of the relative processes.

To analyse the evolution of leptons, one should take into account all the particles which participate in the interactions changing lepton/baryon number density. These particles include leptons, quarks (both left-handed and right-handed), Higgs, RH neutrino and their super-partners in SUSY. The number densities of quark fields are determined by the "spectator processes" [154], which are much faster than the processes of generating and washing out lepton number, and the ratios of quark and Higgs to lepton number densities

are fixed in certain ranges of temperature thanks to the corresponding chemical potentials in equilibrium. For this reason, we can write the Boltzmann Equations using the lepton number density and the number density of the lightest RH neutrino field, and the final baryon number can be converted via the relation of B and L. (In the second approach of flavoured scenarios, we introduce another variable, the inactive $B-L$ number density, which will be discussed in Appendix (F)).

In this thesis, we only consider the case of strong hierarchical RH neutrino masses, where the second and third generation of RH neutrino decay earlier than the first generation of RH neutrino due to their large masses. We assume that the lepton asymmetry produced from the second and the third RH neutrino decay is erased by the later processes involving the lightest RH neutrino. For the details of N_2 in leptogenesis where the lepton asymmetry produced by N_2 is also considered, we refer the reader to [84].

It is convenient to use the dimensionless parameter z to describe processes happening at the scale of $T \sim M_1$. Using the Hubble expansion rate H in radiation dominated universe Eq.(E.5) and the relation of cosmic time t to H, $t = 1/H$, clearly we have

$$\frac{dz}{dt} = -\frac{M_1}{T^2}\frac{dT}{dt} = zH(z) = \frac{H_1}{z}\,, \tag{4.1}$$

where H_1 is the Hubble expansion rate at temperature $T = M_1$.

In addition, the Boltzmann Equations can be simplified if we use the particle abundance (particle number density normalized by the entropy density):

$$y_x \equiv n_x/s, \tag{4.2}$$

where n_x is the particle density in the co-moving volume with the considered particle x and s is entropy density[1]. In this case, the effect of expanding of the universe is embedded in y_x, since both n_x and s are in the co-moving volume, scaled as $1/T^3$.

The reactions play the crucial role of generating lepton number. As an example, let us firstly consider a particle x. To calculate the change of number density of x, one needs

[1]The expression of entropy s in the radiation dominated universe is given in Eq. (E.21)

to take into account the reactions with x in the initial states as well as in the final states. Clearly, the reactions with x in the initial states decrease the number density of x whereas the reaction with x in the final states increase the number density of x

$$\frac{dy_x}{dz} = -\frac{1}{sHz}\sum_{a,i,j\cdots}\left[\frac{y_x y_a\cdots}{y_x^{\rm eq}y_a^{\rm eq}\cdots}\gamma(x+a+\cdots\to i+j+\cdots)\right.$$
$$\left.-\frac{y_i y_j\cdots}{y_i^{\rm eq}y_j^{\rm eq}\cdots}\gamma(i+j+\cdots\to x+a+\cdots)\right], \tag{4.3}$$

where $y^{\rm eq}\equiv n^{\rm eq}/s$ is the abundance of particle x in equilibrium, with $n^{\rm eq}$ calculated in Appendix (E.2):

$$n_i^{\rm eq}(T) = \frac{g_i\,T\,m_i^2}{2\pi^2}K_2\left(\frac{m_i}{T}\right), \tag{4.4}$$

for massive particles with mass m_i, and

$$n_i^{\rm eq}(T) = \frac{g_i\,T^3}{\pi^2}, \tag{4.5}$$

for massless particles, with g_i the internal degrees of freedom of the particle and $K_2(x)$ the second modified Bessel function.

In leptogenesis, we are interested in massless leptons (and quarks/Higgs) and massive RH neutrinos. Inserting Eq.(4.4) and Eq.(4.5) into Eq.(E.18), we can arrive at the abundances of leptons and RH neutrino in equilibrium Eq.(1.68). Note that the total number of degrees of freedom of the plasma in the framework of the Standard Model is given by $g_*^{\rm SM}=106.75$ and $g_*^{\rm MSSM}=228.75$ in the MSSM.

Here γ is the reaction density in equilibrium, which can be calculated from a general equation

$$\gamma(x+a+\ldots\to i+j+\ldots)$$
$$=\int d\Pi_X f_X^{\rm eq}d\Pi_a f_a^{\rm eq}\ldots|\mathcal{M}(x+a+\ldots\to i+j+\ldots)|^2\tilde{\delta}\;d\Pi_i d\Pi_j\,, \tag{4.6}$$

where $\tilde{\delta}\equiv(2\pi)^4\,\delta^4\left(P_i-P_f\right)$, $\mathcal{M}(x+a+\ldots\to i+j+\ldots)$ is the matrix element of the process $x+a+\ldots\to i+j+\ldots$ and Π is the phase space. In the leptogenesis era, all the lepton number changing interaction rates are in equilibrium, so we have

$$\gamma(x+a+\cdots\to i+j+\cdots)=\gamma(i+j+\cdots\to x+a+\cdots)\,. \tag{4.7}$$

These lepton number changing interactions are induced by the Majorana mass terms of the RH neutrinos, and they include[2]

$$
\begin{aligned}
& N_1 \to \ell + H_u\,, \quad N_1 \to \bar{\ell} + H_u^*\,, \\
N_1 + Q_3 \to \ell + t\,, \quad & \ell + t \to N_1 + Q_3\,, \quad N_1 + \bar{t} \to \ell + \bar{Q}_3\,, \quad \ell + \bar{Q}_3 \to N_1 + \bar{t}\,, \\
N_1 + \bar{Q}_3 \to \bar{\ell} + \bar{t}\,, \quad & \bar{\ell} + \bar{t} \to N_1 + \bar{Q}_3\,, \quad N_1 + t \to \bar{\ell} + Q_3\,, \quad \bar{\ell} + Q_3 \to N_1 + t\,, \\
N_1 + \ell \to \bar{t} + Q_3\,, \quad & N_1 + \bar{\ell} \to t + \bar{Q}_3\,, \quad \bar{t} + Q_3 \to N_1 + \ell\,, \quad t + \bar{Q}_3 \to N_1 + \bar{\ell}\,, \\
& \ell + H_u^* \to \bar{\ell} + H_u\,, \quad \bar{\ell} + H_u \to \ell + H_u^*\,,
\end{aligned}
\tag{4.8}
$$

where the first line is the decays (with reaction rate γ_D). The second and third line are the t-channel scatterings (with reaction rate γ_{S_t}). The fourth line is the s-channel scatterings (with reaction rate γ_{S_s}). The last line represents both t-channel and s-channel $\Delta L = \pm 2$ scatterings (reaction rate γ_{N_t} and γ_{N_s}).

For Leptogenesis, the net abundance of leptons (as well as quarks and Higgs) and the abundance of the lightest RH neutrino play the crucial role[3]. For Dirac type particles x, we introduce the net particle abundance:

$$
Y_x \equiv y_x - y_{\bar{x}}\,. \tag{4.9}
$$

On the other hand, for Majorana particles we cannot distinguish particle from its anti-particle. To unify the notation, we use $Y_{N_1} = y_{N_1}$, the abundance of RH neutrinos. For the number density (both Dirac particles and Majorana particles) in equilibrium, we still have $y_x^{\rm eq} = Y_x^{\rm eq}$.

4.1.1 The Decay terms and Inverse Decay term

The RH neutrino decays can change the abundance of the RH neutrino and left-handed leptons. According to Eq.(1.62) and Eq.(4.7), we can write down the reaction rates for

[2]Due to the large Yukawa coupling of the top quark, it is safe to neglect other quark Yukawa interactions.

[3]We will show how quark asymmetry and Higgs asymmetry also play an important role.

$N_1 \leftrightarrow \ell + H_u$ and $N_1 \leftrightarrow \bar{\ell} + H_u^*$ (with reaction rates $\gamma_{N_1\ell} = \gamma_{\ell N_1}$ and $\gamma_{N_1\bar{\ell}} = \gamma_{\bar{\ell}N_1}$ respectively)

$$\begin{aligned}\gamma(N_1 \to \ell + \phi^*) = \gamma(\ell + \phi^* \to N_1) &= \frac{1}{2}(1+\varepsilon)\gamma_D\,, \\ \gamma(N_1 \to \bar{\ell} + \phi) = \gamma(\bar{\ell} + \phi \to N_1) &= \frac{1}{2}(1-\varepsilon)\gamma_D\,,\end{aligned} \tag{4.10}$$

where $\gamma_D \equiv \gamma(N_1 \to \ell + \phi^*) + \gamma(N_1 \to \bar{\ell} + \phi)$ is the reaction rate of total decay of N_1. Using Eq.(4.3), the decay terms for N_1 and net ℓ are

$$\Gamma_D^{N_1} = -\frac{1}{sHz}\left[\frac{Y_{N_1}}{Y_N^{eq}}\left(\gamma_{N_1\ell} + \gamma_{N_1\bar{\ell}}\right) - \frac{y_\ell y_{H_u}}{y_\ell^{\rm eq} y_{H_u}^{\rm eq}}\,\gamma_{\ell N_1} - \frac{y_{\bar{\ell}} y_{H_u^*}}{y_{\bar{\ell}}^{\rm eq} y_{H_u^*}^{\rm eq}}\,\gamma_{\bar{\ell}N_1}\right], \tag{4.11}$$

$$\Gamma_D^{\ell} = -\frac{1}{sHz}\left[\frac{Y_{N_1}}{Y_N^{eq}}\left(\gamma_{N_1\ell} - \gamma_{N_1\bar{\ell}}\right) - \frac{y_\ell y_{H_u}}{y_\ell^{\rm eq} y_{H_u}^{\rm eq}}\,\gamma_{\ell N_1} + \frac{y_{\bar{\ell}} y_{H_u^*}}{y_{\bar{\ell}}^{\rm eq} y_{H_u^*}^{\rm eq}}\,\gamma_{\bar{\ell}N_1}\right]. \tag{4.12}$$

Notice that we have $y_x \simeq y_x^{\rm eq}$ for all massless particles. Using Eq.(4.9) and Eq.(4.10), we can simplify the term for net lepton asymmetry Y_ℓ , keeping the terms of order Y_ℓ, Y_{H_u} and ϵ. Then Eq. (4.11) and (4.12) turn into

$$\Gamma_D^{N_1} = -\frac{1}{sHz}\left(\frac{Y_{N_1}}{Y_N^{eq}} - 1\right)\gamma_D\,, \tag{4.13}$$

$$\Gamma_D^{\ell} = \frac{1}{sHz}\left[\epsilon\left(\frac{Y_{N_1}}{Y_{N_1}^{eq}} - 1\right) - \frac{1}{2}\left(\frac{Y_\ell}{Y_\ell^{\rm eq}} + \frac{Y_{H_u}}{Y_{H_u}^{\rm eq}}\right)\right]\gamma_D\,. \tag{4.14}$$

One may notice that the lepton asymmetry is generated when the lightest RH neutrino is "out-of-thermal equilibrium" ($Y_{N_1} \neq Y_{N_1}^{\rm eq}$). Since $Y_{N_1}^{\rm eq}$ drops as the temperature T of the universe drops, the out-of-thermal equilibrium can be satisfied when the Universe is cooling down.

The reaction density for a decay $x \to i + j + \cdots$ can be calculated via Eq.(4.6). For the RH neutrino decay it is given by

$$\gamma_D = \gamma(N_1 \to \ell + H_u) = n_{N_1}^{\rm eq}\,\frac{K_1(z)}{K_2(z)}\,\Gamma\,, \tag{4.15}$$

where Γ is the decay width in the rest frame (at zero temperature).

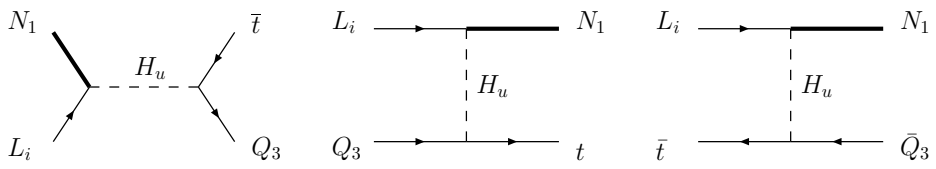

Figure 4.1: The $\Delta L = \pm 1$ scatterings which change N_1 abundance and wash out lepton asymmetry.

4.1.2 $\Delta L = 1$ Scatterings as Washing Out Process

The $\Delta L = \pm 1$ processes include 2 to 2 scattering with a RH neutrino, a left-handed lepton, an up-type quark and a down-type quark as the external lines, and a Higgs field in the propagator. We include t-channel scattering and its charge conjugate process (the second and third line of Eq.(4.8)) and s-channel scatterings (the fourth line in Eq.(4.8)). We neglect three-body decay and 2 to 3 scatterings, as they are strongly suppressed by the phase space integration. In principle the $\Delta L = \pm 1$ scattering can generate lepton number at one loop. Calculation finds that the CP violation is the same as the RH neutrino. However, we do not discuss the lepton asymmetry generated by scattering in this thesis.

On the other hand, more importantly, the $\Delta L = \pm 1$ processes wash out the lepton asymmetries produced by RH neutrino decay. At tree level, the scattering has the same reaction density as its charge conjugate scattering. The only difference is the abundance of the initial state y_ℓ and $y_{\bar{\ell}}$. Using Eq.(4.3), we can write down the contribution of $\Delta L = \pm 1$ scattering to the lightest RH neutrino, $\Gamma_S^{N_1}$ and the contribution to the lepton asymmetry $\Gamma_{S_t}^\ell$, $\Gamma_{S_s}^\ell$ (t-channel and s-channel, respectively):

$$\Gamma_S^{N_1} = -\frac{1}{sHz}\left(\frac{Y_{N_1}}{Y_N^{eq}} - 1\right)(2\gamma_{Ss} + 4\gamma_{St}) \,, \tag{4.16}$$

$$\Gamma_{S_t}^\ell = \frac{1}{sHz}\left[2\frac{Y_\ell}{Y_\ell^{\rm eq}} + \left(\frac{Y_t}{Y_t^{\rm eq}} - \frac{Y_{Q_3}}{Y_{Q_3}^{\rm eq}}\right)\left(\frac{Y_{N_1}}{Y_{N_1}^{eq}} + 1\right)\right]\gamma_{St} \,, \tag{4.17}$$

$$\Gamma_{S_s}^\ell = \frac{1}{sHz}\left(\frac{Y_{N_1}}{Y_{N_1}^{eq}}\frac{Y_\ell}{Y_\ell^{\rm eq}} + \frac{Y_t}{Y_t^{\rm eq}} - \frac{Y_{Q_3}}{Y_{Q_3}^{\rm eq}}\right)\gamma_{Ss} \,. \tag{4.18}$$

The reaction density for a two body scattering can be calculated from Eq.(4.6). The

integration reads:

$$\gamma^{\rm eq}(x+a\to i+j+\cdots)=\frac{T}{64\pi^4}\int_{(m_x+m_a)^2}^{\infty}{\rm d}s\,\sqrt{s}\,K_1\left(\frac{\sqrt{s}}{T}\right)\hat{\sigma}(s)\,, \tag{4.19}$$

where s is the integral parameter standing for the squared centre of mass energy and $\hat{\sigma}(s)$ is the reduced cross section defined by

$$\hat{\sigma}(s)=\frac{2\lambda(u,m_x^2,m_a^2)}{s}\,\sigma(s)\,, \tag{4.20}$$

with the kinematic function

$$\lambda(s,m_x^2,m_a^2)\equiv[s-(m_x+m_a)^2]\,[s-(m_x-m_a)^2]\,, \tag{4.21}$$

and $\sigma(s)$, the rest frame cross section.

4.1.3 $\Delta L=2$ Scatterings as Washing Out Process

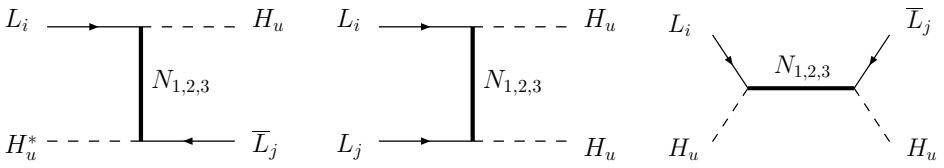

Figure 4.2: The $\Delta L=\pm2$ scatterings which change N_1 abundance and wash out lepton asymmetry.

The $\Delta L=2$ processes include 2 to 2 scattering with a RH neutrino in the propagator. Lepton number is violated in this process due to the Majorana nature of the RH neutrino. The $\Delta L=\pm2$ scattering wash out the lepton asymmetry, similar to $\Delta L=\pm1$ processes, however it does not change the number density of the RH neutrino N_1. The contribution to lepton asymmetry reads:

$$\Gamma^{\ell}_{N_t+N_s} \;=\; \frac{1}{sHz}\cdot 2\left(\frac{Y_\ell}{Y_\ell^{\rm eq}}+\frac{Y_{H_u}}{Y_{H_u}^{\rm eq}}\right)(\gamma_{Ns}+\gamma_{Nt})\;, \tag{4.22}$$

where the factor 2 represents this process changes lepton number by 2 units. The reaction rates $\gamma_{Ns}+\gamma_{Nt}$ can be calculated similarly as the method in last subsection. In this thesis, we use the result presented in [155][156].

In canonical Leptogenesis, when the lightest RH neutrino is heavier than $\sim 10^5$GeV, due to the smallness of RH neutrino Yukawa couplings, the $\Delta L = \pm 2$ scatterings are negligible. However, they become prominent when exotic Yukawa couplings are introduced.

Moreover, for $\Delta L = 2$ scattering process with the heavy RH neutrinos in the propagator, the lightest RH neutrino can be on-shell. So the on-shell part is double counted with the decaying term and inversed decaying term. We have to substract the on-shell part of the scattering. Generally, for a $2 \leftrightarrow 2$ scattering $\ell_\alpha + H_u \leftrightarrow \ell_\beta + H_u^*$, the on-shell part can be expressed as

$$\gamma_\beta^{\alpha\,(\mathrm{os})} = \gamma_{N_1}^{\alpha}\, B_\beta^{N_1}\,, \tag{4.23}$$

where $B_\beta^{N_1}$ is the branching ratio of decay $N_1 \to \ell_\beta + H_u$. The expressions of reaction density of $\Delta L = \pm 2$ scattering can be found in [155].

4.2 Boltzmann Equations in the Non-supersymmetric and Supersymmetric Case

In this section, we discuss the Boltzmann Equations in the SM plus RH neutrinos and MSSM plus RH neutrinos. Firstly, in the case without "spectator" process (the process converting left-handed leptons into other components with non-vanishing $B-L$ number), we can arrive at Boltzmann Equations for leptogenesis in MSSM+RHN by adding all the lepton number changing processes together [4]:

$$\frac{\mathrm{d}Y_{N_1}}{\mathrm{d}z} = \Gamma_D^{N_1} + \Gamma_S^{N_1}\,, \tag{4.24}$$

$$\frac{\mathrm{d}Y_\ell}{\mathrm{d}z} = \Gamma_D^{\ell} - \Gamma_{S_t}^{\ell} - \Gamma_{S_s}^{\ell} - \Gamma_{N_t+N_s}^{\ell}\,. \tag{4.25}$$

These Boltzmann Equations are used as an approximation, one can arrive at the final lepton asymmetry within one order of magnitude. After wash-out processes become neg-

[4]This Equation is given in [160], but the inverse decay term is missed.

ligible (when $z \sim 10$), one can use the lepton number - baryon number relation, Eq.(1.58) to estimate the final baryon number.

Now we can extend the Boltzmann Equations into the framework of Supersymmetry. In Supersymmetry, the super-partners of leptons, quarks, RH neutrinos and Higgses (sleptons, squarks, RH sneutrinos and Higgsinos respectively) also enter the thermal plasma of the Universe. RH sneutrino decays also produce lepton asymmetries; RH (s)neutrinos decay into sleptons; Sleptons and squarks also contain $B - L$ number; Sleptons squarks and Higgsinos plays the role of washing-out, therefore we need to take them into account in the Boltzmann Equations. However the abundances of particles and sparticles have a simple algebraic relation. In the hot plasma of the early universe, chemical potentials of particles in equilibrium are kept in certain ratios by the relevant interactions. The ratios can be calculated by the equilibrium conditions of respective interactions[5]. And the number density of particle (specie x) is related to its chemical potential (See Eq.(1.50)). We notice that there is a difference of factor 2 between bosons and fermions. In Supersymmetry, the fermion-gaugino-sfermion interactions in equilibrium result in that the chemical potential of a fermion is the same as its superpartner, $\mu_x = \mu_{\tilde{x}}$ (Gauginos being Majorana particle have zero chemical potential). Therefore we can define the total number density and abundance of particle species x as:

$$\hat{n}_x \equiv n_x + n_{\tilde{x}}\,, \quad \hat{Y}_x \equiv Y_x + Y_{\tilde{x}}\,. \tag{4.26}$$

We will find it is very convenient to work in $\hat{Y}$ as particles and super-particles have similar behavior in leptogenesis. Also one notices that in this notation, we do not need to worry about the factor 2 between fermion fields and boson fields. Under this notation, the Boltzmann Equations turn into

$$\frac{\mathrm{d}\hat{Y}_{N_1}}{\mathrm{d}z} = \Gamma_D^{\hat{N}_1} + \Gamma_S^{\hat{N}_1} \equiv \Gamma_{D+S}^{\hat{N}_1}\,, \tag{4.27}$$

$$\frac{\mathrm{d}\hat{Y}_\ell}{\mathrm{d}z} = \Gamma_D^{\hat{\ell}} - \Gamma_{S_t}^{\hat{\ell}} - \Gamma_{S_s}^{\hat{\ell}} - \Gamma_{N_t+N_s}^{\hat{\ell}}\,. \tag{4.28}$$

[5]The details of the calculation will be given in Section (4.5).

And the terms are

$$\Gamma^{\hat{N}_1}_{D+S} = -\frac{2}{sHz}\left(\frac{\hat{Y}_{N_1}}{\hat{Y}^{eq}_{N}} - 1\right)(\gamma_D + 2\gamma_{Ss} + 4\gamma_{St}) \,, \tag{4.29}$$

$$\Gamma^{\hat{\ell}}_{D} = \frac{2}{sHz}\left[\epsilon\left(\frac{\hat{Y}_{N_1}}{\hat{Y}^{eq}_{N_1}} - 1\right) - \frac{1}{2}\left(\frac{\hat{Y}_{\ell}}{\hat{Y}^{\rm eq}_{\ell}} + \frac{\hat{Y}_{H_u}}{\hat{Y}^{\rm eq}_{H_u}}\right)\right]\gamma_D \,, \tag{4.30}$$

$$\Gamma^{\hat{\ell}}_{S_t} = \frac{2}{sHz}\left[2\frac{\hat{Y}_{\ell}}{\hat{Y}^{\rm eq}_{\ell}} + \left(\frac{\hat{Y}_{t}}{\hat{Y}^{\rm eq}_{t}} - \frac{\hat{Y}_{Q_3}}{\hat{Y}^{\rm eq}_{Q_3}}\right)\left(\frac{\hat{Y}_{N_1}}{\hat{Y}^{eq}_{N_1}} + 1\right)\right]\gamma_{St} \,, \tag{4.31}$$

$$\Gamma^{\hat{\ell}}_{S_s} = \frac{2}{sHz}\left(\frac{\hat{Y}_{N_1}}{\hat{Y}^{eq}_{N_1}}\frac{\hat{Y}_{\ell}}{\hat{Y}^{\rm eq}_{\ell}} + \frac{\hat{Y}_{t}}{\hat{Y}^{\rm eq}_{t}} - \frac{\hat{Y}_{Q_3}}{\hat{Y}^{\rm eq}_{Q_3}}\right)\gamma_{Ss} \,, \tag{4.32}$$

$$\Gamma^{\hat{\ell}}_{N_t+N_s} = \frac{2}{sHz}\cdot 2\left(\frac{\hat{Y}_{\ell}}{\hat{Y}^{\rm eq}_{\ell}} + \frac{\hat{Y}_{H_u}}{\hat{Y}^{\rm eq}_{H_u}}\right)(\gamma_{Ns} + \gamma_{Nt}) \,. \tag{4.33}$$

Compared with Eq.(4.16)-(4.22), one finds that additional SUSY interactions result in a factor 2 for each term. But notice that the reaction rate $\gamma_D\,, \gamma_{Ss}\,\cdots$ are still the same as the ones in the non-supersymmetric case. In Eq.(4.29) and (4.29), we have used $Y^{\rm eq}_{N_1} = Y^{\rm eq}_{\tilde{N}_1}$, as N_1 and $\tilde{N}_1$ have approximately the same mass before SUSY breaking.

4.3 Initial Conditions

To solve the Boltzmann Equations, we need the initial conditions for RH neutrinos and leptons. We discuss the effect of initial conditions for MSSM+RHN Boltzmann Equations. In the scenario of thermal Leptogenesis, the RH neutrinos are singlets which only interact with other particles via Yukawa couplings. Hence they are produced by inverse decay[6]. In this case, the initial number density for RH neutrino when $T \gg T_{\rm Leptogenesis} \sim M_1$ is zero. However, model-dependent modifications of thermal Leptogenesis are considered, which dramatically change the initial condition of the Boltzmann Equations.

In the "equilibrium" scenario, one assumes the RH neutrinos also participate in other interactions beside the Yukawa interaction. Therefore the number density of RH neutri-

[6] $\Delta L = 2$ scattering $\ell + \ell \to N_1 + N_1$ also generates RH neutrino, but negligible provided the Yukawa couplings are much smaller than unity.

nos is brought into equilibrium ($Y_{N_1}(z_{\rm ini}) = Y^{\rm eq}_{N_1}$) before Leptogenesis happens. In the "dominant" scenario, the RH neutrinos may be generated by the decay of heavier particles (*e.g.* the inflaton) [157]. In this case, the initial number density of RH neutrinos can be much larger than $Y^{\rm eq}_{N_1}$. In all these scenarios, one assumes that the initial lepton asymmetry is zero, and the mechanism which generates RH neutrinos does not alter the lepton asymmetries of the RH neutrino decay and the Boltzmann Equations.

In Fig. 4.3, we illustrate the evolution of RH neutrino density and lepton asymmetry with different initial conditions. We find that the initial condition is most important in the weak-wash out scenario. We find that the sign of Y_ℓ does not change in plot (b) and plot (c) because we always have $Y_{N_1} \geq Y^{\rm eq}_{N_1}$ for the era of Leptogenesis.

4.4 A Brief Review of the Approach of Transition Matrix $A_{\alpha\beta}$

In this section, we briefly review the approach of the leptogenesis Boltzmann Equations with a transition matrix[7] [158]. In this approach a flavoured $B-L$ number $\Delta_\alpha \equiv B - L_\alpha$ where α is the flavour index for left-handed leptons, is introduced. The abundances of the left-handed leptons Y_{ℓ_α} is related to the Y_{Δ_β} via a transition matrix $A_{\alpha\beta}$ by $Y_{\ell_\alpha} = \sum_\beta A_{\alpha\beta} Y_{\Delta_\beta}$.

To obtain the matrix $A_{\alpha\beta}$, one should firstly express Y_{Δ_α} in terms of Y_{ℓ_β}, using the equilibrium conditions Eq.(1.51)-(1.56). This can be written as $Y_{\Delta_\beta} = \sum_\beta B_{\alpha\beta} Y_{\ell_\alpha}$. Clearly, we have $A_{\alpha\beta} = B^{-1}_{\alpha\beta}$. The elements of the transition matrix vary when the universe temperature changes. In MSSM, when the temperature $T \lesssim 10^9\,{\rm GeV}$, the A matrix is given

[7] It is also called "conversion matrix" in some literature.

by [145]

$$A^{\rm MSSM} = \begin{pmatrix} -93/110 & 6/55 & 6/55 \\ 3/40 & -19/30 & 1/30 \\ 3/40 & 1/30 & -19/30 \end{pmatrix} . \tag{4.34}$$

When three flavours of leptons are taken into account, there are a set of four Boltzmann Equations, one for the lightest RH neutrino and the othre three for Δ_α. Since only the left-handed leptons participate in the wash-out processes, one can use the transition matrix to convert Y_{Δ_α} into Y_{ℓ_α}. In the case where the contribution of quarks and Higgs in wash-out processes and $\Delta L = \pm 2$ scattering are ignored, the Boltzmann Equations are

$$\frac{{\rm d}\hat{Y}_{N_1}}{{\rm d}z} = -\frac{2}{sHz}\left(\frac{\hat{Y}_{N_1}}{\hat{Y}_N^{eq}} - 1\right)\left(\gamma_D + 2\gamma_{Ss} + 4\gamma_{St}\right) , \tag{4.35}$$

$$\frac{{\rm d}\hat{Y}_{\Delta_\alpha}}{{\rm d}z} = -\frac{2}{sHz}\left\{\epsilon_{1,\alpha}\left(\frac{\hat{Y}_{N_1}}{\hat{Y}_{N_1}^{eq}} - 1\right)\gamma_D + \left(\gamma_{S_s}^{\alpha} + \gamma_{S_t}^{\alpha}\right) A_{\alpha\beta}\,\frac{\hat{Y}_{\Delta_\beta}}{\hat{Y}_\Delta^{\rm eq}}\right\} . \tag{4.36}$$

Here, $\epsilon_{1,\alpha}$ are the flavoured lepton asymmetries of the RH neutrino decay and $\gamma_{S_s}^{\alpha}$, $\gamma_{S_t}^{\alpha}$ are the $\Delta L = \pm 1$ scattering rate for flavour α. And we have $\hat{Y}_\Delta^{\rm eq} \equiv \hat{Y}_\ell^{\rm eq}$. However, if one outputs Y_{ℓ_α} when z varies, we find that they are not kept in certain ratios, as required by the equilibrium conditions.

4.5 "Uni-flavoured" Boltzmann Equations

In this section, we investigate the role of spectator processes in leptogenesis where three generations of leptons and quarks are considered. We find that three left-handed components of leptons are guaranteed to have an equal abundance due to spectator processes. And one can calculated the total $B - L$ number in the universe instead of three separate left-handed leptons, ℓ_α. This method is presented briefly in Ref. [159]. And in the meantime, the we approach the flavoured Boltzmann Equations by a more tedious method (presented in Appendix F), but we agree with the result in [159].

When the spectator processes are active, the left-handed leptons are converted into right-handed leptons via Yukawa interactions and into left-handed quarks via electroweak sphaleron process. Also the left-handed quarks can be converted into right-handed quarks via Yukawa interactions. However, the total $B-L$ number is conserved, and distributed in different components with certain ratios. Moreover, the abundances of Higgs fields are also related to the quark/lepton abundances due to Yukawa interactions in equilibrium. In this section, we calculate the relations of number densities of relevant particles in leptogenesis. We are interested in leptogenesis at low energy scale, $10^2\,\mathrm{GeV} < T < 10^9\,\mathrm{GeV}$. In this temperature range, the QCD sphaleron processes, which effectively convert left-handed quarks (both up type and down type) into right-handed quarks and electroweak sphaleron which converts left-handed leptons to left-handed quarks are in equilibrium. In addition, Yukawa interactions for all the three generations of quarks and leptons are in equilibrium.

Due to the gauge transformation, all the particles in the same multiplet of $SU(3)_C \times SU(2)_W \times U(1)_Y$ have the same chemical potential and all gauge fields have vanishing chemical potentials $\mu_W = \mu_Z = \mu_B = \mu_g = 0$. So we can use ℓ_i to denote both e_i^L and ν_i^L, where i is the generation index and q_i, u_i, d_i can represent all color states of left-handed quark (u_i^L and d_i^L), right-handed u-type quarks and right-handed d-type quarks. And as discussed in Chapter 1, the non-perturbative electroweak sphaleron process conserves $B-L$. Since the generation indices for B and L are not certainly related in the electroweak sphaleron process, the transitions of any generation of L to B are allowed. In addition, in Ref. [159], supersymmetric off-diagonal soft breaking terms lead to the mixing of scalar leptons, resulting in chemical potentials of different generations of leptons and quarks being equal. So we can have the relation $\mu_{Q_i} = \mu_Q$, $\mu_{\ell_i} = \mu_\ell$[8].

In the temperature range, since all the Yukawa interactions are in equilibrium, making the left-handed and right-handed components in a certain ratio, we can deduce the chemical potential relations for right-handed u-type and d-type quarks: $\mu_u = \mu_c = \mu_t$ and $\mu_d = \mu_s = \mu_b$. Similarly in the lepton sector, e, μ and τ Yukawa couplings in equilibrium

[8]Since all the three left-handed leptons have the same chemical potential is guaranteed, we call this approach "Uni-flavoured" Boltzmann Equations.

results in $\mu_e = \mu_\mu = \mu_\tau$. In addition, the Higgs field H_u and H_d have the same value of chemical potential but opposite signs due to the mixing term $W = \mu H_u H_d$:

$$\mu_{H_u} = -\mu_{H_d} \,. \tag{4.37}$$

Therefore, we need to deal with six chemical potentials for Q, u, d, ℓ, μ and H_u/H_d fields. The relations of them are from the following constraints

- The Yukawa interactions in equilibrium ($Q \leftrightarrow u + H_u$, $Q \leftrightarrow d + H_d$ and $\ell \leftrightarrow e + H_d$) gives[9]

$$\mu_Q - \mu_u + \mu_{H_u} = 0 \,, \tag{4.38}$$

$$\mu_Q - \mu_d + \mu_{H_d} = 0 \,, \tag{4.39}$$

$$\mu_\ell - \mu_e + \mu_{H_d} = 0 \,. \tag{4.40}$$

  As discussed in Section 1.3.2.a, the electron Yukawa interaction is not in equilibrium until $T \sim 10^{4-5}\,\mathrm{GeV}$. When $T > 10^{4-5}\,\mathrm{GeV}$, the right-handed electron can not be generated effectively and its chemical potential should be 0. This would lead to a small change in the chemical potential relations [159].

- The electroweak sphaleron process erase left-handed $B + L$, which guarantees the total $B - L$ number in the plasma vanishes (See. Eq.(1.51)). One may see that the electroweak sphaleron process, 12-fermion interaction[10] doesn't conserve fermion number.

- All the spectator processes, including electroweak sphaleron, conserve hyper-charge. Thus, the hypercharge neutrality is required in the thermal plasma, which gives[11]

$$3\left(\mu_Q + 2\mu_u - \mu_d - \mu_\ell - \mu_e\right) + \mu_{H_u} - \mu_{H_d} = 0 \,. \tag{4.41}$$

  Notice there is a colour factor 3 for both LH and RH quarks and a factor of 2 for the doublets of Q, ℓ and H_u too.

---

[9] Similar to the non-supersymmetric case, Eq.(1.55) and (1.56).

[10] See section (1.3.2).

[11] Similar to Eq.(1.54) in the SM.

Hence, we have 5 equations and 6 variables and we can express all these chemical potentials in term of μ_ℓ:

$$\mu_Q = -\frac{\mu_\ell}{3}; \quad \mu_{H_u} = \frac{4\mu_\ell}{7}; \quad \mu_u = \frac{5\mu_\ell}{21}; \quad \mu_d = -\frac{19\mu_\ell}{21}; \quad \mu_e = \frac{3\mu_\ell}{7}\,. \tag{4.42}$$

Conventionally, ones work with variable total $B-L$ number in the Boltzmann Equations. Therefore the $B-L$ number in the SM+N, defined by

$$\hat{n}_{B-L}^{\rm MSSM+N} \equiv N_f \times (\hat{n}_Q \times \frac{1}{3} \times 2 \times 3 + \hat{n}_u \times \frac{1}{3} \times 3 + \hat{n}_d \times \frac{1}{3} \times 3 - \hat{n}_\ell \times 2 - \hat{n}_e)\,, \tag{4.43}$$

can be re-expressed by $\hat{n}_\ell$. Here N_f is the family number. And the factor 1/3 inside the bracket stands for one quark with 1/3 $B-L$ number and factor 3 and 2 inside the bracket are the color factor and $SU(2)_W$ factor respectively. Inserting Eq.(4.42) into Eq.(4.43), we can arrive at

$$\hat{n}_{B-L} = -\frac{79}{21} N_f \hat{n}_\ell\,. \tag{4.44}$$

Therefore all the components in equilibrium in the thermal plasma of the Universe can be expressed by n_{B-L}, which we will use in the Boltzmann Equations, using Eq.(1.50), (4.26), (4.42) and (4.44):

$$\begin{aligned} \hat{n}_Q = \frac{7}{79}\frac{1}{N_f}\hat{n}_{B-L}\,, \quad \hat{n}_u = -\frac{5}{79}\frac{1}{N_f}\hat{n}_{B-L}\,, \quad \hat{n}_d = \frac{19}{79}\frac{1}{N_f}\hat{n}_{B-L}\,, \\ \hat{n}_e = -\frac{9}{79}\frac{1}{N_f}\hat{n}_{B-L}\,, \quad \hat{n}_{H_u} = -\frac{12}{79}\frac{1}{N_f}\hat{n}_{B-L}\,. \end{aligned} \tag{4.45}$$

Now we can rewrite the terms in the Boltzmann Equations, using Eq.(4.44) and (4.45). Thus Eq.(4.31)-(4.33) turn into

$$\Gamma^{\hat{\ell}}_{St} = -\frac{2}{sHz}\frac{1}{N_f}\left(\frac{12}{79}\frac{\hat{Y}_{N_1}}{\hat{Y}^{\rm eq}_{N_1}} + \frac{54}{79}\right)\frac{\hat{Y}_{B-L}}{\hat{Y}^{\rm eq}_{B-L}}\,\gamma_{St}\,, \tag{4.46}$$

$$\Gamma^{\hat{\ell}}_{Ss} = -\frac{2}{sHz}\frac{1}{N_f}\left(\frac{21}{79}\frac{\hat{Y}_{N_1}}{\hat{Y}^{\rm eq}_{N_1}} + \frac{12}{79}\right)\frac{\hat{Y}_{B-L}}{\hat{Y}^{\rm eq}_{B-L}}\,\gamma_{Ss}\,, \tag{4.47}$$

$$\Gamma^{\hat{\ell}}_{N_t+N_s} = -\frac{2}{sHz}\frac{1}{N_f}\frac{66}{79}\frac{\hat{Y}_{B-L}}{\hat{Y}^{\rm eq}_{B-L}}\left(\gamma_{Ns}+\gamma_{Nt}\right)\,, \tag{4.48}$$

where we have used the $\hat{Y}^{\rm eq}_\ell = \hat{Y}^{\rm eq}_{H_u} = \hat{Y}^{\rm eq}_{B-L}$, as both ℓ and H_u are massless particles in the leptogenesis era ($T \gg E_{\rm EW}$, where $E_{\rm EW}$ is the energy scale of electroweak symmetry

breaking). Boltzmann Equation terms in Eq.(4.29) and (4.30) hold, as they only contains $\hat{Y}_{N_1}$. Thus, Eq.(4.27) and Eq.(4.28) becomes solvable.

To sum up, the Boltzmann Equations for MSSM+RHN are

$$\frac{\mathrm{d}\hat{Y}_{N_1}}{\mathrm{d}z} = -\frac{2}{sHz}\left(\frac{\hat{Y}_{N_1}}{\hat{Y}_N^{eq}}-1\right)\left(\gamma_D+2\gamma_{Ss}+4\gamma_{St}\right), \tag{4.49}$$

$$\begin{aligned}\frac{\mathrm{d}\hat{Y}_{B-L}}{\mathrm{d}z} = &-\frac{2}{sHz}\left\{\epsilon^{\mathrm{tot}}\left(\frac{\hat{Y}_{N_1}}{\hat{Y}_{N_1}^{eq}}-1\right)\gamma_D+\frac{1}{N_f}\left[\left(\frac{12}{79}\frac{\hat{Y}_{N_1}}{\hat{Y}_{N_1}^{\mathrm{eq}}}+\frac{54}{79}\right)\gamma_{St}\right.\right.\\ &\left.\left.+\left(\frac{21}{79}\frac{\hat{Y}_{N_1}}{\hat{Y}_{N_1}^{\mathrm{eq}}}+\frac{12}{79}\right)\gamma_{Ss}+\frac{66}{79}\left(\gamma_{Ns}+\gamma_{Nt}\right)\right]\frac{\hat{Y}_{B-L}}{\hat{Y}_{B-L}^{\mathrm{eq}}}\right\}.\end{aligned} \tag{4.50}$$

Notice that the ϵ^{tot} in Eq.(4.50) is the total (sum over all lepton flavours) CP asymmetry of the RH neutrino decay. We do not do the numerical calculation in this case, as we are more interested in leptogenesis in E_6SSM.

4.6 The Boltzmann Equations in the E_6SSM

Now the Boltzmann Equations in the canonical scenario are set, we can move on to the case of E_6SSM. We investigate the case where Z_2^H symmetry is conserved in section (4.6.1), the case of inert Higgs (Model I) in section (4.6.2) and the case of leptoquark (Model II) in section (4.6.3).

4.6.1 The case of L_4 only (Z_2^H symmetry conserved)

In E_6SSM, the additional lepton doublet L_4 and $\bar{L}_4$ participates the EW interaction. In order to know how L_4 and $\bar{L}_4$ behave in the Boltzmann Equation, we need to know if they can be in equilibrium with other components (*e.g.* Q, u, d, e, ℓ and $H_{u,d}$).

Due to the super-potential term $\lambda H_d L_4 e$, the Yukawa interaction $L_4+H_d \leftrightarrow e$ happens in the hot plasma of the early Universe. If we assume there is no strong suppression of this Yukawa interaction, it would be in equilibrium as the same as the SM LH leptons ℓ.

So, we have the relation of chemical potential of L_4, H_d and e, similar to Eq.(4.40):

$$\mu_{L_4} - \mu_e + \mu_{H_d} = 0\,. \tag{4.51}$$

We can simply compare ordinary lepton Yukawa interaction condition, Eq.(4.40) with Eq.(4.51), and derive that the chemical potential for L_4

$$\mu_{L_4} = \mu_\ell. \tag{4.52}$$

In addition, due to the bilinear term $\mu' L_4 \bar{L}_4$ in the super-potential, we can immediately write down the relation between the chemical potential of L_4 and $\bar{L}_4$[12]:

$$\mu_{L_4} = -\mu_{\bar{L}_4}\,. \tag{4.53}$$

And we can calculate the chemical potential relations with L_4 and $\bar{L}_4$ now. First of all, Eq.(4.38-4.40) still hold. And since both L_4 and $\bar{L}_4$ participate in electroweak sphaleron process, Eq.(1.51)[13], the condition for a vanishing $B - L$ number turns into

$$3\mu_Q + \mu_\ell + \mu_{L_4} - \mu_{\bar{L}_4} = 0\,. \tag{4.54}$$

The interactions of L_4 and $\overline{L}_4$ conserve hyper charge. Thus the total hyper-charge vanishes, and we have

$$3\left(\mu_Q + 2\mu_u - \mu_d - \mu_\ell - \mu_e\right) - \mu_{L_4} + \mu_{\bar{L}_4} + \mu_{H_u} - \mu_{H_d} = 0\,. \tag{4.55}$$

Here we have used the fact that L_4 carries hyper-charge -1 and $\bar{L}_4$ carries hyper-charge 1. Using Eq.(4.38)-(4.40) and Eq.(4.52)-(4.55), we can arrive at the chemical potential relations of these particles:

$$\mu_Q = -\mu_\ell; \quad \mu_{H_u} = \mu_\ell; \quad \mu_u = 0; \quad \mu_d = -2\mu_\ell; \quad \mu_e = 0; \quad \mu_{L_4} = \mu_\ell; \quad \mu_{\bar{L}_4} = -\mu_\ell \tag{4.56}$$

---

[12]This is similar to the situation of H_u and H_d.

[13]Since particles in the sphaleron processes carry certain $U(1)_N$ charges, one finds that the conservation of $U(1)_N$ charge might forbid the electroweak sphaleron process. In this situation, the electroweak sphaleron process can only happen when the $U(1)_N$ symmetry breaks. This might require writing Boltzmann Equations in a flavour independent way. And the B to L transition happens in a window between the $U(1)_N$ breaking scale and the electroweak scale. Alternatively, higher gauge symmetry in the E$_6$SSM may also result in some $B + L$ number breaking operator, allowing the L to B transition. The details will be discussed in a work in progress.

The the total $B-L$ with L_4 and $\bar{L}_4$ is

$$\begin{aligned}\hat{n}_{B-L}^{\mathrm{E_6SSM}} &\equiv N_f \times (\hat{n}_Q \times \frac{1}{3} \times 2 \times 3 + \hat{n}_u \times \frac{1}{3} \times 3 + \hat{n}_d \times \frac{1}{3} \times 3 - \hat{n}_\ell \times 2 - \hat{n}_e) - \hat{n}_{L_4} + \hat{n}_{\bar{L}_4} \\ &= -20\,\hat{n}_\ell\,, \end{aligned} \tag{4.57}$$

where we use the ordinary family number $N_f = 3$. And we can write down the number densities of relevant particles in terms of $\hat{n}_{B-L}$:

$$\begin{gathered}\hat{n}_Q = \frac{1}{20}\hat{n}_{B-L}\,, \quad \hat{n}_u = 0\,, \quad \hat{n}_d = \frac{1}{10}\hat{n}_{B-L}\,, \\ \hat{n}_e = 0\,, \quad \hat{n}_{L_4} = -\frac{1}{20}\hat{n}_{B-L}\,, \quad \hat{n}_{\bar{L}_4} = \frac{1}{20}\hat{n}_{B-L}\,, \quad \hat{n}_{H_u} = -\frac{1}{20}\hat{n}_{B-L}\,. \end{gathered} \tag{4.58}$$

As the $\Delta L = \pm 2$ scatterings play a much more important role than $\Delta L = \pm 1$ scatterings, we neglect the terms of γ_{S_s}, and γ_{S_t}. The Boltzmann Equations in $\mathrm{E_6SSM}$, Z_2^H symmetry conserved case turns into

$$\frac{\mathrm{d}\hat{Y}_{N_1}}{\mathrm{d}z} = -\frac{2}{sHz}\left(\frac{\hat{Y}_{N_1}}{\hat{Y}_N^{eq}} - 1\right)\left(\gamma_D + 2\gamma_{Ss} + 4\gamma_{St}\right)\,, \tag{4.59}$$

$$\frac{\mathrm{d}\hat{Y}_{B-L}}{\mathrm{d}z} = -\frac{2}{sHz}\left\{\epsilon^{\mathrm{tot}}\left(\frac{\hat{Y}_{N_1}}{\hat{Y}_{N_1}^{eq}} - 1\right)\gamma_D + \frac{1}{10}\left(\gamma_{Ns}^{L_4} + \gamma_{Nt}^{L_4}\right)\frac{\hat{Y}_{B-L}}{\hat{Y}_{B-L}^{\mathrm{eq}}}\right\}. \tag{4.60}$$

Here, $\gamma_{Ns}^{L_4}$ and $\gamma_{Nt}^{L_4}$ is the scattering rate of $L_4 + H_u \leftrightarrow \bar{L}_4 + H_u^*$. We neglect scatterings with ordinary lepton number due to their small Yukawa couplings. In addition, one should notice that the total degrees of freedom in this case is $g_*^{ESSM} = 232.5$ due to the additional L_4. An example of the evolution of $B-L$ number is illustrated in Fig. (4.4). We can read that the final $\hat{Y}_{B-L}$ number 7.7×10^{-10}. And in this case, From Eq.(4.56), (4.57) and (4.58), we can see that $\hat{n}_B = \frac{3}{5}\hat{n}_{B-L}$. Then an approximatly correct baryon number can be generated.

4.6.2 The case of inert Higgs

In this subsection, we discuss the case with additional inert Higgs H_2. Since we turn off the Yukawa couplings of L_4 and $\overline{L}_4$, they do not appear in the thermal plasma of

the universe. For $B-L$ number, we only need to consider three generations of quarks and leptons (both left-handed and right-handed). The number density relations of these particles, togeter with "active Higgs" in MSSM+RHN, Eq.(4.44)-(4.45) still hold.

Concerning the extra inert Higgs field, H_2 only participates in N_1 decay and scatterings. We can calculate the asymmetry of H_2 via Boltzmann Equations. The reason is the "inert Higgs number" can only be changed by RH neutrino decay and lepton number changing scatterings. Therefore, the net number density of H_2 have to be considered as a separate variable in the Boltzmann Equations. For $B-L$ number, inert Higgs appears in the washing-out terms of $B-L$ number.

Also, due to the large (lepton)-(inert Higgs)-(RH neutrino) Yukawa couplings, the major contribution of washing-out terms is the $\Delta L=\pm 2$ scatterings $\ell+H_2\leftrightarrow\bar{\ell}+H_2^*$. We notice that this process washes both $B-L$ number and H_2 number by 2 units. The contribution is

$$\Gamma^{\rm H_2}_{N_t+N_s} = -\frac{2}{sHz}\left(\frac{\hat{Y}_\ell}{\hat{Y}^{\rm eq}_\ell}+\frac{\hat{Y}_{H_2}}{\hat{Y}^{\rm eq}_{H_2}}\right)\left(\gamma^{H_2}_{Ns}+\gamma^{H_2}_{Nt}\right) \tag{4.61}$$

where $\gamma^{H_2}_{Ns}$ and $\gamma^{H_2}_{Nt}$ are the s-channel and t-channel reaction rate for $\ell+H_2\leftrightarrow\bar{\ell}+H_2^*$ respectively. Then, the Boltzmann Equations for $B-L$ number and inert Higgs are

$$\frac{{\rm d}\hat{Y}_{N_1}}{{\rm d}z} = -\frac{2}{sHz}\left(\frac{\hat{Y}_{N_1}}{\hat{Y}^{eq}_N}-1\right)\left(\gamma_D+2\gamma_{Ss}+4\gamma_{St}\right), \tag{4.62}$$

$$\frac{{\rm d}\hat{Y}_{B-L}}{{\rm d}z} = -\frac{2}{sHz}\left\{\epsilon^{\rm tot}\left(\frac{\hat{Y}_{N_1}}{\hat{Y}^{eq}_{N_1}}-1\right)\gamma_D+\left(\frac{\hat{Y}_\ell}{\hat{Y}^{\rm eq}_\ell}+\frac{\hat{Y}_{H_2}}{\hat{Y}^{\rm eq}_{H_2}}\right)\left(\gamma^{H_2}_{Ns}+\gamma^{H_2}_{Nt}\right)\right\}, \tag{4.63}$$

$$\frac{{\rm d}\hat{Y}_{H_2}}{{\rm d}z} = -\frac{2}{sHz}\left\{\epsilon^{H_2}_{1,\tau}\left(\frac{\hat{Y}_{N_1}}{\hat{Y}^{eq}_{N_1}}-1\right)\gamma_D+\left(\frac{\hat{Y}_\ell}{\hat{Y}^{\rm eq}_\ell}+\frac{\hat{Y}_{H_2}}{\hat{Y}^{\rm eq}_{H_2}}\right)\left(\gamma^{H_2}_{Ns}+\gamma^{H_2}_{Nt}\right)\right\}. \tag{4.64}$$

where $\epsilon^{\rm tot}$ is the total CP asymmetry, including H_2 in the final state and

$$\epsilon^{H_2}_{1,\tau}\equiv\frac{\Gamma(N_1\to\tau+H_2)-\Gamma(N_1\to\bar{\tau}+H_2^*)}{\Gamma(N_1\to{\rm everthing})} \tag{4.65}$$

is the decaying asymmetry with only H_2 in the final state[14].

[14]Actually, taking $\epsilon^{\rm tot}\simeq\epsilon^{H_2}_{1,\tau}$, we can arrive at $\hat{Y}_{B-L}=\hat{Y}_{H_2}$.

Fig. 4.5 shows a successful leptogenesis in this scenario. We notice the final $Y_{B-L} = 2.7 \times 10^{-10}$. And in this case baryon number and $B - L$ number are kept in a ratio $\hat{n}_B = \frac{84}{79}\hat{n}_{B-L}$[15].

4.6.3 The case of exotic quark (leptoquark)

In the case of leptoquarks D and $\overline{D}$ involved, the RH neutrino decays into quark fields and leptoquark fields, $N_1 \to \tilde{d}D$. Notice that $\tilde{d}^*$ has $-1/3$ baryon number and D has $1/3$ unit of baryon number and 1 unit of lepton number ($\overline{D}$ has $-1/3$ baryon number and -1 lepton number, but it does not appear in the final state of the RH neutrino decay), therefore -1 unit of $B - L$ number is in the final states of this decay channel, which will enter the thermal plasma.

Since we are interested in the $\Delta L = \pm 2$ scatterings, $\ell + H_u \to \bar{\ell} + H_u^*$, and $D + \tilde{d} \to D^c + \tilde{d}^*$, which play the role of washing out process, we need to know the particle density relations of relevant particles to the $B-L$ number. And we need to calculate the chemical potentials again. First of all, we notice that both D and $\overline{D}$ are singlets of $SU(2)_W$. Therefore they cannot participate in the electroweak sphaleron process. However, due to the coupling $g^E_{ijk} e^c_i D_j u^c_k$ in the E$_6$SSM super-potential, the baryon number and lepton number can be released to ordinary (s)quark and (s)lepton via scattering $e + \tilde{u} \leftrightarrow D$, which allows us to write down the relation of chemical potentials of e, u and D, μ_e, μ_u and μ_D:

$$\mu_e + \mu_u = \mu_D \,, \tag{4.66}$$

unless the couling constants g^E_{ijk} are strongly suppressed. Similarly, for $\overline{D}$, the coupling $g^D_{ijk}(Q_i L_j)\bar{D}_k$ results in the scattering $\bar{Q} + \bar{\ell} \leftrightarrow \bar{D}$ in equilibrium. And this can be used to calculate the chemical potential of $\overline{D}$ via

$$-\mu_Q - \mu_\ell = \mu_{\bar{D}} \,. \tag{4.67}$$

[15]This can be calculated from Eq.(4.44) and (4.45).

Notice that both Eq.(4.66) and Eq.(4.67) are valid for all three generations of D and $\overline{D}$. And we can derive that the chemical potentials for different generations of D and $\overline{D}$ are equal respectively.

The relations of ordinary lepton and quark Yukawa interaction, Eq.(4.38)-Eq.(4.40) still hold. Moreover, since D and $\overline{D}$ do not participate in the electroweak sphaleron process, the relation of left-handed $B-L$ number vanishes, Eq.(1.51) also holds. Finally, the relation of the total hyper-charge vanishes, Eq.(4.41) need to be rewritten, adding D and $\overline{D}$:

$$3\left(\mu_Q + 2\mu_u - \mu_d - \mu_\ell - \mu_e - \mu_D + \mu_{\bar{D}}\right) + \mu_{H_u} - \mu_{H_d} = 0\,. \tag{4.68}$$

Here, we have used the hyper-charge of -1/3 for D and 1/3 for $\overline{D}$, and summed over three colors of D and $\overline{D}$. So the algebraic relations can be calculated from Eq.(4.38)-(1.51),(4.66),(4.67) and Eq.(4.68). The result is given by

$$\begin{aligned} \mu_Q = -\frac{1}{3}\ell\,, \quad \mu_{H_u} = \frac{6}{7}\mu_\ell\,, \quad \mu_u = \frac{11}{21}\mu_\ell\,, \quad \mu_d = -\frac{25}{21}\mu_\ell\,, \\ \mu_e = \frac{1}{7}\mu_\ell\,, \quad \mu_D = \frac{2}{3}\mu_\ell\,, \quad \mu_{\bar{D}} = -\frac{2}{3}\mu_\ell\,. \end{aligned} \tag{4.69}$$

In this case, the total $B-L$ number includes the three generations of leptoquarks (D carries $-2/3$ $B-L$ number and $\overline{D}$ carries $2/3$ $B-L$ number.):

$$\begin{aligned} \hat{n}_{B-L}^{\rm ESSM,II} &= N_f \times \left(\hat{n}_Q \times \frac{1}{3} \times 2 \times 3 + \hat{n}_u \times \frac{1}{3} \times 3 + \hat{n}_d \times \frac{1}{3} \times 3 \right. \\ &\qquad \left. + \hat{n}_D \times \left(-\frac{2}{3}\right) \times 3 + \hat{n}_{\bar{D}} \times \frac{2}{3} \times 3 + \hat{n}_\ell \times (-1) \times 2 + \hat{n}_e \times (-1) \right) \\ &= -\frac{129}{7}\,\hat{n}_\ell\,. \end{aligned} \tag{4.70}$$

where we also take $N_f = 3$. Therefore the $\Delta L = \pm 2$ scattering $\tilde{q}^* + D \leftrightarrow \tilde{q} + D^c$ has the reaction rates γ_{Ns}^D (s-channel) and γ_{Nt}^D (t-channel) and reaction density:

$$\begin{aligned} \Gamma_{N_t+N_s}^D + \Gamma_{N_t+N_s}^D &= \frac{2}{sHz} \cdot 2 \cdot \left(-\frac{\hat{Y}_d}{\hat{Y}_d^{\rm eq}} + \frac{\hat{Y}_D}{\hat{Y}_D^{\rm eq}} \right) \left(\gamma_{Ns}^D + \gamma_{Nt}^D \right) \\ &= \frac{2}{sHz} \cdot \frac{26}{129} \cdot \frac{\hat{Y}_{B-L}}{\hat{Y}_{B-L}^{\rm eq}} \cdot \left(\gamma_{Ns}^D + \gamma_{Nt}^D \right)\,. \end{aligned} \tag{4.71}$$

The Boltzmann Equations for leptogenesis with leptoqaurks are

$$\frac{\mathrm{d}\hat{Y}_{N_1}}{\mathrm{d}z} = -\frac{2}{sHz}\left(\frac{\hat{Y}_{N_1}}{\hat{Y}_N^{eq}}-1\right)\left(\gamma_D+2\gamma_{Ss}+4\gamma_{St}\right), \tag{4.72}$$

$$\frac{\mathrm{d}\hat{Y}_{B-L}}{\mathrm{d}z} = -\frac{2}{sHz}\left\{\epsilon^{\mathrm{tot}}\left(\frac{\hat{Y}_{N_1}}{\hat{Y}_{N_1}^{eq}}-1\right)\gamma_D+\frac{26}{129}\cdot\frac{\hat{Y}_{B-L}}{\hat{Y}_{B-L}^{\mathrm{eq}}}\cdot\left(\gamma_{Ns}^D+\gamma_{Nt}^D\right)\right\}. \tag{4.73}$$

Notice that the total CP asymmetry of RH neutrino decay is defined as

$$\epsilon^{\mathrm{tot}} \equiv \frac{\sum_\alpha(\Gamma_{N_1\to\ell_\alpha}-\Gamma_{N_1\to\bar{\ell}_\alpha})+(\Gamma_{N_1\to D}-\Gamma_{N_1\to\bar{D}})}{\Gamma_{N_1\to\mathrm{everything}}}. \tag{4.74}$$

Since the color factor of the exotic quark, we have to modify the total degrees of freedom of the plasma $g_*^{ESSM,II}=240$ due to the additional L_4. An example of the evolution of $B-L$ number in E_6SSM model II is illustrated in Fig. 4.6. The final $B-L$ number reads 4.3×10^{-8}. Also we can calculate that the ratio of B and $B-L$ is $\hat{n}_B=\frac{11}{89}\hat{n}_{B-L}$. Hence, a successful leptogenesis is also achieved in this scenario.

In conclusion, although the Boltzmann Equations are slightly different, correct amounts of baron asymmetry can be achieved in all these three cases when the lightest RH neutrino mass $\sim 10^7\,\mathrm{GeV}$. Therefore we can bring down the reheating temperature and avoid the gravitino-over-production problem.

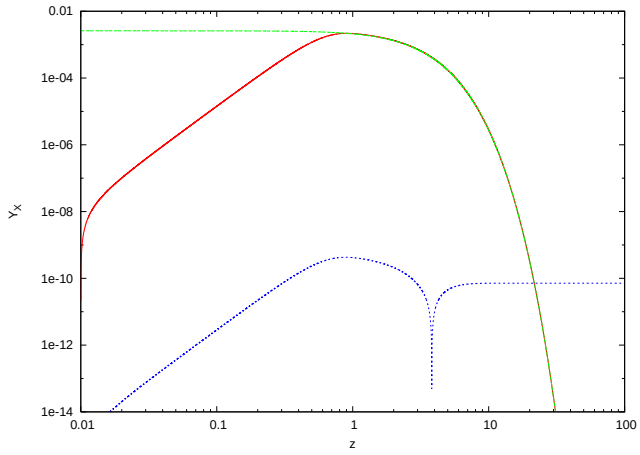

(a)

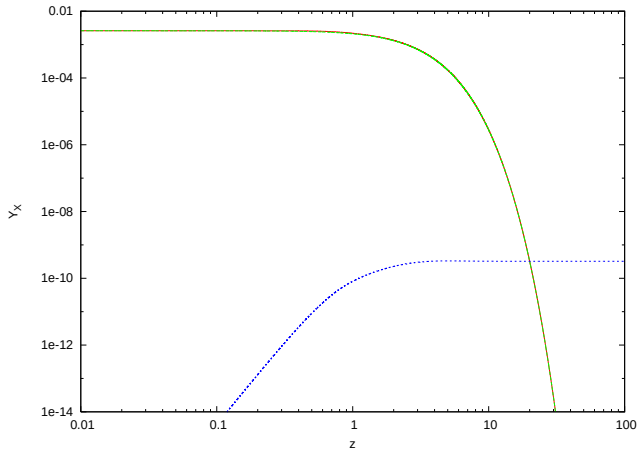

(b)

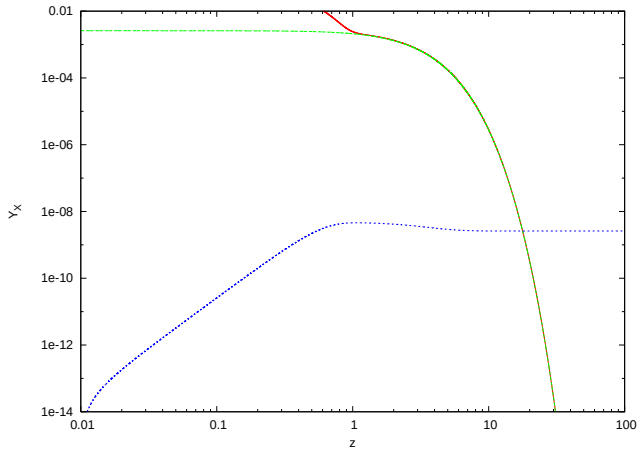

(c)

Figure 4.3: The evolution of Y_{N_1} and $|Y_\ell|$ in a toy model (one flavour and only the inverse decay as the washing-out process), with different initial conditions: (a) $Y_{N_1} = 0$; (b) $Y_{N_1} = Y_{N_1}^{\rm eq}$; (c) $Y_{N_1} = 10\, Y_{N_1}^{\rm eq}$. In these plots, the red/solid lines represent the evolution of Y_{N_1}. The greeen/dash lines are $Y_{N_1}^{\rm eq}$. The blue/dot lines stand for $Y_{|\ell|}$.

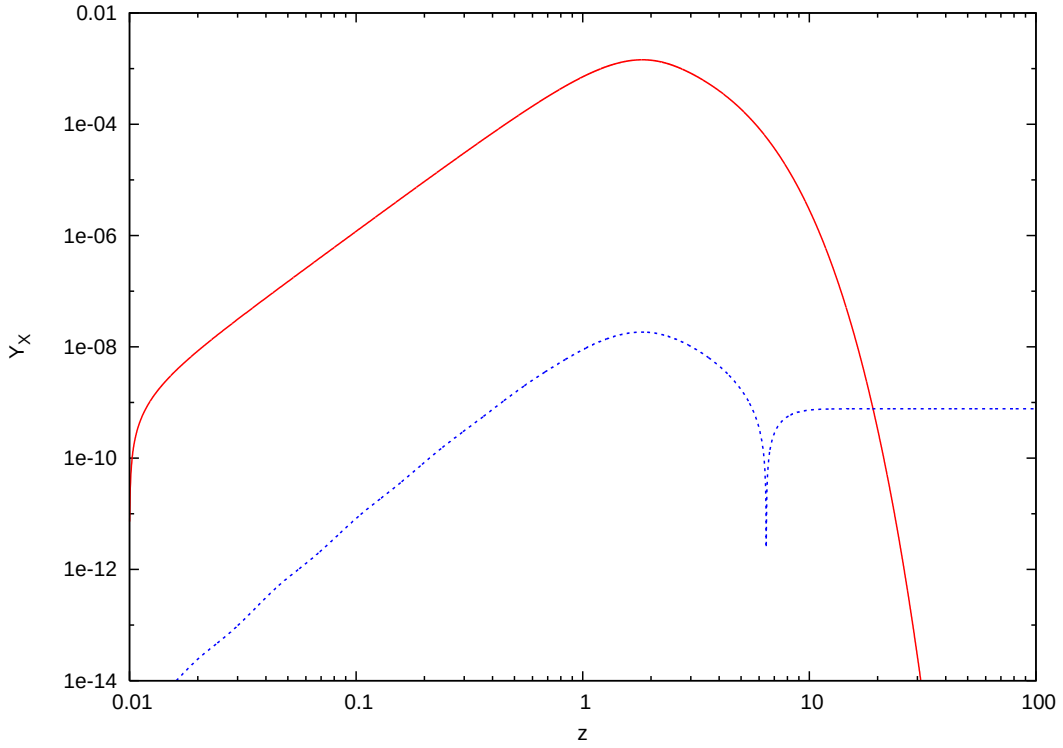

Figure 4.4: The evolution of N_1 (the red/solid line) and $B-L$ (the blue/dash line) number in E_6SSM, Z_2^H symmetry conserved case, for $M_1 = 10^7$ GeV, $h^N_{H_3^u L_4 N_1} = 10^{-5}$, $h^N_{H_3^u L_4 N_2} = 0.1$.

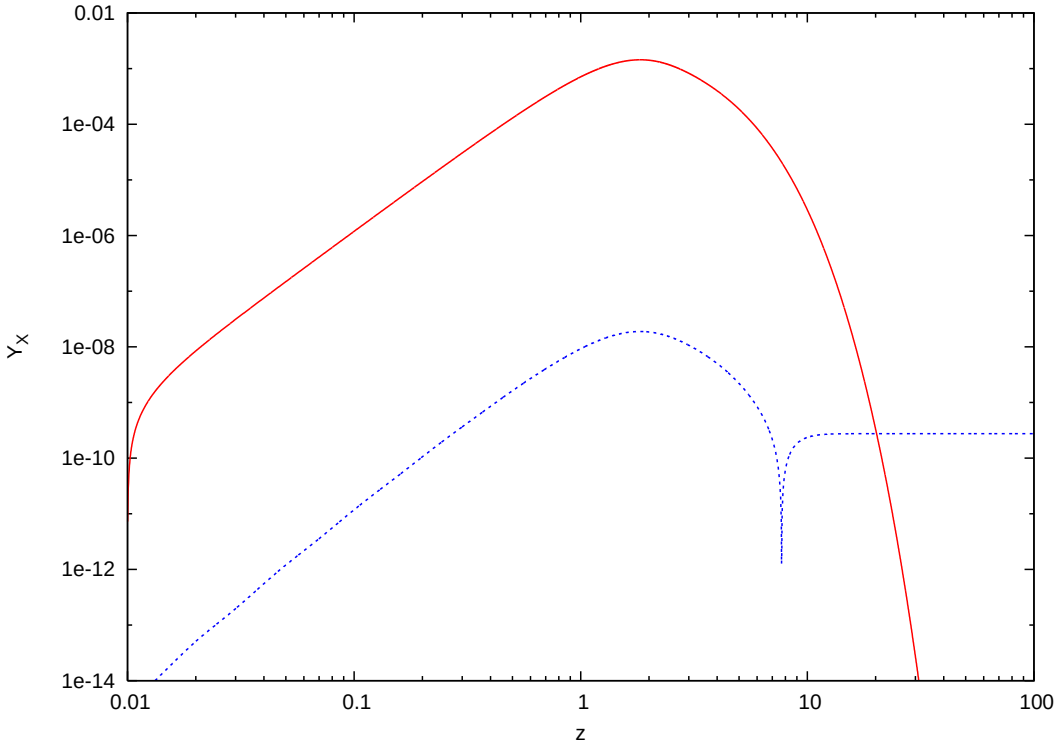

Figure 4.5: The evolution of N_1 (the red/solid line) and $B-L$ (the blue/dash line) number in E_6SSM, model I, for $M_1 = 10^7$ GeV, $h^N_{H_2^u L_3 N_1} = 10^{-5}$, $h^N_{H_2^u L_3 N_2} = 0.1$.

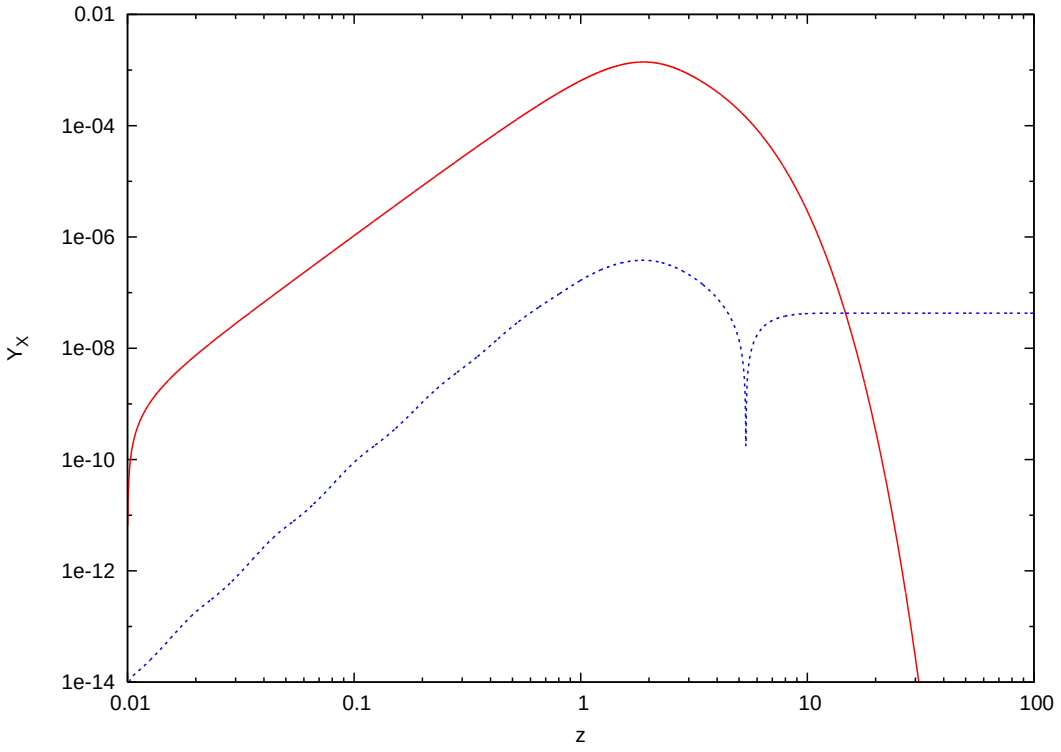

Figure 4.6: The evolution of N_1 (the red/solid line) and $B-L$ (the blue/dash line) number in E_6SSM, model II, for $M_1 = 10^7$ GeV, $g^N_{D_3 d_3 N_1} = 10^{-5}$, $g^N_{D_3 d_3 N_2} = 0.2$.

Chapter 5

Conclusion and Outlook

Neutrinos are particles in the SM that only participate in the electroweak interaction. In the SM, they are described as massless particles. However, when neutrinos are produced in coherent sources (the electroweak interactions), they oscillate between the three families due to their mass differences and the mixing. The neutrino mass squared differences and three mixing angles are well measured by solar, atmospheric and terrestrial neutrino oscillation experiments, whereas the exact scale or the pattern of neutrino masses is still unclear. Neutrinoless double beta decay is the most promising experiment to measure the neutrino mass spectrum. They have masses at least six orders of magnitude lighter than the electron. The lightness of neutrinos indicates that neutrino masses may come from physics at scale much higher than the electroweak scale $\sim$ 100 GeV.

A intriguing mechanism of light neutrino masses is the seesaw model, one explains the lightness of LH neutrino by introducing heavy Majorana RH neutrinos to the SM. The RH neutrinos couple to the left-handed neutrinos via Yukawa couplings. The Yukawa couplings turn into Dirac mass terms. By diagonalising the mass matrix of LH neutrinos and RH neutrinos, one can obtain the effective light LH neutrino masses, which are inversely proportional to the RH neutrino Majorana masses. One also notice that the Majorana nature of neutrinos results in lepton number violation.

The luminous matter of the universe consists of baryon, the ratio of which is well measured from light element abundances and CMB temperature anisotropy. The WMAP data reads the baryon to photon ratio $\eta_B = 6.225 \pm 0.17 \times 10^{-10}$. One need to explain why it is the baryons generated rather than anti-baryons, the so called BAU puzzle. There are three main mechanisms: *(a)* Leptogenesis, in which lepton number is produced from RH neutrino CP violating decay, and sphaleron processes convert lepton number into baryon number; *(b)* the Electroweak Baryogenesis, where net baryon number is generated via electroweak phase transition; *(c)* the Affleck-Dine mechanism, where leptons are produced from scalar dynamics in the early universe, and converted into baryon number via EW sphaleron process.

In the present thesis, we concentrated on Leptogenesis from RH neutrino decay. The RH neutrino, being a Majorana particle, decays into leptons and anti-leptons via Yukawa couplings. The CP asymmetry arises due to the interference of the loop diagrams and tree-level diagrams, which leads to a small difference of leptons and anti-leptons in the final state per RH neutrino decay. Assuming strong hierarchical RH neutrino masses, $M_1 \ll M_2 \ll M_3$, the CP asymmetry is a function of the lightest RH neutrino mass and Yukawa couplings. Since in the seesaw model, the light neutrino masses can be expressed in terms of masses of RH neutrino and Yukawa couplings, the CP asymmetry of RH neutrino decay is constrained by the masses of light neutrino. The so-called Davidson-Ibarra bound on CP asymmetry $|\varepsilon_1| \leq \frac{3}{8\pi}\frac{M_1}{v^2}(m_3 - m_1)$ requires the mass of the lightest RH neutrino $M_1 \gtrsim 10^{8-9}\,\mathrm{GeV}$ in the case of efficiency factor $\eta_{\mathrm{eff}} = 10^{-(2-3)}$ to generate the correct baryon-entropy ratio. However, in the super-gravity theories, the temperature of Leptogenesis $T \sim M_1 \gtrsim 10^{8-9}\,\mathrm{GeV}$ results in a large abundance of gravitinos generated at the reheating era, which might be a catastrophe, since the decay of gravitino can dilute the light elements from BBN. One viable solution is Leptogenesis in the E_6SSM model.

The E_6SSM model is based on E_6 symmetry from string theory, and at low energy scale, it has an effective extra $U(1)_N$ symmetry under which the RH neutrinos are neutral. An exotic lepton, behaving as a fourth generation of lepton is introduced in this model

to unify the gauge couplings. And a Z_2^H symmetry is imposed to forbid FCNC processes, and the breaking of Z_2^H symmetry leads to some interesting phenomena, including the two families of inert Higgs and exotic quarks. These exotic quarks could be leptoquarks or diquarks. The exotic lepton L_4 contributes to the light neutrino masses due to its mixing with the RH neutrino.

In E_6SSM, the RH neutrinos couple to the SM lepton and the exotic lepton via the Yukawa coupling, when the Z_2^H symmetry is conserved. In the case of broken Z_2^H symmetry, the RH neutrino can couples to the inert Higgs and the leptoquark. These extra Yukawa couplings contribute to the lepton asymmetry of RH neutrino decay. We analysis three different cases: *(a)* the case of Z_2^H symmetry conserved *(b)* model I, the inert Higgs is included *(c)* model II, the leptoquark is included. We found in all the three cases, the lepton asymmetries can be enhanced drastically with respect to the CP asymmetries in the framework of MSSM plus RH neutrinos in the region of low RH neutrino mass/reheating temperature $T \sim 10^{6-7}\,\mathrm{GeV}$.

We considered the evolution of lepton/baryon number densities in the E_6SSM through solving the Boltzmann Equations for Leptogenesis. We start from the flavour independent Boltzmann Equations, where the sphaleron processes are assumed to be not active. The evolution of lepton number densities has been analysed for the cases of L_4 and inert Higgses. In these cases, the $\Delta L = 2$ scatterings are more important than $\Delta L = 1$ scatterings thanks to the large exotic Yukawa couplings. The numerical results have showed that a correct baryon abundance can be achieved in either case despite the wash out processes being strong.

We studied the effect of flavour in Boltzmann Equations. We took into account the electroweak sphaleron processes, the QCD sphaleron processes and Yukawa interactions in equilibrium. The ratios of elements, including left-handed and right-handed components of quarks and leptons, Higgs fields are calculated through the relations of chemical potentials of corresponding particles in equilibrium. In the canonical approach, different flavours of $B - L_\alpha$ and left-handed lepton components L_β are connected by a transi-

tion matrix $A_{\alpha\beta}$. The transition matrix describes the abundance of $B - L_\alpha$ converted by sphaleron processes and Yukawa interactions per left-handed lepton generated by RH neutrino decay. In this thesis, we proposed an alternative approach to the flavoured Boltzmann Equations. Based on that only the left-handed components of lepton doublets are active in the processes of RH neutrino decay, $\Delta L = \pm 1$, $\Delta L = \pm 2$ scattering, we distinguish the non-left-handed leptons and consider it as an extra quantity in the Boltzmann Equations. In addition, extra spectator processes terms are introduced in the Boltzmann Equations for left-handed leptons ℓ_α and the non-left-handed components. The spectator terms obey *(a)* being much faster than RH neutrino decay/inverse decay and scattering *(b)* conserving $B - L$ number in the plasma *(c)* making corresponding components in certain ratios calculated from chemical potential relations. We take a different approach where we consider all relevant particle number densities are in certain ratios due to the spectator processes. Then we can calculate total $B - L$ number in the Boltzmann Equations. We investigate the evolution of lepton/baryon number density within this approach. And we found that a successful leptogenesis can happen at low energy scale $T \sim 10^{6-7}$ GeV. We concentrate on three different scenarios: *(a)* E_6SSM with unbroken Z_2^H symmetry (exotic lepton L_4 and $\overline{L}_4$), *(b)* E_6SSM Model I (with inert Higgs fields) and *(c)* E_6SSM Model II (with exotic leptoquarks). We find that when the exotic Yukawa couplings are relatively large, the CP asymmetries of RH neutrino decay can be $\sim 10^{-6}$, so that enough lepton/baryon asymmetry can be generated in the hot plasma in the universe. So we can avoid the problem of gravitino-over-production.

There are still many unsolved problems and potential problems of neutrinos and baryon asymmetry universe. On the side of experiments, we need to measure the exact scale of neutrino mass, more accurate value of the mixing angles, the CP phase of PMNS matrix, and hopefully, the properties of exotic quarks, inert Higgs and RH neutrino. On the side of theory, there are still unsolved problems for neutrino and leptogenesis.

(i) What is the reason of tri-bi-maximal mixing for neutrinos? What leads to the hierarchy of fermion masses? Family symmetry of some unknown mechanism?

(ii) Which mechanism contributes most to the baryon number at present universe? Is there any way to disprove any of them?

(iii) When does leptogenesis happen? Or what is the exact scale of RH neutrino mass? Is gravitino a serious problem in leptogenesis?

(iv) What is the CP phase in the Yukawa couplings of RH neutrino? Is it enough to generate lepton asymmetry for leptogenesis?

(v) How is leptogenesis linked to Dark Matter, considering the fact that $\Omega_{\rm b} \sim \Omega_{\rm DM}$?

More straightforwardly, in Affleck-Dine mechanism, the requirement of enough lepton/baryon number be generated restricts the lightest left-handed neutrino mass. However, the spectator processes are not taken into account in the previous study of the Affleck-Dine mechanism. It would be interesting to investigate the restriction of light neutrino masses when the "flavoured Affleck-Dine" mechanism is considered.

Appendix A

The Spinors in the Standard Model

The Dirac Equation can be split into

$$(\not{p} - m)\, u^{(i)}(p) = 0 \quad (\not{p} + m)\, v^{(i)}(p) = 0\,, \tag{A.1}$$

where $i = 1, 2$, denoting the spin up and spin down states. In the Weyl representation, where

$$\gamma^0 = \begin{pmatrix} 0 & \mathbf{1}_2 \\ \mathbf{1}_2 & 0 \end{pmatrix}, \quad \gamma^i = \begin{pmatrix} 0 & \sigma^i \\ -\sigma^i & 0 \end{pmatrix}, \quad \gamma^5 = \begin{pmatrix} -\mathbf{1}_2 & 0 \\ 0 & \mathbf{1}_2 \end{pmatrix}. \tag{A.2}$$

the spinor $u(p)$ and $v(p)$ can be expressed as

$$u^s(p) = \begin{pmatrix} \sqrt{\mathbf{E} + \vec{p}\cdot\vec{\sigma}}\ \xi^s \\ \sqrt{\mathbf{E} - \vec{p}\cdot\vec{\sigma}}\ \xi^s \end{pmatrix}, \quad v^s(p) = \begin{pmatrix} \sqrt{\mathbf{E} + \vec{p}\cdot\vec{\sigma}}\ \eta^s \\ -\sqrt{\mathbf{E} - \vec{p}\cdot\vec{\sigma}}\ \eta^s \end{pmatrix}. \tag{A.3}$$

Here, ξ and η are two components spinors. $\xi^1 = (1, 0)^T$ and $\xi^2 = (0, 1)^T$

Weyl chiral spinors are projection of left-handed operator and right-handed operator:

$$P_L, \psi_L = \psi_L \quad \text{and} \quad P_R\, \psi_R = \psi_R\,. \tag{A.4}$$

The projection operators are given by:

$$P_L = \frac{1}{2}(1 - \gamma^5)\,, \quad P_R = \frac{1}{2}(1 + \gamma^5). \tag{A.5}$$

The charge conjugate of spinor is defined as

$$\psi^C = C\overline{\psi}^T \,, \tag{A.6}$$

with the charge conjugation matrix $C \equiv \gamma^0\gamma^2$. ψ^C has the opposite chirality to ψ.

Appendix B

Supersymmetry and Beyond

B.1 The Standard Model and Need for New Physics

The Standard Model, based on a $U(1)_Y \times SU(2)_w \times SU(3)_c$ gauge symmetry describes phenomenon of particle physics below $\mathcal{O}(100\,\mathrm{GeV})$. It has 19 parameters: three gauge couplings, nine masses for quarks (up and down type) and charged leptons, three quark mixing angles and one CP phase for this mixing, a QCD CP phase, a Higgs coupling and the Higgs mass. It is a triumph of physics since it is tested precisely in a quite large range, including QED, (*for example* the magnetic moment of electron), QCD and weak processes. However itself suffers some potential problems.

First of all, as mentioned in the previous chapter, the neutrino masses, possibly together with RH neutrino(s) need to be introduced in the Lagrangian. In the QCD part, the strong CP phase θ_{QCD} is strongly suppressed for some unknown reason so that there is no observable CP violation in the strong interaction. On the cosmology side, the Dark Matter (DM), which is neutral and quite stable can not be a SM particle, which indicates that the content of the SM particle need to be extended. In addition, it seems the 19 parameters in the SM is too many. Certain mechanism is needed to reduce the number of parameters.

The SM itself, has a unstable electro-weak scale, suffering from the hierarchy problem due to the loop correction gives a large mass to Higgs particle.

Supersymmetry (SUSY) is the most promising candidate of TeV scale physics, which tend to solve parts of the problems in the SM. In SUSY, particles have their own Supersymmetric partner. So the number of particle is doubled. the large Higgs mass correction is cancelled by additional loop diagram involved supersymmetric particles. Supersymmetry also changes the renormalization group equations, making three gauge couplings unified at one point. The simplest version of Supersymmetry is a model with only SM particles and their Supersymmetric partners, called

The 2-component Weyl spinor Q and its conjugate $\bar{Q}$ obey relations

$$\{Q_\alpha, Q_\beta\} = \{\bar{Q}_{\dot{\alpha}}, \bar{Q}_{\dot{\beta}}\} = 0\,, \quad \{Q_\alpha, \bar{Q}_{\dot{\beta}}\} = 2\sigma^\mu_{\alpha\dot{\beta}} P_\mu\,, \quad [Q_\alpha, P_\mu] = 0\,. \tag{B.1}$$

where $\alpha\,, \beta\,, \dot{\alpha}\,, \dot{\beta} = 1, 2$ and P_μ is the translation generator.

Two fermionic coordinator θ and $\bar{\theta}$, which behave like two-component spinors. They are anti-commutators:

$$\{\theta, \theta\} = \{\theta, \bar{\theta}\} = \{\bar{\theta}, \bar{\theta}\} = 0\,, \tag{B.2}$$

And the finite SUSY transformation reads

$$\exp\left[i\left(\theta\theta + \bar{\theta}\bar{\theta} - x_\mu P^\mu\right)\right]\,. \tag{B.3}$$

The superfields Φ_i can be understood as functions of fermionic coordinator θ, $\bar{\theta}$ and space-time coordinator x_μ. The superpotential

$$f(\Phi_i) = \sum_i k_i \Phi_i + \frac{1}{2}\sum_{i,j} m_{ij}\Phi_i\Phi_j + \frac{1}{3}\sum_{i,j,k} g_{ijk}\Phi_i\Phi_j\Phi_k\,. \tag{B.4}$$

The superpotential can lead to Lagrangian

$$\mathcal{L} = \sum_i \left(F_i F_i^* + |\partial_\mu \phi|^2 - i\bar{\psi}_i \sigma_\mu \partial^\mu \psi_i\right) \tag{B.5}$$

$$+ \left[\sum_j \frac{\partial f(\phi_i)}{\partial \phi_j} F_j - \frac{1}{2}\sum_{j,k} \frac{\partial^2 f(\phi_i)}{\partial\phi_j \partial\phi_k}\psi_j\psi_k + \text{h.c.}\right]\,, \tag{B.6}$$

where the auxiliary field

$$F_j = - \left[\frac{\partial f(\phi_i)}{\partial \phi_j} \right] . \tag{B.7}$$

Supersymmetry may lead to large lepton number violation and baryon number violation at low energy scale, and therefore a discrete symmetry R-parity is imposed in SUSY to forbid lepton number/baryon number violating operators:

$$P_R = (-1)^{3\,(B-L)+2\,s} \tag{B.8}$$

where s is the spin of the particle. The particles in the SM have R-parity of 1 and the SUSY particles have R-parity of -1. Without R-parity violation, a production of a single SUSY particle is forbidden, and the lightest -1 R-parity particle is stable, hence playing a role of the Dark Matter particle.

Appendix C

Hyper Charges of the SM and MSSM Particles

The electric charge Q, isospin operator I_3 and Hyper-charge Y obey the relation:

$$Q = I_3 + \frac{1}{2} Y \,, \tag{C.1}$$

The electric charge, weak isospin and Hyper charge can be found in table (C.1). Notice that fermions from different generations have the same quantum numbers.

In the context of MSSM, the hyper charges of the SUSY particles are the same as their super-partners. In addition, the down-type Higgs H_d and up-type Higgs H_u have hyper-charge $Y_{H_u} = -Y_{H_d}$.

Particle	Electric Charge	Weak Isospin	Hyper Charge
e^L	-1	-1/2	-1
e^R	-1	0	-2
ν_e^L	0	1/2	-1
u^L	2/3	1/2	1/3
u^R	2/3	0	4/3
d^L	-1/3	-1/2	1/3
d^R	-1/3	0	-2/3
H^+	1	1/2	1
H^0	0	-1/2	1
W^+	1	1	0
W^-	-1	-1	0
Z^0	0	0	0
B	0	0	0

Table C.1: The electric charge, weak isospin and Hyper charge of particles in the SM.

Appendix D

The Big Bang Nucleosynthesis Reactions

Before the nucleosynthesis, when the temperature $T \geq 1$ MeV, protons and neutrons participate in weak interaction and they convert into each other via

$$\mathrm{p} + \mathrm{e}^- \leftrightarrow \mathrm{n} + \nu_e\,, \quad \mathrm{p} + \bar{\nu}_e \leftrightarrow \mathrm{n} + e^+\,. \tag{D.1}$$

These two reactions are in chemical equilibrium, and therefore the ratio of neutron to proton density can be calculated according to Boltzmann distribution

$$\frac{n_n}{n_p} = \exp\left(-\frac{m_n - m_p}{T}\right)\,. \tag{D.2}$$

Processes (D.1) are frozen when the Hubble parameter $H = \Gamma_{\mathrm{weak}}$. One can calculates that this happens when the temperature drops to 0.8 MeV. The ratio of neutron to proton is fixed as $n_n/n_p = 1/7$.

Meanwhile, proton and neutron combine into Deuterium:

$$\mathrm{p} + \mathrm{n} \leftrightarrow \mathrm{D} + \gamma\,, \tag{D.3}$$

The binding energy for Deuterium $B_D = 2.2$ MeV. When the temperature drops to 0.06 MeV, a certain amount of Deuterium (the same order of baryon) is yielded. The major

processes at this time are

$$^2\mathrm{D} + \mathrm{p} \rightarrow {}^3\mathrm{He} + \gamma\,, \tag{D.4}$$

$$^2\mathrm{D} + {}^2\mathrm{D} \rightarrow {}^3\mathrm{He} + \mathrm{n}\,, \tag{D.5}$$

$$^2\mathrm{D} + {}^2\mathrm{D} \rightarrow {}^3\mathrm{T} + \mathrm{p}\,, \tag{D.6}$$

which yield ^{3}T[1] and ^{3}He. The sequence processes include

$$^3\mathrm{He} + \mathrm{n} \rightarrow {}^3\mathrm{T} + \mathrm{p}\,, \tag{D.7}$$

$$^3\mathrm{T} + {}^2\mathrm{D} \rightarrow {}^3\mathrm{He} + \mathrm{n}\,, \tag{D.8}$$

$$^3\mathrm{He} + {}^2\mathrm{D} \rightarrow {}^4\mathrm{He} + \mathrm{p}\,. \tag{D.9}$$

At this stage, the major nucleus produced by BBN is ^{4}He. ^{2}D, ^{3}T and ^{3}He are intermediate products, which has number density 3 to 4 orders of magnitude smaller than ^{4}He. When enough ^{4}He is accumulated, the reactions yielding heavier nuclei begins

$$^4\mathrm{He} + {}^3\mathrm{T} \rightarrow {}^7\mathrm{Li} + \gamma\,, \tag{D.10}$$

$$^4\mathrm{He} + {}^4\mathrm{He} \rightarrow {}^7\mathrm{Be} + \gamma\,. \tag{D.11}$$

^{7}Be can convert to ^{7}Li via

$$^7\mathrm{Be} + e^- \rightarrow {}^7\mathrm{Li} + \nu_e\,. \tag{D.12}$$

Part of ^{7}Li collapse with proton and generate ^{4}He

$$^7\mathrm{Li} + \mathrm{p} \rightarrow {}^4\mathrm{He} + {}^4\mathrm{He}\,. \tag{D.13}$$

Considering all these processes together, one finds the final number density of ^{7}Li is 7 to 8 orders of magnitude smaller than ^{4}He. The network of BBN reaction chain is illustrated in Fig. D.1 When the temperature of the universe drops to $\sim$0.01 MeV(10^8 K), the Nucleosynthesis finishes and all light elements abundances are "locked".

[1] ^{3}T is unstable. It will decay into ^{3}He after BBN.

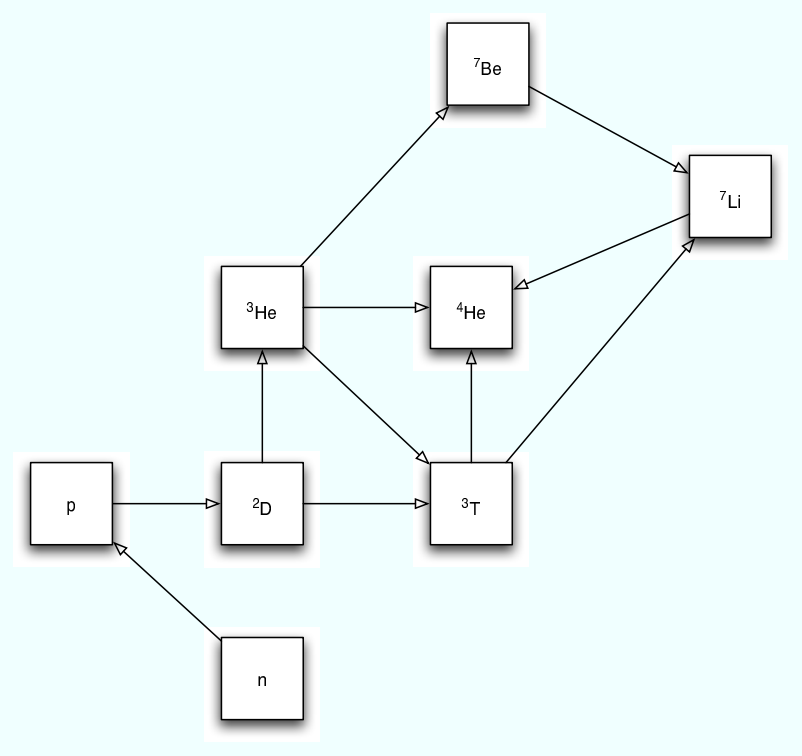

Figure D.1: The network of primary nucleosynthesis reactions.

Appendix E

Cosmology Thermodynamics

Here, we present some rudimentary thermodynamics of the early universe, showing that the particle physics phenomenology plays an important role in cosmology.

E.1 The expansion of the Universe

The expansion of the universe is described by a factor $a(t)$, which is defined as $l(t) = l_0 \dot{a}(t)$ and Hubble parameter

$$H = \frac{\dot{a}}{a} \,. \tag{E.1}$$

The Friedman function of the dynamics of the expanding universe is given by

$$\frac{\ddot{a}}{a} = -\frac{4}{3}\,\pi\, G(\rho_b + 3p_b) + \frac{\Lambda}{3}\,, \tag{E.2}$$

where ρ_b and p_b are the density and pressure of the matter in the universe, $G = \frac{1}{M_{\rm pl}^2}$ is the Newton's constant and Λ is the cosmological constant.

Integrating Eq.(E.2), one finds the cosmological equation

$$H^2 = \left(\frac{\dot{a}}{a}\right)^2 = \frac{8}{3}\pi G\rho_b \pm \frac{1}{a^2R^2} + \frac{\Lambda}{3}\,. \tag{E.3}$$

In the above equation, we use the special Einstein-de Sitter limit, where $p_b \ll \rho_b$. R and the plus minus sign describe the curvature of the universe. In the radiation dominanted universe, the energy density is a function of particle DoF g_* and temperature T

$$\rho_b = g_* \frac{\pi^2}{30} T^4 \,, \tag{E.4}$$

In the radiation dominated universe, we can further neglect the curvature term and cosmological constant term and therefore the Hubble parameter can be expressed as

$$H = \sqrt{\frac{4\pi^3 g_*}{45}} \frac{T^2}{M_{\rm pl}} \,. \tag{E.5}$$

E.2 Number density of particles

In the plasma of the hot universe, the number of microstates with energy density ε is given by

$$\Delta g_\epsilon = \frac{gV}{2\pi^2} \int_\epsilon^{\epsilon+\Delta\epsilon} |p|^2 \, d|p| \;\simeq\; \frac{gV}{2\pi^2} \sqrt{\epsilon^2 - m^2}\, \epsilon \, \Delta\epsilon \,, \tag{E.6}$$

where p is the momentum of the particle V is the volume and g is the internal degrees of freedom of the particle. It is convenient to work in the unit volume where $V = 1$. Bosons in the plasma satisfy the Bose-Einstein distribution:

$$n_\epsilon = \frac{1}{e^{\frac{\epsilon-\mu}{T}} - 1} \,, \tag{E.7}$$

whereas Fermi-Dirac distribution for fermions:

$$n_\epsilon = \frac{1}{e^{\frac{\epsilon-\mu}{T}} + 1} \,. \tag{E.8}$$

In the above two equations, μ is the chemical potential of the corresponding particle. Integrating the energy density, one can find the number density of each particle as a function of temperature T, mass m and the chemical potential μ:

$$n = \sum_\epsilon n_\epsilon \Delta g_\epsilon = \frac{g}{2\pi^2} \int_m^\infty \frac{\sqrt{\epsilon^2 - m^2}}{e^{(\epsilon-\mu)/T} \mp 1} \, \epsilon \, d\epsilon \,, \tag{E.9}$$

where the minus sign is for bosons and plus sign is for fermions. The density of particles in equilibrium satisfies

$$n_i^{\rm eq}(T) = \frac{g_i}{(2\pi)^3}\int d^3\, p_i\, f_i^{\rm eq}\,, \tag{E.10}$$

where $f_i^{\rm eq}(E_i, T) = e^{-E_i/T}$. The integral reads

$$n_i^{\rm eq}(T) = \frac{g_i\, T\, m_i^2}{2\pi^2} K_2(\frac{m_i}{T})\,, \tag{E.11}$$

for massive particle with mass m_i. And

$$n_i^{\rm eq}(T) = \frac{g_i\, T^3}{\pi^2}\,, \tag{E.12}$$

for massless particles. It is important to calculate the excess of number density of particle and antiparticle in the limit of ultra-high temperature $\mu \ll T$ and massless particle $m = 0$. For bosons, we have

$$n_b - n_{\bar{b}} \simeq \frac{gT^3}{3}\frac{\mu_b}{T}\,, \tag{E.13}$$

whereas for fermions

$$n_f - n_{\bar{f}} \simeq \frac{gT^3}{6}\frac{\mu_b}{T}\,. \tag{E.14}$$

E.3 The Entropy of Particles

The energy density of bosons and fermions in the hot plasma in the universe can be calculated from integration

$$\rho = g\int \epsilon\, n_\epsilon\, {\rm d}^3\mathbf{p}\,, \tag{E.15}$$

where n_ϵ, the distribution function in Eq.(E.7) and Eq.(E.8) need to be treated differently for bosons and fermions. Then the energy density is a function of temperature and particle degree of freedom, for bosons, it reads

$$\rho_b \simeq \frac{\pi^2}{30}\, g\, T^4\,, \tag{E.16}$$

and for fermions, then we have

$$\rho_f \simeq \frac{7\pi^2}{240}\, g\, T^4\,, \tag{E.17}$$

From the point of view of total entropy of the plasma, see Eq.(E.4), total degrees of freedom of a mixture of bosons and fermions can be effectively expressed as

$$g_* = \sum_{m \ll T} g_b + \frac{7}{8} \sum_{m \ll T} g_f\,, \tag{E.18}$$

We can see that for bosons and fermions which have the same internal degrees of freedom, the entropies satisfy

$$s_f = \frac{7}{8}\, s_b\,, \tag{E.19}$$

The entropy of the universe is defined as

$$s \equiv \frac{\rho + p}{T} \tag{E.20}$$

In the radiation dominated universe, we have relation $p = \frac{1}{3}\rho$, using Eq.(E.4) the total entropy density can be easily expressed as

$$s = g_*\, \frac{2\pi^2}{45} T^3\,. \tag{E.21}$$

Appendix F

An Alternative Method to the Flavoured Boltzmann Equations

The Boltzmann Equations in Chapter 4 discribe the evolution of lepton/quarks in an elegant way. In the meantime, an alternative method is derived and used by the authors to solve the evolution of $B-L$ number in the early Universe. Although this method is much more tedious, we think it is still useful to present this method in this thesis. One can expect that when the spectator processes are considered in other situation (*e.g.* the Affleck-Dine mechanism, mentioned in Chapter 4, the method in Chapter 4 may be not working.

Firt of all, we use the number density relations of the relevent components of leptogenesis (Eq. 4.42)

$$\mu_Q = -\frac{\mu_\ell}{3}; \quad \mu_\phi = \frac{4\mu_\ell}{7}; \quad \mu_u = \frac{5\mu_\ell}{21}; \quad \mu_d = -\frac{19\mu_\ell}{21}; \quad \mu_e = \frac{3\mu_\ell}{7}\,, \tag{F.1}$$

because only the left-handed leptons are active in generating $L-B$ number, we distinguish left-handed leptons from non left-handed lepton $L-B$s (labelled with $\Upsilon = (L-\ell)-B$). The ratio of left-handed lepton ℓ_i to Υ,

$$c_\Upsilon = \frac{e - 6\,Q - 3\,u - 3\,d}{2\,\ell}\,. \tag{F.2}$$

In the temperature range 10^2 GeV- 10^9 GeV, inserting Eq.(4.42) into Eq.(F.2), we can have $c_\Upsilon = 31/14$.

Since the role of spectator processes is to keep lepton flavours and baryon flavours in the ratio, one can consider them effectively as processes with arbitrarily large rate. The fast processes keeping $\hat{Y}_{\ell_\alpha}, (\alpha = 1, 2, 3)$ and $\hat{Y}_\Upsilon$ in a ratio of c_Υ correspond to a term $\Theta \sum_{\beta\neq\alpha}(c_\Upsilon \hat{Y}_\Upsilon + \hat{Y}_{\ell_\beta} - N_f \hat{Y}_{\ell_\alpha})$ and $\Theta \sum_\beta (\hat{Y}_{\ell_\beta} - N_f\, c_\Upsilon\, \hat{Y}_\Upsilon)$ in the Boltzmann Equation of $\hat{Y}_{\ell_\alpha}$, where Θ is a positive number, which makes the last term much larger than the previous terms. Notice that the Θ terms cancel each other so that total $L-B$ is conserved.

$$\frac{\mathrm{d}\hat{Y}_{N_1}}{\mathrm{d}z} = -\frac{2}{sHz}\left(\frac{\hat{Y}_{N_1}}{\hat{Y}_N^{eq}} - 1\right)(\gamma_D + 2\gamma_{Ss} + 4\gamma_{St})\,, \tag{F.3}$$

$$\begin{aligned}\frac{\mathrm{d}\hat{Y}_{\ell_\alpha}}{\mathrm{d}z} = & -\frac{2}{sHz}\left\{\epsilon_{1,\alpha}\left(\frac{\hat{Y}_{N_1}}{\hat{Y}_{N_1}^{eq}} - 1\right)\gamma_D + \left(\gamma_{S_s}^\alpha + \gamma_{S_t}^\alpha\right)\frac{\hat{Y}_{\ell_\beta}}{\hat{Y}_\ell^{\mathrm{eq}}}\right\} \\ & +\Theta \sum_{\beta\neq\alpha}(c_\Upsilon \hat{Y}_\Upsilon + \hat{Y}_{\ell_\alpha} - N_f\, \hat{Y}_{\ell_\alpha})\,,\end{aligned} \tag{F.4}$$

$$\frac{\mathrm{d}\hat{Y}_\Upsilon}{\mathrm{d}z} = \Theta \sum_\beta (\hat{Y}_{\ell_\beta} - N_f\, c_\Upsilon\, \hat{Y}_\Upsilon)\,. \tag{F.5}$$

These equations can be solved numerically, and the value of Θ is empirically set to ensure the ratio of $\hat{Y}_\ell$ and $\hat{Y}_\Upsilon$ and a reasonable computer time.

To illustrate the result of the uni-flavour Boltzmann Equations, we take the scenario of Consequential Dominance in Section 3.3.1. We take the right-handed neutrino masses $M_{1,2,3} = 10^9, 10^{10}, 10^{11}\,\mathrm{GeV}$, and the maximal CP asymmetry of right-handed neutrino decay can be calculated

$$\varepsilon_{1,\beta} = 4.6 \times 10^{-6}\,, \quad \varepsilon_{1,e} = 0\,, \tag{F.6}$$

where $\beta = \mu, \tau$.

Here we have taken the assumption of thermally produced right-handed neutrino, in which $Y_X = 0$ $X = N_1$, when $z \ll 1$. The evolution of $\hat{Y}_\ell$ and $\hat{Y}_\Upsilon$ is showed in Figure F.1. We can clearly see that the $\hat{Y}_\ell$ and $\hat{Y}_\Upsilon$ are kept in a ratio during the leptogenesis era. The final $L - B$ number abundance reads $\hat{Y}_{L-B} = 1.25 \times 10^{-9}$, and the total $L - B$ number for flavour independent Boltzmann Equations is $\hat{Y}_{L-B} = 2.17 \times 10^{-9}$.

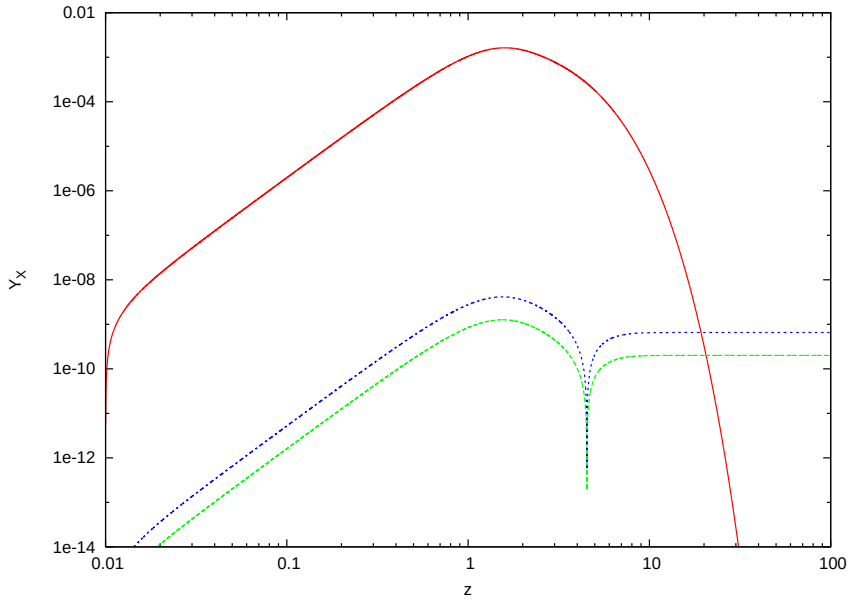

Figure F.1: The evolution of N_1 abundance (the solid line) left-handed lepton asymmetries Y_{ℓ_α} (the dash line) and Υ total abundance (dot-dash line), for $M_1 = 10^8\,\mathrm{GeV}$.

Appendix G

An illustration of flavours in Boltzmann Equations

In this appendix, we illustrate a visible model to explain how flavours play the role in leptogenesis Boltzmann Equations.

We image there are three tanks (Fig. G.1). On the top of each tank, there is one tap, filling water into these three separate tanks. And there is a small hole in the bottom of each tank, from which the water flows out. The incoming water flow depends on the taps, and the outgoing water flow is proportional to the volume/height of water in each tank. (The more water in the tank, the more pressure on the hole.)

If we want to calculate how much water in these tanks at time t (assuming in the beginning all these three tanks are empty), the situation is like calculating flavour-independent lepton asymmetries from the RH neutrino decay:

- The incoming water flow of each tank stands for the rate of generating lepton asymmetries from the RH neutrino decay.
- The outgoing water flow of each tank is propotional to the volume/height of water in respective tank stands for the washing-out rates of lepton asymmetries are

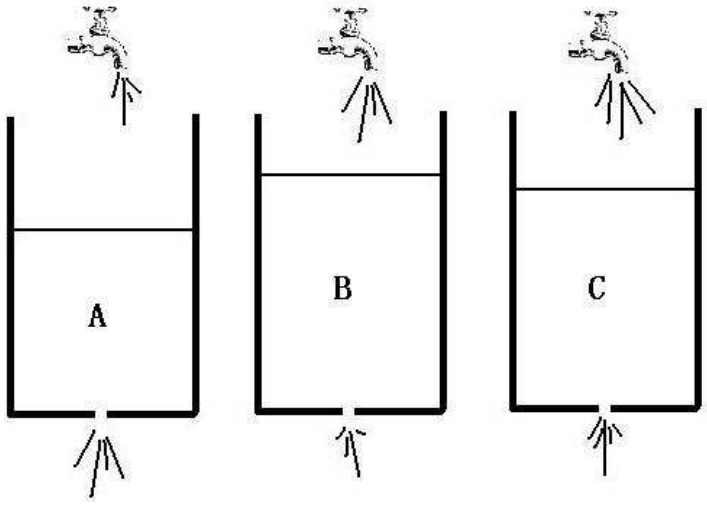

Figure G.1: An illustration of a generating-erasing system with three independent variables.

propotional to number densities of respective (left-handed) leptons.

And this is the flavour independent case, where we assume the sphaleron processes are still not active, and the $B - L$ number is conserved in three left-handed leptons only.

Now, let's investigate the flavoured case. When we take into account the 'spectator process', (including sphaleron processes and Yukawa interactions), these water tanks need to be modified. Notice that the 'spectator process' converts left-handed leptons to right-handed leptons, left-handed quarks and right-handed quarks, conserving $B - L$ number. The asymmetries of all these components, together with Higgs fields, go into equilibrium. So, we can image a situation where these three tanks are connected by pipes. And an additional tank is also connected to them, but there is no hole in the bottom of it. The pipes between these tanks are large enough so that the water levels are always even (Fig. G.2).

So, in leptogenesis, the spectator processes play the role of these pipes - converting left-handed leptons into each other and inactive components (quarks and right-handed leptons), keeping them in certain ratios. We can image that the water in the additional tank is the inactive components - there is no hole in the bottom to "wash it out".

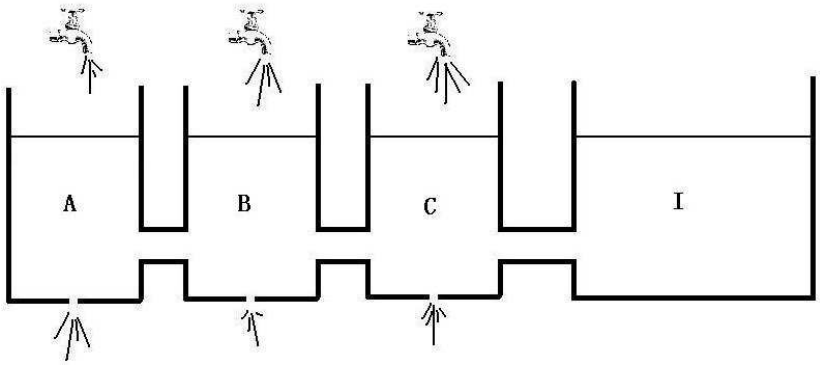

Figure G.2: An illustration of a generating-erasing system with communicating (spectator process).

To calculate how much water in these tanks, we only need to consider one variable - the volume of water in all these tanks together. Similarly, in leptogenesis, we can only consider the total $B - L$ number in the Boltzmann Equations, and left-handed lepton number in each flavour can be algebraically expressed by $B - L$ number.

As for the case of E_6SSM, with L_4 only, we can image there is another additional tank with a hole in the bottom (Fig. G.3). This tank represents L_4. The calculation in this scenario is very straightforward. And for the case of inert Higgs and leptoquark, we still can have water-tank models to describe them.

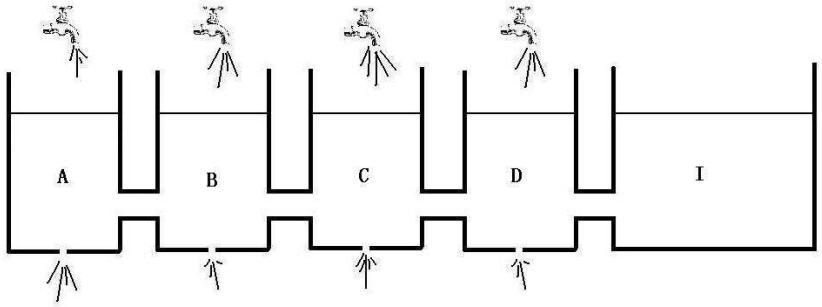

Figure G.3: An illustration of a generating-erasing system with communicating (spectator process) and an additional variable.

Bibliography

[1] W. Pauli, *IN *ENZ, C.P. (ED.), V. MEYENN, K. (ED.): WOLFGANG PAULI* 481-483.*

[2] F. Reines and C. L. Cowan, Nature **178** (1956) 446.

[3] C. L. Cowan, F. Reines, F. B. Harrison, H. W. Kruse and A. D. McGuire, Science **124** (1956) 103.

[4] G. Danby, J. M. Gaillard, K. Goulianos, L. M. Lederman, N. B. Mistry, M. Schwartz and J. Steinberger, Phys. Rev. Lett. **9** (1962) 36.

[5] M. L. Perl *et al.*, Phys. Lett. B **63** (1976) 466.

[6] R. N. Cahn, Phys. Rev. D **36** (1987) 2666 [Erratum-ibid. D **40** (1989) 922]. A. Borrelli, L. Maiani, R. Sisto, G. C. Rossi and M. Testa, Nucl. Phys. B **333**, 335 (1990). D. Y. Bardin and G. Passarino, arXiv:hep-ph/9803425. D. Y. Bardin, M. Grunewald and G. Passarino, arXiv:hep-ph/9902452.

[7] Y. Fukuda *et al.* [Super-Kamiokande Collaboration], Phys. Rev. Lett. **81** (1998) 1562 [arXiv:hep-ex/9807003].

[8] M. H. Ahn *et al.* [K2K Collaboration], Phys. Rev. D **74** (2006) 072003 [arXiv:hep-ex/0606032].

[9] Y. Itow *et al.* [The T2K Collaboration], arXiv:hep-ex/0106019.

[10] D. S. Ayres *et al.* [NOvA Collaboration], arXiv:hep-ex/0503053; O. Mena Requejo, S. Palomares-Ruiz and S. Pascoli, Phys. Rev. D **72** (2005) 053002 [arXiv:hep-ph/0504015]; A. Donini, E. Fernandez-Martinez, D. Meloni and S. Rigolin, Nucl. Phys. B **743** (2006) 41 [arXiv:hep-ph/0512038].

[11] D. G. Michael *et al.* [MINOS Collaboration], Phys. Rev. Lett. **97** (2006) 191801 [arXiv:hep-ex/0607088].

[12] P. Adamson *et al.* [MINOS Collaboration], Phys. Rev. D **77** (2008) 072002 [arXiv:0711.0769 [hep-ex]].

[13] P. Adamson *et al.* [MINOS Collaboration], Phys. Rev. Lett. **101** (2008) 131802 [arXiv:0806.2237 [hep-ex]].

[14] G. Iovane, arXiv:hep-ex/9812015; M. Komatsu, P. Migliozzi and F. Terranova, J. Phys. G **29** (2003) 443 [arXiv:hep-ph/0210043]; H. Pessard and f. t. O. Collaboration, arXiv:0910.5701 [hep-ex].

[15] M. Apollonio *et al.* [CHOOZ Collaboration], Phys. Lett. B **420** (1998) 397 [arXiv:hep-ex/9711002].

[16] M. Apollonio *et al.* [CHOOZ Collaboration], Phys. Lett. B **466** (1999) 415 [arXiv:hep-ex/9907037].

[17] M. Apollonio *et al.* [CHOOZ Collaboration], Eur. Phys. J. C **27** (2003) 331 [arXiv:hep-ex/0301017].

[18] S. Abe *et al.* [KamLAND Collaboration], Phys. Rev. Lett. **100** (2008) 221803 [arXiv:0801.4589 [hep-ex]].

[19] D. V. Ahluwalia, Int. J. Mod. Phys. A **11** (1996) 1855 [arXiv:hep-th/9409134].

[20] B. Kayser, J. Phys. Conf. Ser. **173** (2009) 012013 [arXiv:0903.0899 [hep-ph]].

[21] A. Strumia and F. Vissani, arXiv:hep-ph/0606054.

[22] S. M. Bilenky and B. Pontecorvo, Phys. Rept. **41** (1978) 225; S. M. Bilenky and C. Giunti, Int. J. Mod. Phys. A **16** (2001) 3931 [arXiv:hep-ph/0102320]; S. M. Bilenky, arXiv:hep-ph/0512215.

[23] C. Giunti, J. Phys. G **34** (2007) R93 [arXiv:hep-ph/0608070].

[24] B. T. Cleveland *et al.*, Astrophys. J. **496** (1998) 505.

[25] Q. R. Ahmad *et al.* [SNO Collaboration], Phys. Rev. Lett. **89** (2002) 011301 [arXiv:nucl-ex/0204008].

[26] P. Anselmann *et al.* [GALLEX Collaboration], Phys. Lett. B **285** (1992) 376; W. Hampel *et al.* [GALLEX Collaboration], Phys. Lett. B **420** (1998) 114.

[27] M. Altmann *et al.* [GNO Collaboration], Phys. Lett. B **490** (2000) 16 [arXiv:hep-ex/0006034]; M. Altmann *et al.* [GNO COLLABORATION Collaboration], Phys. Lett. B **616** (2005) 174 [arXiv:hep-ex/0504037].

[28] J. Hosaka *et al.* [Super-Kamkiokande Collaboration], Phys. Rev. D **73** (2006) 112001 [arXiv:hep-ex/0508053]; J. P. Cravens *et al.* [Super-Kamiokande Collaboration], Phys. Rev. D **78** (2008) 032002 [arXiv:0803.4312 [hep-ex]].

[29] P. Bhattacharjee and G. Sigl, Phys. Rept. **327** (2000) 109 [arXiv:astro-ph/9811011].

[30] E. Andres *et al.*, Astropart. Phys. **13** (2000) 1 [arXiv:astro-ph/9906203].

[31] M. Ackermann *et al.* [IceCube Collaboration], Astrophys. J. **675** (2008) 1014 [arXiv:0711.3022 [astro-ph]].

[32] R. Abbasi *et al.* [IceCube Collaboration], Phys. Rev. D **79** (2009) 102005 [arXiv:0902.0675 [astro-ph.HE]].

[33] A. Schukraft, J. P. Huelss and f. t. I. Collaboration, arXiv:0906.3942 [astro-ph.HE].

[34] A. Letessier-Selvon, Nucl. Phys. Proc. Suppl. **118** (2003) 399 [arXiv:astro-ph/0208526]; J. W. Cronin, arXiv:0911.4714 [astro-ph.HE].

[35] F. Halzen and D. Hooper, JCAP **0308** (2003) 006 [arXiv:astro-ph/0305234].

[36] F. Halzen and D. Hooper, JCAP **0401** (2004) 002 [arXiv:astro-ph/0310152].

[37] M. C. Gonzalez-Garcia, F. Halzen and M. Maltoni, Phys. Rev. D **71** (2005) 093010 [arXiv:hep-ph/0502223].

[38] F. Halzen, Eur. Phys. J. C **46** (2006) 669 [arXiv:astro-ph/0602132].

[39] R. Adler *et al.* [CPLEAR Collaboration], Phys. Lett. B **363** (1995) 243. R. Adler *et al.* [CPLEAR Collaboration], Phys. Lett. B **403** (1997) 383.

[40] B. Pontecorvo, Zh. Eksp. Teor. Fiz. (JETP) 33 (1957) 549; ibid. 34 (1958) 247; ibid. 53 (1967) 1717; Z. Maki, M. Nakagawa, S. Sakata, Prog. Theor. Phys. 28 (1962) 870.

[41] N. Cabibbo, Phys. Rev. Lett. **10** (1963) 531; M. Kobayashi and T. Maskawa, Prog. Theor. Phys. **49** (1973) 652.

[42] E. K. Akhmedov, JHEP **0709** (2007) 116 [arXiv:0706.1216 [hep-ph]].

[43] E. K. Akhmedov and A. Y. Smirnov, arXiv:0905.1903 [hep-ph].

[44] L. Wolfenstein, Phys. Rev. D **17** (1978) 2369.

[45] S. P. Mikheev and A. Y. Smirnov, Sov. J. Nucl. Phys. **42** (1985) 913 [Yad. Fiz. **42** (1985) 1441].

[46] T. Schwetz, AIP Conf. Proc. **981** (2008) 8 [arXiv:0710.5027 [hep-ph]].

[47] S. Hannestad, JCAP **0305** (2003) 004 [arXiv:astro-ph/0303076]; O. Elgaroy and O. Lahav, JCAP **0304** (2003) 004 [arXiv:astro-ph/0303089].

[48] J. Lesgourgues, M. Viel, M. G. Haehnelt and R. Massey, JCAP **0711** (2007) 008 [arXiv:0705.0533 [astro-ph]].

[49] E. Komatsu *et al.* [WMAP Collaboration], arXiv:0803.0547 [astro-ph].

[50] C. Kraus *et al.*, Eur. Phys. J. C **40** (2005) 447 [arXiv:hep-ex/0412056].

[51] KATRIN web site: `http://www-ik.fzk.de/tritium/`

[52] C. Weinheimer *et al.*, Phys. Lett. B **460** (1999) 219.

[53] H. V. Klapdor-Kleingrothaus, A. Dietz, H. L. Harney and I. V. Krivosheina, Mod. Phys. Lett. A **16** (2001) 2409 [arXiv:hep-ph/0201231].

[54] V. A. Rodin, A. Faessler, F. Simkovic and P. Vogel, Nucl. Phys. A **766** (2006) 107 [Erratum-ibid. A **793** (2007) 213] [arXiv:0706.4304 [nucl-th]].

[55] J. Menendez, A. Poves, E. Caurier and F. Nowacki, Nucl. Phys. A **818** (2009) 139 [arXiv:0801.3760 [nucl-th]].

[56] R. N. Mohapatra *et al.*, Rept. Prog. Phys. **70** (2007) 1757 [arXiv:hep-ph/0510213].

[57] P. F. Harrison, D. H. Perkins and W. G. Scott, Phys. Lett. B **530** (2002) 167 [arXiv:hep-ph/0202074].

[58] N. Arkani-Hamed, S. Dimopoulos, G. R. Dvali and J. March-Russell, Phys. Rev. D **65** (2002) 024032 [arXiv:hep-ph/9811448].

[59] P. H. Gu and H. J. He, JCAP **0612**, 010 (2006) [arXiv:hep-ph/0610275].

[60] N. Arkani-Hamed, S. Dimopoulos and G. R. Dvali, Phys. Lett. B **429** (1998) 263 [arXiv:hep-ph/9803315].

[61] N. Haba, S. Matsumoto and K. Yoshioka, Phys. Lett. B **677** (2009) 291 [arXiv:0901.4596 [hep-ph]].

[62] W. Buchmuller, R. D. Peccei and T. Yanagida, Ann. Rev. Nucl. Part. Sci. **55** (2005) 311 [arXiv:hep-ph/0502169].

[63] K. Hamaguchi, arXiv:hep-ph/0212305.

[64] F. X. Josse-Michaux, arXiv:0809.4960 [hep-ph].

[65] S. S. C. Law, arXiv:0901.1232 [hep-ph].

[66] Yunqiang Yu, "A Note on Particle Cosmology," (in Chinese) Peking University Press, Beijing, China, November 2002.

[67] G. Steigman, Int. J. Mod. Phys. E **15** (2006) 1 [arXiv:astro-ph/0511534].

[68] V. Simha and G. Steigman, JCAP **0806** (2008) 016 [arXiv:0803.3465 [astro-ph]].

[69] B. Fields and S. Sarkar, arXiv:astro-ph/0601514.

[70] J. C. Mather *et al.*, Astrophys. J. **354** (1990) L37.

[71] J. C. Mather *et al.*, Astrophys. J. **420** (1994) 439.

[72] D. J. Fixsen, E. S. Cheng, J. M. Gales, J. C. Mather, R. A. Shafer and E. L. Wright, Astrophys. J. **473** (1996) 576 [arXiv:astro-ph/9605054].

[73] L. Page *et al.* [WMAP Collaboration], Astrophys. J. Suppl. **148** (2003) 233 [arXiv:astro-ph/0302220]. C. L. Bennett *et al.*, "First Year Wilkinson Microwave Anisotropy Probe (WMAP) Observations: Preliminary Maps and Basic Results," Astrophys. J. Suppl. **148** (2003) 1.

[74] W. Hu and N. Sugiyama, Phys. Rev. D **51** (1995) 2599 [arXiv:astro-ph/9411008].

[75] A. Strumia, arXiv:hep-ph/0608347.

[76] A. D. Sakharov, Pisma Zh. Eksp. Teor. Fiz. **5** (1967) 32 [JETP Lett. **5** (1967 SOPUA,34,392-393.1991 UFNAA,161,61-64.1991) 24].

[77] G. 't Hooft, Phys. Rev. Lett. **37** (1976) 8.

[78] V. Mukhanov, "Physical fundations of cosmology," Cambridge University Press 2005.

[79] V. A. Kuzmin, V. A. Rubakov and M. E. Shaposhnikov, Phys. Lett. B **155** (1985) 36; V. A. Rubakov and M. E. Shaposhnikov, Usp. Fiz. Nauk, **166** (1996) 493.

[80] M. Fukugita and T. Yanagida, Phys. Lett. B **174** (1986) 45.

[81] *for a recent review, see* S. Davidson, E. Nardi and Y. Nir, arXiv:0802.2962 .

[82] W. Buchmuller, P. Di Bari, and M. Plumacher, Ann. Phys. **315** (2005) 305.

[83] P. H. Y. Gu and U. Sarkar, arXiv:0903.3473 [hep-ph].

[84] G. Engelhard, Y. Grossman, E. Nardi and Y. Nir, Phys. Rev. Lett. **99** (2007) 081802 [arXiv:hep-ph/0612187].

[85] M. A. Luty, Phys. Rev. D **45** (1992) 455; M. Flanz, E. A. Paschos and U. Sarkar, Phys. Lett. B **345** (1995) 248 [Erratum-ibid. B **382** (1996) 447] [arXiv:hep-ph/9411366]; M. Plumacher, Z. Phys. C **74** (1997) 549 [arXiv:hep-ph/9604229].

[86] J. Liu and G. Segre, Phys. Rev. D **48** (1993) 4609 [arXiv:hep-ph/9304241].

[87] B. A. Campbell, S. Davidson and K. A. Olive, Nucl. Phys. B **399** (1993) 111; L. Covi, E. Roulet and F. Vissani, Phys. Lett. B **384** (1996) 169;

[88] S. Davidson and A. Ibarra, Phys. Lett. B **535** (2002) 25 [arXiv:hep-ph/0202239].

[89] M. Yu. Khlopov and A. D. Linde, Phys. Lett. B **138** (1984) 265; J. R. Ellis, J E. Kim, and D. V. Nanopoulos, Phys. Lett. B **145** (1984) 181.

[90] T. Moroi, arXiv:hep-ph/9503210.

[91] M. Endo, F. Takahashi and T. T. Yanagida, Phys. Rev. D **76** (2007) 083508 [arXiv:hep-ph/0702247].

[92] M. Bolz, W. Buchmuller and M. Plumacher, Phys. Lett. B **443** (1998) 209; J. L. Feng, S. Su and F. Takayama, Phys. Rev. D **70** (2004) 075019; T. Kanzaki, M. Kawasaki, K. Kohri and T. Moroi, Phys. Rev. D **75** (2007) 025011.

[93] A. Pilaftsis and T. E. J. Underwood, Nucl. Phys. B **692** (2004) 303 [arXiv:hep-ph/0309342].

[94] A. Pilaftsis and T. E. J. Underwood, Phys. Rev. D **72** (2005) 113001 [arXiv:hep-ph/0506107].

[95] A. Anisimov, A. Broncano and M. Plumacher, Nucl. Phys. B **737** (2006) 176 [arXiv:hep-ph/0511248].

[96] I. Affleck and M. Dine, Nucl. Phys. B **249** (1985) 361; M. Dine, L. Randall and S. D. Thomas, Nucl. Phys. B **458** (1996) 291.

[97] A. Riotto and M. Trodden, Ann. Rev. Nucl. Part. Sci. (1999) **49** 35; J. M. Cline. hep-ph/0609145.

[98] S. J. Huber and M. G. Schmidt, Nucl. Phys. B **606** (2001) 183.

[99] M. Yoshimura, Phys. Rev. Lett. **41** (1978) 281 [Erratum-ibid. **42** (1979) 746].

[100] A. G. Cohen, D. B. Kaplan and A. E. Nelson, Ann. Rev. Nucl. Part. Sci. **43** (1993) 27 [arXiv:hep-ph/9302210].

[101] S. F. King, S. Moretti and R. Nevzorov, Phys. Rev. D **73** (2006) 035009.

[102] S. F. King, S. Moretti and R. Nevzorov, Phys. Lett. B **634** (2006) 278.

[103] P. Athron, S. F. King, D. J. Miller, S. Moretti and R. Nevzorov, arXiv:0910.0705 [hep-ph].

[104] M. B. Green, J. H. Schwarz, E. Witten, Superstring Theory (Cambridge Univ. Press, Cambridge, 1987).

[105] H. Georgi, S. L. Glashow, Phys. Rev. Lett. **32** (1974) 438.

[106] H. P. Nilles, M. Srednicki, D. Wyler, Phys. Lett. B **120** (1983) 346; J. M. Frere, D. R. T. Jones, S. Raby, Nucl. Phys. B **222** (1983) 11; J. P. Derendinger, C. A. Savoy, Nucl. Phys. B **237** (1984) 307; M. I. Vysotsky, K. A. Ter-Martirosian, Sov. Phys. JETP **63** (1986) 489; J. Ellis, J. F. Gunion, H. Haber, L. Roszkowski, F. Zwirner, Phys. Rev. D **39** (1989) 844.

[107] L. Durand, J. L. Lopez, Phys. Lett. B **217** (1989) 463; L. Drees, Int. J. Mod. Phys. A **4** (1989) 3635.

[108] G. F. Giudice and A. Masiero, Phys. Lett. B **206** (1988) 480.

[109] S. A. Abel, S. Sarkar and P. L. White, Nucl. Phys. B **454**, 663 (1995) [arXiv:hep-ph/9506359].

[110] S. F. King, S. Moretti and R. Nevzorov, *In *Moscow 2006, ICHEP* 1125-1128*

[111] B. Zumino, Phys. Lett. B **87** (1979) 203.

[112] J. Rich, M. Spiro, J. Lloyd-Owen, Phys. Rept. **151** (1987) 239; P.F. Smith, Contemp. Phys. **29** (1988) 159; T.K. Hemmick *et al.*, Phys. Rev. D **41** (1990) 2074.

[113] S. Kraml *et al.* (eds.), *Workshop on CP studies and non-standard Higgs physics*, CERN–2006–009, hep-ph/0608079; S.F. King, S. Moretti, R. Nevzorov, hep-ph/0601269; S.F. King, S. Moretti, R. Nevzorov, hep-ph/0610002; R. Howl and S. F. King, JHEP **0801** (2008) 030.

[114] F. Abe *et al.* [CDF Collaboration], Phys. Rev. Lett. **79** (1997) 2192.

[115] P. Abreu et al. [DELPHI Collaboration], Phys. Lett. B **485** (2000) 45; R. Barate et al. [ALEPH Collaboration], Eur. Phys. J. C **12** (2000) 183.

[116] J. Erler, P. Langacker, S. Munir and E. R. Pena, JHEP **0908** (2009) 017 [arXiv:0906.2435 [hep-ph]].

[117] P. Abreu *et al.* [DELPHI Collaboration], Phys. Lett. B **446** (1999) 62; J. Breitweg *et al.* [ZEUS Collaboration], Phys. Rev. D **63** (2001) 052002; C. Adloff *et al.* [H1 Collaboration], Phys. Lett. B **523** (2001) 234; G. Abbiendi *et al.* [OPAL Collaboration], Phys. Lett. B **526** (2002) 233; V. M. Abazov *et al.* [D0 Collaboration], Phys. Rev. D **71** (2005) 071104; [CDF Collaboration], hep-ex/0506074.

[118] F. Abe *et al.* [CDF Collaboration], Phys. Rev. Lett. **77** (1996) 5336 [Erratum-ibid. **78** (1997) 4307]; B. Abbott *et al.* [D0 Collaboration], Phys. Rev. Lett. **80** (1998) 666.

[119] R. N. Mohapatra, A. Perez-Lorenzana and C. A. de Sousa Pires, Phys. Lett. B **474** (2000) 355 [arXiv:hep-ph/9911395].

[120] S. M. Barr, Phys. Rev. Lett. **92** (2004) 101601 [arXiv:hep-ph/0309152].

[121] C. H. Albright and S. M. Barr, Phys. Rev. D **69** (2004) 073010 [arXiv:hep-ph/0312224].

[122] S. M. Barr and I. Dorsner, Phys. Lett. B **632** (2006) 527 [arXiv:hep-ph/0507067].

[123] S. Antusch and S. F. King, Phys. Lett. B **597** (2004) 199 [arXiv:hep-ph/0405093].

[124] E. Ma, N. Sahu and U. Sarkar, arXiv:hep-ph/0611257.

[125] T. Hambye, E. Ma, M. Raidal and U. Sarkar, Phys. Lett. B **512** (2001) 373 [arXiv:hep-ph/0011197].

[126] M. Frigerio, T. Hambye and E. Ma, JCAP **0609** (2006) 009 [arXiv:hep-ph/0603123].

[127] A. Abada, H. Aissaoui and M. Losada, Nucl. Phys. B **728** (2005) 55 [arXiv:hep-ph/0409343].

[128] K. S. Babu, R. N. Mohapatra and S. Nasri, Phys. Rev. Lett. **97** (2006) 131301 [arXiv:hep-ph/0606144].

[129] N. Sahu and U. Sarkar, arXiv:hep-ph/0701062.

[130] E. Ma and U. Sarkar, Phys. Rev. Lett. **80** (1998) 5716; T. Hambye, E. Ma, and U. Sarkar, Nucl. Phys. B **602** (2001) 23; E. J. Chun and S. K. Kang, Phys. Rev. D **63** (2001) 097902; A. S. Joshipura, E. A. Paschos, and W. Rodejohann, *Nucl. Phys.*, B611:227–238, 2001; B. Brahmachari, E. Ma, and U. Sarkar, Phys. Lett. B **520** (2001) 152; T. Hambye and G. Senjanovic, Phys. Lett. B **582** (2004) 73; W. l. Guo, Phys. Rev. D **70** (2004) 053009; S. Antusch and S. F. King, Phys. Lett. B **597** (2004) 199; S. Antusch and S. F. King, JHEP **0601** (2006) 117; T. Hambye, M. Raidal, and A. Strumia, Phys. Lett. B **632** (2006) 667; E. J. Chun and S. Scopel, Phys. Rev. D **75** (2007) 023508; S. Antusch, Phys. Rev. D **76** (2007) 023512; W. Chao, S. Luo and

Z. z. Xing, Phys. Lett. B **659** (2008) 281; T. Hallgren, T. Konstandin and T. Ohlsson, JCAP **0801** (2008) 014.

[131] G. D'Ambrosio, T. Hambye, A. Hektor, M. Raidal, and A. Rossi, Phys. Lett. B **604** (2004) 199; E. J. Chun and S. Scopel, Phys. Lett. B **636** (2006) 278.

[132] Y. Grossman, T. Kashti, Y. Nir and E. Roulet, Phys. Rev. Lett. **91** (2003) 251801; G. D'Ambrosio, G. F. Giudice and M. Raidal, Phys. Lett. B **575** (2003) 75; Y. Grossman, T. Kashti, Y. Nir and E. Roulet, JHEP **0411** (2004) 080; E. J. Chun, Phys. Rev. D **69** (2004) 117303; L. Boubekeur, T. Hambye and G. Senjanovic, Phys. Rev. Lett. **93** (2004) 111601; M. C. Chen and K. T. Mahanthappa, Phys. Rev. D **70** (2004) 113013; T. Kashti, Phys. Rev. D **71** (2005) 013008; Y. Grossman, R. Kitano and H. Murayama, JHEP **0506** (2005) 058; A. D. Medina and C. E. M. Wagner, JHEP **0612** (2006) 037; J. Garayoa, M. C. Gonzalez-Garcia and N. Rius, JHEP **0702** (2007) 021; E. J. Chun and L. Velasco-Sevilla, JHEP **0708** (2007) 075. S. Dar, S. J. Huber, V. N. Senoguz and Q. Shafi, Phys. Rev. D **69** (2004) 077701;

[133] A. Pilaftsis and T. E. J. Underwood, Nucl. Phys. B **692** (2004) 303; T. Hambye, J. March-Russell and S. M. West, JHEP **0407** (2004) 070; C. H. Albright and S. M. Barr, Phys. Rev. D **70** (2004) 033013; S. Dar, S. J. Huber, V. N. Senoguz and Q. Shafi, Phys. Rev. D **69** (2004) 077701; A. Pilaftsis and T. E. J. Underwood, Phys. Rev. D **72** (2005) 113001; A. Pilaftsis, Phys. Rev. Lett. **95** (2005) 081602; A. Anisimov, A. Broncano and M. Plumacher, Nucl. Phys. B **737** (2006) 176; S. M. West, Mod. Phys. Lett. A **21** (2006) 1629; Z. z. Xing and S. Zhou, Phys. Lett. B **653** (2007) 278; A. De Simone and A. Riotto, JCAP **0708** (2007) 013; V. Cirigliano, A. De Simone, G. Isidori, I. Masina and A. Riotto, JCAP **0801** (2008) 004.

[134] T. Hambye, Nucl. Phys. B **633** (2002) 171; A. Abada and M. Losada, Nucl. Phys. B **673** (2003) 319; A. Abada, H. Aissaoui and M. Losada, Nucl. Phys. B **728** (2005) 55; A. Abada, G. Bhattacharyya and M. Losada, Phys. Rev. D **73** (2006) 033006; D. Atwood, S. Bar-Shalom and A. Soni, Phys. Lett. B **635** (2006) 112; M. Frigerio, T. Hambye and E. Ma, JCAP **0609** (2006) 009; E. Ma, N. Sahu and U. Sarkar, J.

Phys. G **34** (2007) 741; M. Hirsch, J. W. F. Valle, M. Malinsky, J. C. Romao and U. Sarkar, Phys. Rev. D **75** (2007) 011701; N. Sahu and U. Sarkar, Phys. Rev. D **76** (2007) 045014.

[135] R. Barbieri, P. Creminelli, A. Strumia, and N. Tetradis, Nucl. Phys. B **575** (2000) 61; T. Endoh, T. Morozumi, and Z. h. Xiong, Prog. Theor. Phys. **111** (2004) 123; O. Vives, Phys. Rev. D **73** (2006) 073006; A. Abada, S. Davidson, F. X. Josse-Michaux, M. Losada and A. Riotto, JCAP **0604** (2006) 004; E. Nardi, Y. Nir, E. Roulet and J. Racker, JHEP **0601** (2006) 164; A. Abada, S. Davidson, A. Ibarra, F. X. Josse-Michaux, M. Losada and A. Riotto, JHEP **0609** (2006) 010; A. De Simone and A. Riotto, JCAP **0702** (2007) 005; S. Blanchet, P. Di Bari and G. G. Raffelt, JCAP **0703** (2007) 012.

[136] P. Minkowski, Phys. Lett. B **67** (1977) 421; M. Gell-Mann, P. Ramond and R. Slansky, *Proceedings of the Supergravity Stony Brook Workshop*, New York 1979, eds. P. Van Nieuwenhuizen and D. Freedman; T. Yanagida, *Proceedings of the Workshop on Unified Theory and Baryon Number in the Universe*, Tsukuba, Japan 1979, eds. A. Sawada and A. Sugamoto; R. N. Mohapatra, G. Senjanovic, Phys. Rev. Lett. **44** (1980) 912.

[137] S. F. King, Phys. Lett. B **439** (1998) 350; S. F. King, Nucl. Phys. B **562** (1999) 57; S. F. King, Nucl. Phys. B **576** (2000) 85; S. F. King, JHEP **0209** (2002) 011.

[138] S. F. King, JHEP **0209** (2002) 011.

[139] S. F. King, Phys. Rev. D **67** (2003) 113010.

[140] K. S. Babu, C. N. Leung and J. T. Pantaleone, Phys. Lett. B **319** (1993) 191 [arXiv:hep-ph/9309223]; J. R. Ellis, G. K. Leontaris, S. Lola and D. V. Nanopoulos, Eur. Phys. J. C **9** (1999) 389 [arXiv:hep-ph/9808251]; A. Dighe, S. Goswami and P. Roy, Phys. Rev. D **76** (2007) 096005.

[141] B. Pontecorvo, Zh. Eksp. Teor. Fiz. **33** (1957) 549; *ibid.* **34** (1958) 247; *ibid.* **53** (1967) 1717; Z. Maki, M. Nakagawa and S. Sakata, Prog. Theor. Phys. **28** (1962) 870.

[142] S. F. King and N. N. Singh, Nucl. Phys. B **591** (2000) 3.

[143] P. F. Harrison, D. H. Perkins and W. G. Scott, Phys. Lett. B **458** (1999) 79; P. F. Harrison, D. H. Perkins and W. G. Scott, Phys. Lett. B **530** (2002) 167; P. F. Harrison and W. G. Scott, Phys. Lett. B **535** (2002) 163; P. F. Harrison and W. G. Scott, Phys. Lett. B **557** (2003) 76; C. I. Low and R. R. Volkas, Phys. Rev. D **68** (2003) 033007. A similar but physically different form was proposed earlier by: L. Wolfenstein, Phys. Rev. D **18** (1978) 958.

[144] S. F. King, JHEP **0508** (2005) 105.

[145] S. Antusch, S. F. King and A. Riotto, JCAP **0611** (2006) 011.

[146] S. Davidson and A. Ibarra, Phys. Lett. B **535** (2002) 25; K. Hamaguchi, H. Murayama and T. Yanagida, Phys. Rev. D **65** (2002) 043512.

[147] A. De Simone and A. Riotto, JCAP **0708** (2007) 002 [arXiv:hep-ph/0703175].

[148] A. De Simone, arXiv:0805.2354 [hep-ph].

[149] A. De Simone and A. Riotto, JCAP **0708** (2007) 013 [arXiv:0705.2183 [hep-ph]].

[150] C. S. Fong and M. C. Gonzalez-Garcia, JCAP **0808** (2008) 008 [arXiv:0806.3077 [hep-ph]].

[151] A. Anisimov, W. Buchmuller, M. Drewes and S. Mendizabal, Annals Phys. **324** (2009) 1234 [arXiv:0812.1934 [hep-th]].

[152] V. Cirigliano, C. Lee, M. J. Ramsey-Musolf and S. Tulin, arXiv:0912.3523 [hep-ph].

[153] J. Garayoa, S. Pastor, T. Pinto, N. Rius and O. Vives, arXiv:0905.4834 [hep-ph].

[154] W. Buchmuller and M. Plumacher, Phys. Lett. B **511** (2001) 74 [arXiv:hep-ph/0104189].

[155] M. Plumacher, Nucl. Phys. B **530** (1998) 207 [arXiv:hep-ph/9704231].

[156] M. Plumacher, arXiv:hep-ph/9807557.

[157] G. Lazarides and Q. Shafi, Phys. Lett. B **258** (1991) 305; T. Asaka, K. Hamaguchi, M. Kawasaki and T. Yanagida. Phys. Lett. B **464** (1999) 12.

[158] A. Abada, S. Davidson, F. X. Josse-Michaux, M. Losada and A. Riotto, JCAP **0604** (2006) 004 [arXiv:hep-ph/0601083]; E. Nardi, Y. Nir, E. Roulet and J. Racker, JHEP **0601** (2006) 164 [arXiv:hep-ph/0601084]; A. Abada, S. Davidson, A. Ibarra, F. X. Josse-Michaux, M. Losada and A. Riotto, JHEP **0609** (2006) 010 [arXiv:hep-ph/0605281]. S. Blanchet and P. Di Bari, JCAP **0703** (2007) 018 [arXiv:hep-ph/0607330]; S. Antusch, Phys. Rev. D **76** (2007) 023512 [arXiv:0704.1591 [hep-ph]]. F. X. Josse-Michaux and A. Abada, JCAP **0710** (2007) 009 [arXiv:hep-ph/0703084].

[159] D. Aristizabal Sierra, M. Losada and E. Nardi, arXiv:0905.0662 [hep-ph].

[160] E. Nardi, Y. Nir, J. Racker and E. Roulet, JHEP **0601** (2006) 068 [arXiv:hep-ph/0512052].